INFLAMMATION AND BENIGN PROSTATIC HYPERPLASIA: ROLE OF IMMUNE CELLS AND THEIR INTERACTIONS IN CHRONIC INFLAMMATION AND CELLULAR HYPERPLASIA

by

Meaghan M Broman

A Dissertation

Submitted to the Faculty of Purdue University

In Partial Fulfillment of the Requirements for the degree of

Doctor of Philosophy

Department of Comparative Pathobiology

West Lafayette, Indiana

August 2021

THE PURDUE UNIVERSITY GRADUATE SCHOOL
STATEMENT OF COMMITTEE APPROVAL

Dr. Timothy Ratliff, Chair

Department of Comparative Pathobiology

Dr. Chang-deng Hu

Department of Medicinal Chemistry and Molecular Pharmacology

Dr. Shihuan Kuang

Department of Animal Science

Dr. Suresh Mittal

Department of Comparative Pathobiology

Approved by:

Dr. Sanjeev K. Narayanan

Dedicated to my family for their unwavering support.

ACKNOWLEDGMENTS

The studies presented here involved the contributions and support of many people over the years. First, I would like to thank Dr. Timothy Ratliff for the opportunity to work in this field and for his guidance and support. Also, thanks to my committee members Dr. Changdeng Hu, Dr. Shihuan Kuang, and Dr. Suresh Mittal for their valuable input and guidance. I would like to thank the current and past members of the Ratliff lab for their help and support over the years, including Dr. Ben Elzey, Dr. Jiang Yang, Dr. Hsing Hui Wang, Dr. Renee Vickman, Dr. Erin Kischuk, Dr. Greg Cresswell, Dr. Paula Cooper, Dr. Scott Crist, and Tripti Bera. Thanks to the members of the Hayward lab and researchers at NorthShore Research Institute including Dr. Simon Hayward, Dr. Renee Vickman (again), Dr. Omar Franco, and Dr. Susan Crawford for their hard work with the human BPH project that made these studies possible. And a special thanks to Dr. Nadia Lanman and Juan Sebastian Paez Paez of the Purdue University Genomics Core Facility, the Collaborative Core for Cancer Bioinformatics (C3B), which is funded by the Walther Cancer Foundation and the Purdue University Center for Cancer Research (NIH grant P30 CA023168), for their bioinformatics expertise, without which none of these sequencing studies would have been possible.

I would also like to thank the staff of the various Purdue core facilities that have contributed to various aspects of this work, including Dr. Philip San Miguel of the Purdue Genomics Core and Dr. Jill Hutchcroft of the Purdue Flow Cytometry Core, and Victor Bernal-Crespo and MacKenzie Macintosh of the Purdue University Histology Research Laboratory, a core facility of the NIH-funded Indiana Clinical and Translational Science Institute. I would also like to thank Sandra Torregrosa-Allen, Melanie Currie, and Heidi Cervantes of the Biological Evaluation Shared Resource in the Purdue University Center for Cancer Research for their assistance in animal studies. I would also like to acknowledge the researchers and staff of Indiana University that have provided their assistance, including Dr. Travis Jerde for his assistance in immunofluorescence staining, Dr. Constance Temm of the Indiana University Immunohistochemistry Laboratory for the preparation of histologic and immunohistologic sections, and Veronika Slivova of Indiana University Health Methodist Hospital for procurement of human prostate specimens.

Thank you all, I am truly grateful for your support.

TABLE OF CONTENTS

LIST OF TABLES

LIST OF FIGURES

ABSTRACT

Benign prostatic hyperplasia (BPH) is a common urologic condition among older men, affecting approximately half of men by age 50 and nearly 80% by age 80. Lower urinary tract symptoms (LUTS) associated with BPH may significantly impact quality of life for many of these men. Inflammation has been associated with the development and progression of BPH however, the precise impact and role(s) of immune cells in these conditions remains unclear. Many previous studies over the decades have explored the roles of immune cells in prostate disease in animal models and prostate tissues from human patients, and, more recently, through transcriptomic analyses of bulk cell populations and of single cells. These and other emerging technologies continue to add to the body of knowledge related to this area.

The prostate is a complex organ composed of multiple epithelial and mesenchymal cell types and subtypes. The growth, morphology, and function of these cells is influenced by autocrine and paracrine cell-cell interactions in ways that are largely not yet understood. A better understanding of the composition, heterogeneity, morphology, interactions, and functional features of various prostate cell types, particularly involving immune cells in the context of inflammatory processes, is expected to improve our understanding of the impact of altered cellular composition and communication on prostate homeostasis and disease.

Inflammation has been shown to impact the growth, morphology, and function of various prostate cell types. It is hypothesized that inflammation promotes epithelial cell proliferation and differentiation in BPH despite androgen-targeted therapy. It is hypothesized that communications between and within various immune cell populations perpetuate the non-resolving inflammatory microenvironment that promotes prostate cell expansion. In this research, the POET-3 mouse model of inducible autoimmune inflammation is used to evaluate the impact of autoimmune-type inflammation on basal epithelial cell progenitor growth and differentiation in the absence of androgens mimicking the conditions of androgen deprivation therapy (ADT), and to demonstrate the enhanced growth and differentiation potential conferred on basal progenitors by inflammation.

Additionally, this research evaluates the morphology, gene expression, and cell-cell interaction predictions of BPH prostate immune cells to explore the role of immune cells and their interactions in driving BPH inflammation.

Overall, inflammation induced epithelial and stromal expansion and basal progenitor cell proliferation in vivo and promoted basal progenitor cell growth and differentiation in vitro under androgen-deficient conditions mimicking androgen-targeted therapy. Histologic evaluation of BPH specimens reveals the composition and distribution of immune cells, including organizing lymphoid structures resembling tertiary lymphoid structures (TLS). Also, analyses of single cell RNA sequencing data of gene expression patterns and signaling pathways reveal a mixed inflammatory microenvironment in BPH. Furthermore, predicted ligand-receptor interactions indicate mixed inflammatory signaling between and among immune cell populations, including T cells, macrophages, and mast cells, that likely to the unresolving nature of BPH inflammation.

In all, the results of these studies demonstrate inflammation-induced epithelial and stromal expansion in a mouse model of resolving prostatitis and indicate potential roles for multiple immune cell populations and their interactions in driving the ongoing inflammation of BPH, suggesting that this ongoing inflammation may impact the progressive stromal and epithelial expansion characteristic of BPH.

CHAPTER 1. INTRODUCTION

1.1 Biology of the human prostate

The prostate is a component of both the urinary and reproductive systems and is present in all mammals, although anatomy varies among species [1]. Many studies have explored the autocrine and paracrine communications among epithelial, stromal, and immune cells and their impact on prostatitis, BPH, and cancer. However, many questions regarding the roles and mechanisms of these cells and their interactions in prostate disease remain. More specifically, the roles of immune cell populations and their interactions in the perpetuation of the non-resolving inflammation of BPH and in cellular hyperplasia.

The anatomy and cellular composition of the prostate and communications among the various cell types impact the response to inflammatory stimuli and the clinical manifestations of prostate inflammation and hyperplasia. Therefore, defining the composition, heterogeneity, and interactions of immune cell populations is anticipated to provide insights into the pathogenesis of BPH inflammation and hyperplasia.

1.1.1 Anatomy and Development

The normal human prostate is an alobular organ situated in the lower pelvic cavity distal to the urinary bladder that surrounds the proximal prostatic urethra as it exits the urinary bladder [1]. The prostate arises from the primitive urogenital sinus which originates from the caudal hindgut endoderm [2]. The developing prostate is composed of an outer urogenital sinus mesenchyme (UGSM) layer and an inner urogenital sinus epithelium (UGSE) layer, from which the prostate stromal and epithelial compartments arise, respectively [3, 4]. At around 10 weeks gestation (human) or 17.5 days post coitus (mouse), the prostate begins to form through epithelial budding of the urogenital sinus under the influence of androgens produced by the fetal testes [2, 5]. These buds elongate and undergo branching morphogenesis, a process that continues through puberty [5]. At puberty when androgen levels increase, the prostate further develops and enlarges due to expansion and differentiation of epithelial and stromal compartments, eventually reaching a size of approximately 20-25 cm^3 in the normal adult male [1, 6].

The adult prostate is generally divided into three zones: peripheral zone (PZ), transition zone (TZ), and central zone (CZ) [1, 7]. The PZ comprises the bulk (approximately 70%) of the normal adult prostate volume and contains the majority of the glandular epithelial tissue [1, 7]. The TZ is normally the smallest zone, around 5% of the normal young adult prostate volume [1]. The CZ comprises about 25% of the normal prostate volume [1]. Some studies also include a fourth zone, the anterior zone, which is composed only of fibromuscular stromal tissue with no glands [1, 7]. The cellular and structural differences among the prostatic zones contribute to the localization of prostatic disease. The PZ is the most common location for prostate adenocarcinoma development, while the TZ is the usually the most affected zone in benign prostatic hyperplasia [1, 6, 8].

1.1.2 Androgen signaling in the prostate

The prostate develops, matures, and maintains cellular homeostasis under the influence of the androgens testosterone and its more active form 5α-dihydrotestosterone (DHT) through their signaling though the androgen receptor (AR) [3, 9]. Testosterone is produced predominately by Leydig cells of the testes and to a lesser extent in the adrenal cortex [1]. Testosterone is converted to DHT within prostate epithelial cells through the DHT synthesis pathway [1]. This pathway involves the activity of several enzymes at various steps, including the 5α reductase (5αR) enzymes and Cyp17a1 [10]. The 5αR enzymes include 3 isoforms: Srd5a1, Srd5a2, and Srd5a3 [1]. The major 5αR enzymes of the normal adult prostate, Srd5a1 and Srd5a2, are expressed in both the epithelium and stroma [11]. Srd5A1 is the predominate 5αR enzyme within the prostate epithelium, while Srd5a2 is the predominate form in the stromal compartment and the overall predominate form in the normal prostate [11]. Srd5a3 is overexpressed in hormone-refractory PCa [12]. These enzymes have been targeted by anti-androgen therapy in the treatment of PCa and BPH [13, 14].

Testosterone and DHT exert their effects on prostate cells through its interaction with AR [15]. DHT has approximately 5 times the affinity for AR when compared to testosterone. To initiate AR signaling, AR binds to testosterone or DHT in the cytoplasm then translocates to the nucleus where it binds to androgen response elements (ARE) in the DNA and activates AR-associated gene transcription [15]. Inhibition of androgen signaling either through reduction of androgen (castration, testosterone or DHT synthesis inhibition) or AR blockade results in rapid luminal

epithelial cell apoptosis and prostate involution [16, 17]. This process is reversable by reintroduction of androgen, which results in prostate cell proliferation and regrowth of the organ [16].

1.1.3 Prostate cellular populations

Histologically, the prostate is composed of glandular epithelial and stromal compartments. The human prostate is composed of approximately 30-50 glands lined by pseudostratified epithelium surrounded by abundant fibromuscular stromal tissue [1, 2]. The glandular epithelium is composed of luminal cells, basal cells, and rare neuroendocrine cells [2, 18]. The stroma is composed of various cell types including fibroblasts, smooth muscle cells, endothelial cells, immune cells, and extracellular matrix (ECM) [1]. Prostate cell types have typically been identified based on their tissue location, morphology, gene expression, and cell surface antigen expression [18-20]. More recently, advances in cell sequencing technologies have provided insights into the identity, composition, activities, and heterogeneity of prostate cell populations [20, 21].

Prostate epithelial compartment

The larger columnar luminal epithelial cells are the functional secretory cells of the prostate, producing prostatic secretions which fill the glandular lumina and contribute to the ejaculate [1]. These well-differentiated cells are generally identified by their columnar morphology and their expression of specific keratin proteins (Keratin 8, Keratin 18), prostate specific antigen (PSA), and androgen receptor (AR) [17, 22, 23]. Basal epithelial cells lie adjacent to the basement membrane and are identified by their expression of Keratin 5 and 14, p63, and low expression of AR [22, 24]. In contrast to luminal cells, basal cells are considered androgen-independent with a high capacity for proliferation [17]. Intermediate-type cells referred to as transit amplifying cells (TAC) expressing both basal and luminal cell markers are observed in prostate epithelial cell cultures in vitro and in vivo during development, however they are not typically observed in the normal adult prostate (Choi et al., 2012; Hudson et al., 2001; Karthaus et al., 2014; Wang et al., 2001). Neuroendocrine cells are rare and their function in the prostate is unclear; these cells are identified by their expression of the neuroendocrine markers synaptophysin and chromogranin A [18, 22].

Using scRNA-Seq, Henry et al (2018) identified four epithelial populations in whole prostate cell preparations from normal human prostates [20].

Epithelial progenitor cells

Along with mature differentiated cells are populations of self-renewing multipotent or unipotent stem/progenitor cells maintained in tissue-specific niches that replenish the various tissue cell populations under homeostatic or pathologic conditions [25]. Prostate epithelial progenitor cells are heterogeneous cells found mostly in the proximal ducts. [20, 21]. Crowley et al (2020) suggested variable distribution and regenerative capacity of luminal progenitor cells among the four lobes of the mouse prostate [21]. Lineage tracing studies in mouse models have demonstrated that in the normal adult prostate, luminal and basal cells are each maintained by separate populations of unipotent progenitor cells [26, 27]. However, organoid and prostate reconstitution assays have demonstrated the multipotent progenitor capacity of both isolated luminal and basal progenitors [21, 22, 28, 29]. Ousset et al (2012) demonstrated that unipotent luminal progenitor cells and multipotent basal progenitor cells capable of multilineage differentiation contribute to epithelial expansion during postnatal development [30].

Aside from the general luminal and basal cell markers, various markers have been used to identify and isolate potential progenitor cell populations. Functionally, progenitor cells are identified by their properties of self-renewal and differentiation into multiple lineages [31, 32]. Experimentally, these properties have been assessed through 3D organoid culture and through *in vivo* prostate reconstitution assays (Lukacs et al., 2010; Xin et al., 2007)[31]. Chua et al (2014) demonstrated the formation of prostate organoids from dissociated luminal progenitors referred to as castration-resistant Nkx3.1-expressing cells (CARN) [28]. Kwon et al (2016) observed that epithelial progenitor cells from different lineages produced distinct organoid types [27]. Several studies have used Sca-1 to identify both basal and luminal progenitor cells in the adult mouse prostate [27, 31, 33-35]. CD49f has been used in conjunction with Sca-1 and other markers to distinguish basal from luminal progenitor cells [27, 31, 34]. Other basal progenitor markers include Trop2 and Zeb1 [16, 36].

While luminal and basal epithelial populations are mainly maintained by their own progenitors, basal progenitor cells have been shown to be capable of differentiation into all three epithelial lineages under certain pathological conditions such as prostatitis and repeated rounds of androgen deprivation and reintroduction, as well as in experimental conditions such as prostate reconstitution assays [26, 27, 31, 32, 37]. Previous studies in mouse prostatitis models have shown that this basal-to-luminal differentiation capacity is enhanced by prostatic inflammation. Kwon et al (2014) noted that induction of prostatitis enhanced basal-to-luminal epithelial cell differentiation in a mouse model of *E. coli* prostatitis [29]. Wang et al (2015) demonstrated expansion of a Lin^- $Sca\text{-}1^+CD49f^+$ basal progenitor population and enhanced organoid formation from isolated Lin^- $Sca\text{-}1^+CD49f^+$ cells following induction of autoimmune-type prostate inflammation in the POET-3 mouse model [34]. Also, while basal cells do not require AR for their maintenance, the differentiation of basal cells into functional luminal cells is dependent on AR signaling [38].

In the normal prostate, androgen deprivation via castration results in rapid luminal epithelial cell apoptosis and involution of the organ [16, 17]. Some epithelial subpopulations survive castration and regenerate the epithelium following reintroduction of androgen [32, 37, 39, 40]. Lineage tracing experiments suggest that replacement luminal epithelial cells arise from surviving AR^+ luminal cells following reintroduction of androgen [41]. More recently, Karthaus et al (2020) used scRNA-Seq to identify luminal cell subpopulations with enhanced regenerative abilities that persisted following androgen deprivation and suggested that these cells were largely responsible for luminal cell regeneration following androgen reintroduction [39]. Chua et al (2018) suggested that subpopulations of luminal progenitors varied in their requirement for AR [42]. The ability of epithelial subpopulations to survive following androgen deprivation is also observed in a subset of prostatic carcinoma cells that are resistant to androgen deprivation therapy (ADT) known as castration-resistant prostatic carcinoma (CRPC) (Lukacs et al., 2010) [43]. Also, while the cell type of origin for prostate cancer has not been definitively identified, both basal and luminal progenitor cells are susceptible to neoplastic transformation and potential cell types of origin for PCa [24, 26, 44]. Transformed cells may share features with normal progenitor cells such as castration resistance and self-renewal, and some antigens and signaling pathways exhibited by normal progenitor cells have also been identified in cancer cells [16, 45]. Basal cells may also contribute to epithelial hyperplasia observed in BPH prostates [46].

Prostatic inflammation has been shown to promote short-term basal epithelial progenitor cell proliferation and differentiation in mouse models of resolving prostatic inflammation [34, 35, 47]. This is in contrast to the ongoing and worsening inflammation observed in BPH. It is hypothesized that the unresolving inflammatory microenvironment in BPH may promote continual cellular proliferation and hyperplasia.

Prostate stromal compartment

The stroma is composed of various cell types including fibroblasts, smooth muscle cells, endothelial cells, immune cells, and as well as extracellular matrix (ECM) compounds [1, 48]. Under the influence of androgens and AR signaling, paracrine signals from prostate stromal cells support epithelial morphogenesis, differentiation, proliferation, and maintenance [38, 49, 50]. Studies in AR knockout mice with loss of stromal fibroblast or smooth muscle AR have reported altered prostate development and decreased epithelial cell proliferation and prostate size [38, 51, 52]. Following castration, stromal smooth muscle cells are replaced by fibroblasts and myofibroblasts [49]. Androgen replacement results in increased growth factors (EGF, TGFα) [49].

Stromal cells and their communications with immune cells and epithelial cells may contribute to chronic prostatic inflammation, cancer, and BPH. For example, immune cell-derived cytokines such as CCL3 and CCL4 can promote production of the chemokines CCL21 and CXCL13 by stromal cells which in turn attract more immune cells to the inflammatory microenvironment [53, 54]. Cancer associated fibroblasts (CAF) produce chemokines such as CCL2 to attract monocytes to the tumor microenvironment [55]. Also, signaling between cancer cells and CAF may activate both cell types and promote cancer cell epithelial-to-mesenchymal transition, invasion and metastasis [56]. In BPH, stromal cell proliferation and expansion is often a prominent feature and may predominate over epithelial hyperplasia [57, 58]. These cells may also support epithelial proliferation and hyperplasia through secretion of growth factors and cytokines. In transgenic mice, overexpression of certain stromal growth factors including FGF2, FGF7, IGF-1 and TGFα have been shown to promote prostate epithelial cell hyperplasia [59-62]. Kato et al (2013) suggested that FGF2-FGFR signaling may promote prostate epithelial cell proliferation, and that androgens may suppress this signaling [49]. Inflammatory cells may activate stromal cells which recruit additional immune cells and support the formation of TLS [53, 54].

Previously, identification and isolation of specific fibromuscular stromal populations has been hindered by the lack of identified surface marker antigens [20]. More recently, scRNA-Seq studies have been used to identify and define stromal cell populations and their markers [20]. scRNA-Seq analysis techniques may aid in future studies of the roles of stromal cells and their interactions in prostate disease.

Prostate immune cells

In the normal prostate, the immune cell population is small and consists of both lymphoid and myeloid populations [54]. Overall, CD8+ T cells typically predominate with fewer numbers of $CD4^+$ T cells, B cells, macrophages, mast cells, and plasma cells [54, 63]. As men age, overall immune cell numbers in the prostate increase [63, 64].

Prostate-associated lymphoid tissue (PALT) is the most abundant immune tissue in the prostate [54]. Di Carlo et al (2007) described the morphology and composition of PALT in the prostates of men ages 62-70 without reported histologic evidence of BPH. This study divided PALT into intraepithelial immune cells and lymphoid aggregates within the stroma, with intraepithelial PALT consisting predominately of $CD8^+$ T cells and stromal PALT composed of $CD4^+$ T cells, $CD8^+$ T cells, and B cells arranged in follicular structures with or without a germinal center or in loose aggregates [54]. These follicles and aggregates were most commonly located in periglandular areas but some were distributed in other areas within the stroma [54]. Antibody-producing plasma cells are also present and found mostly within the periglandular stroma and in association with lymphoid structures.

The organized lymphoid structures termed tertiary lymphoid structures (TLS), tertiary lymphoid tissue, tertiary lymphoid organs, or ectopic lymphoid tissue have been observed in various tissues [65]. TLS are often associated with epithelial tissues such as the respiratory and intestinal tracts, as well as the prostate [54, 65]. Unlike primary and secondary lymphoid organs, which form during embryologic development, TLS form in non-lymphoid tissues in response to local chronic antigenic stimulation and inflammation [65, 66]. Several inflammatory mediators have been associated with TLS formation and maintenance including the TNF family members TNFα and lymphotoxins α and β, CXCL13, CCL21, and CCL19 [54, 67]. TLS are composed of central B

cell follicles with follicular dendritic cells (FDC) surrounded by parafollicular $CD4^+$ T cells [54]. High endothelial vessels (HEV), vascular structures typically associated with lymphoid follicles of secondary lymphoid organs (lymph nodes, spleen), are also observed in association with these structures in the prostate and other tissues [54, 68]. TLS have been associated with various disease processes including infection, autoimmunity, and neoplasia [69, 70].

The prostate myeloid component consists predominately of macrophages and also includes dendritic cells (DC), mast cells, and neutrophils [54]. Macrophages may be observed within the glandular lumina or distributed within the stroma, and along with DCs may be closely associated with lymphoid structures within the stroma [54]. Mast cells are generally present in loose aggregates within the stroma, often in perivascular or perineural areas [71, 72]. Neutrophils are typically rare in the prostate and are usually associated with acute inflammation [73].

In normal tissues, tissue injury results in an acute pro-inflammatory reaction followed by a shift to a tissue repair phenotype and eventual resolution of inflammation. In BPH, inflammatory cell numbers increase and does not diminish over time. Previous studies have identified a mixed inflammatory phenotype among immune cells within BPH tissues, which may suggest that conflicting pro-inflammatory and pro-tissue repair signals from immune cells perpetuate inflammation and hinder its resolution. However, the mechanisms involved and their implications for the perpetuation of inflammation, cellular hyperplasia, and morphologic changes in BPH are not fully understood.

1.2 Prostate inflammation and prostatic disease

Prostate inflammation has been linked to the development of both BPH and PCa; however, the mechanisms by which inflammation promotes prostate disease are not fully understood. Various immune cell populations may play anti- or pro-inflammatory roles in the microenvironment and altered signaling among immune cells and between immune cells and other prostate cell types may be involved in the perpetuation of prostatic inflammation.

1.2.1 Prostatitis

Previous studies have estimated the overall prevalence of prostatitis as between 2% and 16% [74-76]. The National Institutes of Health (NIH) divides prostatitis into four categories: acute bacterial prostatitis (Type I), chronic bacterial prostatitis (Type II), chronic prostatitis/chronic pelvic pain syndrome (CP/CPPS) (Type III), and asymptomatic inflammatory prostatitis (Type IV) [77, 78]. Around 90% of diagnosed prostatitis cases are categorized as CP/CPPS [77, 78]. Along with pelvic pain, CP/CPPS may involve a variety of symptoms including LUTS, sexual dysfunction, and psychosocial symptoms such as depression and anxiety, all of which negatively impact a patient's quality of life [78]. While an infectious agent may potentially initiate the inflammatory process, no organisms are identified by culture [77, 78]. The underlying cause of CP/CPPS is unclear, and hypothesized causes include infectious agents, autoimmunity, neurologic dysfunction, or endocrine imbalance [77, 78]. T cell reactivity to prostate antigens has been demonstrated in some men with CP/CPPS, suggesting an autoimmune component to CP/CPPS in some patients [79]. Inflammatory immune cells and their modulation of the microenvironment have been linked to many disease states including infectious disease, autoimmunity, and cancer [66].

1.2.2 Prostate cancer

Prostate cancer (PCa) is the commonly diagnosed non-cutaneous cancer and the second deadliest cancer type among men [80]. In contrast to BPH, which typically affects the transition zone, most PCa arise in the peripheral zone, where the bulk of the prostatic glandular tissue resides [7, 81]. Prostatic intraepithelial neoplasia has been described as a precursor lesion to PCa and is divided into low and high grade PIN [82]. Histologic features of PIN include increased cellularity and cells with enlarged hyperchromatic nuclei and prominent nucleoli [82]. Loss of the basal cell layer is a feature of progression to PCa [82]. Adenocarcinoma is the most common tumor type in the prostate [82]. While most human adenocarcinomas are of a luminal type, a single definitive cell type of PCa origin has not been identified [26]. Studies in murine models indicate that both luminal and basal progenitors may undergo carcinogenesis, and basal progenitor cells are hypothesized to be one potential cell type of origin for PCa [24, 26, 27, 44, 45, 83, 84]. Also, a basal cell-associated gene profile in PCa tumors has been associated with aggressiveness, suggesting that transformed

basal cells or potentially other epithelial cells that have transformed to a basal-like phenotype may represent a cellular profile more likely to resist and escape current androgen-based therapies [84].

Other non-epithelial cell types in the local tumor microenvironment may contribute to therapy resistance. In addition to various immune cells, the tumor microenvironment includes cancer-associated fibroblasts (CAF), which have been reported to both hinder and support tumor growth. CAF may secrete cytokines and growth factors that communicate with epithelial cells also contribute to local inflammatory responses by recruiting immune cells to the microenvironment [55, 85]. The extent of this tumor-stromal communication has yet to be fully elucidated. Recently, scRNA-Seq analysis techniques have been developed to predict the cell-cell interactions may elucidate the cellular populations and interactions occurring in the tumor microenvironment [86, 87].

While treatment of localized disease treated through surgery and chemotherapy is often curative, some patients will experience tumor recurrence and undergo androgen deprivation therapy (ADT) [43, 88]. ADT involves the reduction of androgen through androgen synthesis inhibition and/or AR signaling inhibition though castration or drug treatment [43]. Androgen deprivation results in rapid luminal epithelial cell apoptosis, which is followed by prostatic infiltration by various immune cells [43, 89]. In the normal prostate, a population of basal progenitor cells are able to survive and even proliferate and migrate following castration [89]. Shi et al (2014) demonstrated that epithelial cells expressing stem cell markers were enriched in the proximal prostatic ducts and were capable of proliferation and migration following castration [89]. Similarly, subsets of androgen-independent PCa cells exist within the heterogenous tumor cell population which resist ADT [24, 90].

In many patients, ADT ultimately fails as the diseases progresses from an initially androgen-dependent form to a lethal androgen-independent form termed castration-resistant prostate cancer (CRPC) [88, 91, 92]. The mechanisms by which PCa switches from androgen dependence to androgen independence are not clear. Proposed mechanisms have included AR mutations or gene amplification, emergence of AR splice variants, alternate AR-dependent gene activation, or intracrine androgen production by tumor cells [12, 13, 90, 92, 93]. It is hypothesized that

inflammation contributes to one or more of these mechanisms, perhaps through genetic or epigenetic alterations induced by enhanced proliferation and/or oxidative stress.

2.2.1 Immune cells and PCa

Inflammation has been linked to cancer in many tissues, although the precise mechanisms by which inflammation promotes cellular transformation and tumor development and progression are not fully understood, and likely vary among cancer types [94]. Chronic inflammation is commonly observed in prostate biopsy and surgical specimens and has been hypothesized to contribute to prostate carcinogenesis and resistance to therapy; however, the mechanisms by which this may occur are unclear [64, 95, 96] In normal tissue repair, cytokines produced by immune cells promote cell proliferation and differentiation, and it is thought that a similar process may promote prostate progenitor cell or PCa cell proliferation following castration or ADT [89]. Repeated tissue damage, proliferation, and generation of reactive oxygen and nitrogen species by inflammatory cells causing genetic damage in proliferating epithelial cells have been proposed as a trigger for carcinogenesis [97-99]. In addition, epithelial cell apoptosis induced by ADT is followed by prostatic infiltration by various immune cells [43, 89].

Many studies have indicated a link between chronic inflammation and PCa and have suggested anti- and pro-tumor roles for various immune cell types [99]. Tumor infiltrating lymphocytes (TIL), which include T cells, B cells, natural killer (NK) cells, and natural killer T (NKT) cells are often observed in tumors and have been associated with varying effects on the tumor. For example, infiltration by $CD8^+$ T cells has been associated with enhanced tumor cell killing, improved response to treatment, and improved patient survival in many cancer types [66, 100]. In contrast, B cells have been suggested to promote androgen-independent growth of PCa through activation of IKKα-BMI1 signaling via lymphotoxin α and β, and an increased density of intratumoral B cells has been associated with high risk PCa patient tumors [43, 91, 101, 102]. Both B and T cells comprise TLS, which have been observed in association with the local microenvironments of many tumor types including PCa, and have been associated with prolonged survival in both mouse models and human patients and more recently have been explored as an immunotherapy target [66, 67, 103, 104]. Myeloid cells, including macrophages, myeloid-derived suppressor cells (MDSC), dendritic cells (DC), neutrophils, and mast cells, have generally been considered to suppress anti-

tumor activity but may also have varying roles the tumor microenvironment [72, 105]. Mast cells have been observed in association with PCa, and some studies have suggested that intratumoral mast cells may be a positive prognostic indicator in PCa [71, 72, 106].

1.2.3 Benign prostatic hyperplasia

BPH is one of the most common male urologic conditions, affecting approximately 50% of men by age 50 and 80% by age 80 [6, 63, 95, 107]. BPH is the most common cause of lower urinary tract symptoms (LUTS) which include increased urgency and frequency, nocturia, weak urine stream and urine retention [107]. Clinical symptom severity is measured using the International Prostate Symptom Score (IPSS) [108]. While not all men with gross or histologic evidence of BPH experience significant clinical symptoms associated with prostatic enlargement, severe LUTS symptoms may significantly negatively impact quality of life and drive increased healthcare costs for affected patients, and many will eventually require medical and/or surgical intervention to manage their clinical symptoms [95, 107].

BPH predominately affects the TZ and periurethral area and is characterized by progressive stromal and/or glandular proliferation and expansion [7, 8, 20, 46]. While the proportion of glandular epithelial tissue to fibromuscular stromal tissue may vary, fibromuscular stromal tissue is generally increased compared to normal prostate and is often the predominant component of BPH nodules [57]. Bartsch et al (1979) observed a significant increase in the percentage of stroma and a decrease in glandular tissue in BPH prostates compared to normal prostates from young men, suggesting that stromal expansion is the major component of BPH [57]. Also, Shapiro et al (1992) found an increase in the ratio of stroma to epithelium in prostates from patients with symptomatic BPH compared to patients with asymptomatic BPH [58].

The symptoms of BPH are mainly attributed to bladder obstruction resulting from constriction of the prostatic urethra [58, 109]. This constriction is due mainly to prostatic enlargement resulting from androgen-mediated cellular proliferation and expansion and to α-adrenergic receptor-stimulated smooth muscle contraction [108]. To target these two components, treatment for BPH often involves the combination of 5α reductase enzyme inhibitors (5αRI) and α-adrenergic

receptor blockers, respectively [110]. However, many BPH patients eventually fail medical therapy, resulting in the need for surgical intervention for symptomatic BPH [95].

While the underlying cause of prostatic enlargement is not known, several potential causes or contributing factors have been proposed. BPH-associated cellular expansion occurs under the influence of androgens, and it is thought that age-related hormonal changes and changes in AR signaling may play a role in stimulating cellular proliferation [111]. Wu et al (2007) demonstrated that loss of epithelial AR resulted in increased epithelial proliferation and diminished epithelial differentiation in an epithelial AR knockout mouse model [9]. Alterations in growth factor expression such as overexpression of insulin like growth factors (IGFs) and their receptors in BPH cells have been implicated in driving the hyperplasic response [112, 113]. Systemic conditions such as obesity, diabetes, and metabolic syndrome may also contribute [114]. In recent decades, an immune-mediated process has been suggested as discussed below [79, 96, 115, 116].

Immune cells in BPH

Almost 3 decades ago, Nickel et al. (1994) proposed that, in addition to cellular expansion and smooth muscle activity, inflammation may be the "third component" connecting BPH and LUTS, and subsequent studies have associated the degree of inflammation in BPH with LUTS [8, 115]. Chronic inflammation is commonly observed in association with BPH nodules [63, 96, 117, 118]. Delongchamps et al (2008) observed chronic inflammatory infiltrates in 75% (70/93) of BPH prostates and 50% (37/74) of non-BPH prostates [117]. While a study by Robert et al. (2009) involving 282 BPH patient specimens observed inflammatory infiltrates in the majority of specimens similar to previous studies, they also observed an association between the degree of inflammation and IPSS and significantly higher prostate volumes in specimens with high-grade inflammation compared to those with low-grade inflammation [63]. The findings of these studies and others have led to the hypothesis that immune-mediated mechanisms may underlie the development and progression of BPH [96, 116]. However, while inflammation has been implicated in the pathogenesis of BPH, the precise mechanisms by which immune cells may contribute to BPH are not fully understood [96].

A particular feature of BPH inflammation is its progressive and non-resolving nature. In most tissues, inflammation peaks following the initial insult and eventually declines and resolves.

However, in the BPH prostate, inflammation fails to resolve and may worsen over time. It is hypothesized that this unresolving inflammation promotes epithelial and stromal proliferation as well as recruitment of additional immune cells to the prostate microenvironment. The roles of the various prostate immune cell populations and their interactions in the perpetuation of this inflammation is not fully elucidated.

Immune cell populations in BPH

Like the normal prostate, immune cell populations in BPH consist various lymphoid and myeloid populations including T cells, macrophages, B cells, and smaller numbers of other immune cell subtypes such as plasma cells and mast cells [63, 96, 118]. And as in the normal prostate, T lymphocytes represent the majority of immune cells in BPH [63, 64]. Theyer et al (1992) observed that in contrast to normal prostates where the majority of T cells are $CD8^+$ cytotoxic T cells, activated $CD4^+$ memory T cells predominate in BPH [64, 119]. A later study by Robert et al (2009) observed a majority of $CD8^+$ T cells in their specimens; however, the authors noted that differences in the distribution of $CD8^+$ and $CD4^+$ T cells in the epithelial vs stromal compartments and the sampling methods used to create their tissue microarray may account for this difference from the previous study [63, 64]. Also, infiltrating T cells were found to express co-inhibitory receptors (LAG-1, PD-1, TIM-3, CTLA-4) and co-stimulatory receptors (CD28, OX40, 4-1BB) associated with chronic T cell activation at a higher frequency than peripheral blood T cells, supporting the hypothesis that BPH is a chronic inflammatory condition [120].

The inflammatory microenvironment is influenced by cell-cell interactions involving various pro-inflammatory and anti-inflammatory cytokines and chemokines [121]. $CD4^+$ T lymphocytes infiltrate the prostate in response to pro-inflammatory cytokines such as interleukin 15 (IL-15) from BPH stromal, epithelial, and immune cells and interferon γ (IFNγ) from T cells and produce additional inflammatory cytokines [63, 118, 122]. IL-15 induces T cell proliferation and IFNγ production, which in turn stimulates further IL-15 production and lymphocyte recruitment, indicating that this paracrine signaling loop is involved in driving the increase in lymphocyte infiltration in BPH [123]. T lymphocyte-derived cytokines IFNγ, IL-2, IL-4, IL-13, and IL-17 were overall increased in BPH tissues compared to normal prostate and IFNγ and IL-2 stimulated prostate stromal cell proliferation while IL-4 inhibited proliferation, suggesting that infiltrating

lymphocytes modulate prostate stromal cell proliferation [122, 124, 125]. Also, BPH stromal cells stimulated by chronic inflammation may produce cytokines and chemokines such as CCL21 and CXCL13 to recruit immune cells to the prostate and may also act as antigen presenting cells (APC) to induce cytokine secretion by $CD4^+$ T cells [54, 69, 126]. Recruited lymphocytes may form aggregates and organizing tertiary structures under the influence of stromal and immune cell-derived chemokines and cytokines [127]. While TLS have been observed in association with BPH nodules, the potential role of TLS in BPH is not clear. TLS produce cytokines to recruit more T cells, B cells, and NK cells to the local microenvironment [69]. The number of TLS-associated HEV has been associated with both the degree of chronic inflammation and with LUTS in BPH prostates [68]. However, TLS have also been observed in prostates from aged men without histologic evidence of BPH [54]. While Di Carlo's study implies that organized PALT structures may be an age-related development unrelated to BPH, an age-matched comparison between specimens with and without clinical symptoms of BPH or prostatic enlargement above a threshold may be necessary to explore a potential link between formation of lymphoid structures, BPH, and LUTS.

The BPH prostate also contains various myeloid cell populations, including macrophages and mast cells [63]. Previous and current studies suggest significant heterogeneity among prostate myeloid populations, which may arise from bone marrow or from tissue resident hematopoietic cells, and local signals influence recruitment and differentiation of these cells [128]. The origins of myeloid cells and their responses to signals in the local tissue microenvironment may contribute to their observed heterogeneity. While cytokines and factors produced by macrophages impact the local microenvironment, macrophages and other APC such as dendritic cells can influence adaptive immune responses by promoting B cell differentiation into plasma cells by presenting antigens to naïve B cells [129]. Mast cells and mast cell subsets have been identified in neoplastic and non-neoplastic prostate tissue, however the function of these cells in BPH is not fully understood [71, 72, 106]. Mast cells have been associated with chronic pelvic pain syndrome (CPPS) and LUTS in BPH patients by promoting prostatic inflammation, smooth muscle contraction, and fibrosis [77, 130, 131]. Mast cells have also been implicated in the promotion of prostate epithelial proliferation in BPH through IL6/STAT3 signaling, as well as prostate stromal cell expansion/proliferation in the context of *Trichomonas vaginalis* infection [132, 133]. Additionally, mast cell-mediated modulation of other immune cells including Treg, Th17 cells, and B cells may promote

autoimmune inflammatory processes and may potentially contribute to ongoing BPH inflammation [130, 134, 135].

The heterogeneous nature of immune cell populations and their activities in BPH is hypothesized to contribute to the chronic non-resolving inflammatory microenvironment. Steiner et al (2003) noted that the cytokine expression pattern varied with the histological pattern of hyperplastic nodule formation, with increased IL-4 and IL-13 expression within nodules indicative of a Th2 response in infiltrated hyperplastic prostate tissues compared to the Th1 profile of the histologically normal tissue, indicating a mixed lymphoid inflammatory response in the BPH microenvironment [124]. Macrophages are often broadly divided into pro-inflammatory M1 and anti-inflammatory M2 subtypes based on expressed markers mainly identified in *in vitro* polarization experiments [136, 137]. However, more recent studies suggest that this classification does not fully encompass the extent of macrophage heterogeneity and plasticity *in vivo* [136, 138]. All together, these previous studies indicate that interactions among immune cells and other prostate cell populations drive the recruitment and activation of additional immune cells in the BPH microenvironment, and that conflicting pro- and anti-inflammatory signals in BPH prostates may contribute to the continuation and progression of BPH inflammation. And while previous studies have identified potential interactions among heterogeneous prostate cell types involved in BPH inflammation, many of the cell-cell communications that are hypothesized to drive BPH inflammation and hyperplastic responses have yet to be elucidated.

1.3 Animal models and prostate disease

Many animal models have been used in prostate research, with advantages and disadvantages to each. Rodent models have been and remain the most commonly used animal models in prostate research and have provided valuable insights into mechanisms of prostate disease. However, these models present some challenges in modeling human disease in that they do not fully recapitulate the anatomic, morphologic and clinical aspects of human prostate disease [139, 140]. More recently, the canine model of BPH has gained interest due to more similar prostate anatomy than the rodent models as well as the development of spontaneous BPH with age in intact dogs [141]. However, the canine model still differs significantly to humans in terms of anatomy and BPH pathogenesis [141]. Of all current animal models, the non-human primate model, particularly the

chimpanzee, most closely resemble the human anatomy and BPH development and progression [142]. However, the slow progression of BPH in these animals as well as practical and ethical concerns hinder the experimental use of this model [142].

Despite their challenges, rodent models have proven invaluable in the study of urologic disease. More specifically, rodent models of prostatitis have allowed for the study of the roles of various immune, epithelial, and stromal cell populations in inflammation and the impact on prostate disease.

1.3.1 Mouse prostate anatomy

Mouse prostate anatomy differs substantially from that of humans [48]. In contrast to the alobular structure of the human prostate, the mouse prostate is divided into four paired lobes (dorsal, ventral, lateral and anterior) with distinct anatomic and histologic features [2, 18, 48]. While some studies have suggested certain lobes as comparable to specific zones of the human prostate, there is no consensus as to the anatomic equivalence of the human and mouse prostate [143]. Similar to the human prostate, the murine prostate is composed of epithelial and stromal compartments [22, 48]. The epithelial compartment is composed of luminal, basal, and neuroendocrine cells which express many of the same characteristic markers as human prostate epithelial cells, such as Keratin 8 (luminal), Keratin 5 (basal), and Chromogranin A (neuroendocrine) [48]. In addition, some epithelial progenitor markers identified in human prostates have also been used to identify and study epithelial progenitors in mouse prostates. CD49f, used in many murine prostate studies, is a conserved stem cell marker among many mammalian species including rodents and humans [25, 34]. Goldstein et al (2008) identified Trop2 as a marker of a stem-like basal cell subpopulation in both humans and mice [16]. However, some differences exist between murine and human markers. For example, Stem cell antigen-1 (Sca-1), which has been identified in many mouse studies as a marker of both basal and luminal progenitor cells, is not expressed in the human prostate [27, 33, 34]. McAuley et al (2019) identified Sox2 as a marker of castration-resistant epithelial cells in adult mice [144]. The capacity for self-renewal and differentiation of murine progenitor cell populations has been assessed experimentally through their ability to form tissue organoids in 3D culture and form prostate tissue in prostate reconstitution assays (Lukacs et al., 2010; Xin et al., 2007). Additionally, previous studies have shown that the capacity of isolated murine basal

progenitor cells for proliferation and self-renewal is enhanced by inflammation (H. H. Wang et al., 2015; L. Wang et al., 2015; Xin et al., 2007).

Rodent prostates lack the dense fibromuscular stroma characteristic of the human prostate; instead, the smooth muscle is arranged in a thin layer subjacent to the epithelial basement membrane and fibroblasts are loosely arranged within the inter-glandular stroma [48]. These differences are one reason that rodent models of human BPH, where stromal expansion is usually a prominent feature, present a challenge in modeling of the human disease.

1.3.2 Mouse models of prostatitis

Immune cell numbers are low in the normal mouse prostate, consisting of few mixed lymphoid and myeloid populations. While these populations are normally small, they significantly expand and shift under experimental prostatitis conditions. Rodent models of prostatitis include spontaneous inflammation models, infectious agent models, hormone-associated models, and immune-induced models [145, 146]. Each model has its advantages and disadvantages and differ in their comparability to human prostatitis. Spontaneous prostatitis has been described in multiple rat strains, however the incidence and distribution of prostatic inflammation varies among strains and is not entirely predictable [145]. Inducible bacterial models and inducible immune-mediated models will be discussed here in relation to the current research.

Bacterial prostatitis mouse models

Most early mouse models involved induction of prostatitis through inoculation with a pathogenic organism. One of the most often used mouse models of prostatitis have involved transurethral inoculation with bacterial pathogens, most often uropathogenic *E. coli* [29, 35]. While these models are useful in assessing the impact of inflammation on prostate disease, diagnosed human prostatitis is predominately of the chronic abacterial type, and the nature of the inflammatory reaction in bacterial prostatitis differs from that observed in CP/CPPS [78]. However, this model has been useful in demonstrating the impact of inflammation on prostate cell populations and prostatic lesions. The inflammatory populations in this model were initially predominately neutrophils and macrophages, which decrease over time while lymphoid populations increase [73]. Expression of inflammatory genes including interleukins and COX2 increase in conjunction with

inflammation [73]. Furthermore, inflammation induced epithelial cell proliferation and hyperplasia [73]. Wang et al (2015) demonstrated expansion of Sca-1^{+}CD44^{+}CD133^{+}c-Kit^{+} epithelial progenitor cells following induction of prostatitis by *E.coli* strain 1677 [35]. Gao et al (2019) noted that chronic *E.coli*-induced prostatic inflammation induced epithelial morphologic changes consistent with PIA and PIN as well as induced genomic mutations in a C57BL/6 mouse model [147].

POET-3 model

To better model the type of chronic abacterial inflammation observed in most human prostatitis cases, the prostate ovalbumin expressing transgenic (POET)-3 mouse was developed to study the impact of autoimmune inflammation on prostate cell growth and carcinogenesis [47]. The POET-3 mouse expresses ovalbumin in the prostate epithelium under the control of the prostate epithelial cell-specific probasin promoter ARR_2PB, which is activated by binding of AR to the promoter [47]. Adoptive transfer of *in vitro* activated OT-1 T cells results in reproducible induction of prostate-specific inflammation [47]. Previous studies in the intact POET-3 mouse model indicate that induced inflammation peaks around 6-7 days post-OTI injection and declines steadily thereafter and increased immune cell numbers are observed 80 days post-adoptive transfer [47]. Haverkamp et al (2011) observed increased epithelial proliferation and stromal expansion following induction of inflammation [47]. Wang et al (2015) demonstrated expansion and proliferation of Lin-Sca-1^{+}CD$49f^{+}$ basal epithelial progenitor cells *in vivo* and enhanced organoid formation in LSC isolated from inflamed POET-3 mice *in vitro* [34, 35]. This study also found that inflamed LSC formed larger and more hollow-type organoids compared to LSC from non-inflamed mouse prostates in androgen-free 3D culture, indicating that the impact of inflammation on the growth and differentiation of LSC persists after removal from the inflammatory microenvironment [34]. Additionally, this model has been combined with prostate-specific PTEN knockout to generate Luc/$PTEN^{het}$/ROSA26/POET-3 and Luc/$PTEN^{fl/fl}$/ROSA26/POET-3 mice to investigate the role of inflammation in prostate carcinogenesis [148].

The POET-3 mouse represents a model of resolving autoimmune-type prostatic inflammation, which contrasts with the non-resolving nature of human BPH inflammation. However, this model

has been useful in uncovering the impact of this type of inflammation on specific prostate cell types.

Other immune mouse models

Mouse models, both spontaneous and inducible, have been developed to model an autoimmune inflammatory environment. Autoimmune prostatitis may develop in non-obese diabetic (NOD) mice spontaneously [145, 149]. Antigen-induced models using prostate homogenates have been used as inducible autoimmune prostatitis models in various mouse strains. In the same study that demonstrated acceleration of preneoplastic lesions in an *E. coli* prostatitis mouse model, Gao et al (2019) also used a rat prostate extract protein immunization model to demonstrate enhanced formation of PIA and PIN in inflamed C57BL/6 mouse prostates [147]. While this method can induce autoimmune prostatitis in wild type mice, the induction is much less efficient than in mice genetically prone to developing autoimmune inflammation. In one study, Rivero et al (2002) found that 2 injections of rat prostate steroid-binding protein (RSBP) induced prostatitis in 80-100% of NOD mice compared to around 30% of C57BL/6 mice [150].

Mice with a deficiency in the autoimmune regulator (Aire) gene, a transcription factor involved in the expression of self-antigens in the thymus and the development of central tolerance, develop spontaneous autoimmune inflammation in multiple organs [151]. Injection with mouse prostate homogenates plus complete Freud's adjuvant results in subepithelial and stromal lymphocytic and lymphoplasmacytic inflammation. The prostatic inflammation in this model persists instead of resolving, and may form lymphoid aggregates and organizing structures similar to TLS observed in human prostates [54].

1.4 Single cell RNA sequencing in prostate research

Elucidating the mechanisms of disease and exploration of potential therapies require an in-depth knowledge of the cellular composition of the tissue or organ under investigation [20]. Bulk RNA Seq can provide a transcriptional profile of a whole tissue [152]. However, most tissues are composed of multiple cell types and subtypes that cannot be elucidated by bulk analysis [152]. Single cell sequencing has been used to identify cell types and elucidate cellular heterogeneity in healthy and diseased tissues [153]. High-throughput sequencing allows for the transcriptional

profiling of many cells at the same time [153]. Similar cell types are clustered based on their differential gene expression (DGE) patterns [153]. The addition of CITE-seq antibodies to specific cell surface markers allows for further identification of cell types based on surface marker expression [154]. In addition to identification of cell subtypes, scRNA-Seq data may be used to identify unique cell subtype markers and cell signaling pathways [153]. Initial scRNA-Seq studies focused mainly on using gene expression data for identifying cell types or functional states within a sample by means of cell clustering analyses [155]. More recently, the uses of scRNA-Seq data have expanded to involve multiple analyses of the gene expression, epigenetics, and protein expression profiles of a single cell [156].

As described previously, the human prostate is composed of multiple heterogeneous cell types and subtypes [20, 21]. scRNA-Seq has been used to define the heterogeneity of various prostate cell populations [20, 21]. To define the cellular landscape of the normal human prostate and establish a baseline for future prostate disease studies, Henry et al. (2018) performed scRNA-Seq on normal prostates and prostatic urethra from healthy young organ donors [20]. This analysis identified 4 epithelial cell subtypes, two of which had not been previously characterized, illustrating the heterogeneous composition of the epithelial component [20]. This study also describes the challenges of obtaining pure cellular populations by FACS, as well as a scheme for isolating stromal cell populations which had previously been hindered by the lack of adequate cell surface markers for fluorescence activated cell sorting (FACS) [20]. Another scRNA-Seq study by Crowley et al (2020) suggested notable heterogeneity among luminal epithelial cells but less heterogeneity among the basal epithelial cells [21]. This study also suggested that several luminal epithelial progenitor markers were shared between mice and humans, which may aid future comparative studies [21]. As scRNA-Seq data analysis approaches differ between studies and can impact results, it is difficulty to directly compare the results of these studies. However, as more scRNA-Seq datasets are published, individual researchers may apply their analyses of choice. Also, the development of additional techniques such as spatial transcriptomics may allow for the anatomic localization of cells expressing specific gene profiles and provide further insight into their local function and cellular interactions [157].

1.4.1 Cell-cell interactions

Cell-cell communications via ligand-receptor interactions is known to be integral to tissue and organ function [158]. Interactions between prostate epithelial cells and stromal cells are known to influence the embryonic and post-natal development of the organ, and perturbations in these interactions impact normal tissue homeostasis and disease development [49, 59]. Similarly, prostate inflammatory processes are initiated and perpetuated via interactions involving cytokines, chemokines, and their receptors expressed by various cell types [121]. The full extent and roles of cell-cell interactions among prostate cell types is not yet known.

To explore cell-cell interactions within tumors, Kumar et al (2018) developed a method to predict and score ligand-receptor interactions using scRNA-Seq data [86]. This and similar methods predict and score interactions based on ligand and receptor gene expression and cell number and referencing databases of known ligand-receptor pairs [86, 87]. These methods may be applied to various tissue types to predict and compare cell-cell interactions among all cells or subsets of cells between normal and disease states or treatment groups and may indicate targets for treatment. As it is hypothesized that interactions between and among various immune cell populations drive the continuation and progression of prostatic inflammation in BPH, these methods may predict alterations in ligand-receptor interactions in BPH compared to non-BPH prostates and potentially identify interactions involved in perpetuating BPH inflammation.

1.5 Research Questions and Conclusions

The general composition of the immune populations in the normal and diseased prostate have been explored in many studies; however, the roles and impact of immune cells in prostate disease are not fully understood. In particular, the potential roles of immune cells in prostate inflammation and BPH progression. Previous studies by this lab and others have sought to describe and characterize the impact of prostatic inflammation on various prostate cell types. Studies in the POET-3 mouse model have shown expansion of epithelial and stromal cells in response to autoimmune-type inflammation, including a population of basal progenitor cells that are hypothesized to contribute to BPH and PCa [34, 47]. Studies in human specimens have identified a mixed inflammatory phenotype in BPH, as well as paracrine signaling pathways that drive immune cell recruitment, proliferation, and activity [124]. However, many questions regarding

the drivers of non-resolving BPH inflammation and its roles in prostate cell expansion remain. Also, previous studies into the heterogeneity and gene expression of immune cell populations have been limited to the evaluation of previously identified cell markers and genes in tissue specimens. In recent years, the development of RNA sequencing technologies has allowed for in-depth analysis of the transcriptome of bulk and single cells from normal and diseased tissues, providing a valuable tool in uncovering the heterogeneity and gene expression profiles of cell populations [158]. This technology in combination with previously developed histologic, immunohistologic, flow cytometry, and gene expression analysis techniques can provide a deeper understanding of the composition, morphology, and activity of BPH immune cells. The purpose of the research presented here is to further define the impact of immune cells and autoimmune-type inflammation on the prostate by exploring immune cell morphology, gene expression, and interactions in human BPH specimens by means of scRNA-Seq and histologic analyses, as well as basal epithelial progenitor cell morphology and behavior in the POET-3 mouse model of inducible autoimmune prostatitis. It is anticipated that by exploring the immune mechanisms of BPH inflammation and hyperplasia that potential targets for further study and/or treatment may be identified.

In the current studies, we used scRNA-Seq and histologic analyses to examine and compare the immune cell populations, morphology, gene expression, and interactions in BPH and normal non-BPH prostates. Since inflammation has been associated with BPH progression and LUTS, we hypothesized that differences in specific immune cell populations and their cell-cell communications may contribute to the perpetuation of an inflammatory microenvironment. Also, as basal epithelial cells are hypothesized to contribute to BPH and PCa and previous studies have demonstrated that inflammation can drive basal epithelial progenitor cell proliferation, the morphology and behavior of these cells in the POET-3 model of autoimmune-type prostatitis was evaluated [34]. Also, since inflammation is hypothesized to promote epithelial progenitor cell proliferation and differentiation under androgen-deprived conditions, these cells were evaluated *in vivo* in castrate POET-3 mice and *in vitro* in an androgen-free 3D organoid culture model. Also, while further studies are needed to further elucidate the precise mechanisms and impact of the immune cell interactions described here, this research suggests potential immune targets for future studies of the prostate inflammatory microenvironment.

Studies by this lab and others have sought to describe and characterize the impact of prostatic inflammation on various prostate cell types. However, many questions regarding the prostate inflammatory microenvironment and its roles in BPH remain. BPH is characterized by chronic non-resolving inflammation, and the drivers of this ongoing inflammation are not fully understood. Also, the roles of various immune cell subtypes and their communications with each other and other cell types in this inflammation are not fully understood. The purpose of the research presented here is to further define the impact of immune cells and autoimmune-type inflammation on the prostate by exploring immune cell morphology, gene expression, and interactions and basal epithelial progenitor cell morphology and behavior.

1.6 References

1. Steers, W.D., C.P. Evans, and C.R. Chapple, *Urologic principles and practice*. 2nd ed. Springer specialist surgery series. 1 online resource (IX, 677 p. 156 illus., 119 illus. in color.).
2. Toivanen, R. and M.M. Shen, *Prostate organogenesis: tissue induction, hormonal regulation and cell type specification.* Development, 2017. **144**(8): p. 1382-1398.
3. Wen, S., et al., *Stromal androgen receptor roles in the development of normal prostate, benign prostate hyperplasia, and prostate cancer.* Am J Pathol, 2015. **185**(2): p. 293-301.
4. Hayward, S.W., et al., *Stromal development in the ventral prostate, anterior prostate and seminal vesicle of the rat.* Acta Anat (Basel), 1996. **155**(2): p. 94-103.
5. Ricke, W.A., et al., *Hormonal and stromal regulation of normal and neoplastic prostatic growth.* Prog Mol Subcell Biol, 2005. **40**: p. 183-216.
6. Berry, S.J., et al., *The development of human benign prostatic hyperplasia with age.* J Urol, 1984. **132**(3): p. 474-9.
7. McNeal, J.E., *The zonal anatomy of the prostate.* Prostate, 1981. **2**(1): p. 35-49.
8. De Nunzio, C., et al., *The controversial relationship between benign prostatic hyperplasia and prostate cancer: the role of inflammation.* Eur Urol, 2011. **60**(1): p. 106-17.
9. Wu, C.T., et al., *Increased prostate cell proliferation and loss of cell differentiation in mice lacking prostate epithelial androgen receptor.* Proc Natl Acad Sci U S A, 2007. **104**(31): p. 12679-84.
10. Attard, G., et al., *Antitumor activity with CYP17 blockade indicates that castration-resistant prostate cancer frequently remains hormone driven.* Cancer Res, 2009. **69**(12): p. 4937-40.

11. Zhu, Y.S. and G.H. Sun, *5alpha-Reductase Isozymes in the Prostate.* J Med Sci, 2005. **25**(1): p. 1-12.

12. Uemura, M., et al., *Novel 5 alpha-steroid reductase (SRD5A3, type-3) is overexpressed in hormone-refractory prostate cancer.* Cancer Sci, 2008. **99**(1): p. 81-6.

13. Chang, K.H., et al., *Dihydrotestosterone synthesis bypasses testosterone to drive castration-resistant prostate cancer.* Proc Natl Acad Sci U S A, 2011. **108**(33): p. 13728-33.

14. de Bono, J.S., et al., *Abiraterone and increased survival in metastatic prostate cancer.* N Engl J Med, 2011. **364**(21): p. 1995-2005.

15. Feng, Q. and B. He, *Androgen Receptor Signaling in the Development of Castration-Resistant Prostate Cancer.* Front Oncol, 2019. **9**: p. 858.

16. Goldstein, A.S., et al., *Trop2 identifies a subpopulation of murine and human prostate basal cells with stem cell characteristics.* Proc Natl Acad Sci U S A, 2008. **105**(52): p. 20882-7.

17. Schalken, J.A. and G. van Leenders, *Cellular and molecular biology of the prostate: stem cell biology.* Urology, 2003. **62**(5 Suppl 1): p. 11-20.

18. Shen, M.M. and C. Abate-Shen, *Molecular genetics of prostate cancer: new prospects for old challenges.* Genes Dev, 2010. **24**(18): p. 1967-2000.

19. DeMarzo, A.M., et al., *Pathological and molecular aspects of prostate cancer.* Lancet, 2003. **361**(9361): p. 955-64.

20. Henry, G.H., et al., *A Cellular Anatomy of the Normal Adult Human Prostate and Prostatic Urethra.* Cell Rep, 2018. **25**(12): p. 3530-3542 e5.

21. Crowley, L., et al., *A single-cell atlas of the mouse and human prostate reveals heterogeneity and conservation of epithelial progenitors.* Elife, 2020. **9**.

22. Karthaus, W.R., et al., *Identification of multipotent luminal progenitor cells in human prostate organoid cultures.* Cell, 2014. **159**(1): p. 163-175.

23. Zhang, D., et al., *Prostate Luminal Progenitor Cells in Development and Cancer.* Trends Cancer, 2018. **4**(11): p. 769-783.

24. Wang, Z.A., et al., *Lineage analysis of basal epithelial cells reveals their unexpected plasticity and supports a cell-of-origin model for prostate cancer heterogeneity.* Nat Cell Biol, 2013. **15**(3): p. 274-83.

25. Krebsbach, P.H. and L.G. Villa-Diaz, *The Role of Integrin alpha6 (CD49f) in Stem Cells: More than a Conserved Biomarker.* Stem Cells Dev, 2017. **26**(15): p. 1090-1099.

26. Choi, N., et al., *Adult murine prostate basal and luminal cells are self-sustained lineages that can both serve as targets for prostate cancer initiation.* Cancer Cell, 2012. **21**(2): p. 253-65.

27. Kwon, O.J., L. Zhang, and L. Xin, *Stem Cell Antigen-1 Identifies a Distinct Androgen-Independent Murine Prostatic Luminal Cell Lineage with Bipotent Potential.* Stem Cells, 2016. **34**(1): p. 191-202.

28. Chua, C.W., et al., *Single luminal epithelial progenitors can generate prostate organoids in culture.* Nat Cell Biol, 2014. **16**(10): p. 951-61, 1-4.

29. Kwon, O.J., et al., *Prostatic inflammation enhances basal-to-luminal differentiation and accelerates initiation of prostate cancer with a basal cell origin.* Proc Natl Acad Sci U S A, 2014. **111**(5): p. E592-600.

30. Ousset, M., et al., *Multipotent and unipotent progenitors contribute to prostate postnatal development.* Nat Cell Biol, 2012. **14**(11): p. 1131-8.

31. Lawson, D.A., et al., *Isolation and functional characterization of murine prostate stem cells.* Proc Natl Acad Sci U S A, 2007. **104**(1): p. 181-6.

32. Xin, L., et al., *Self-renewal and multilineage differentiation in vitro from murine prostate stem cells.* Stem Cells, 2007. **25**(11): p. 2760-9.

33. Kwon, O.J., et al., *The Sca-1(+) and Sca-1(-) mouse prostatic luminal cell lineages are independently sustained.* Stem Cells, 2020. **38**(11): p. 1479-1491.

34. Wang, H.H., et al., *Characterization of autoimmune inflammation induced prostate stem cell expansion.* Prostate, 2015. **75**(14): p. 1620-31.

35. Wang, L., et al., *Expansion of prostate epithelial progenitor cells after inflammation of the mouse prostate.* Am J Physiol Renal Physiol, 2015. **308**(12): p. F1421-30.

36. Wang, X., et al., *Identification of a Zeb1 expressing basal stem cell subpopulation in the prostate.* Nat Commun, 2020. **11**(1): p. 706.

37. Xin, L., D.A. Lawson, and O.N. Witte, *The Sca-1 cell surface marker enriches for a prostate-regenerating cell subpopulation that can initiate prostate tumorigenesis.* Proc Natl Acad Sci U S A, 2005. **102**(19): p. 6942-7.

38. Haverkamp, J.M., et al., *An inducible model of abacterial prostatitis induces antigen specific inflammatory and proliferative changes in the murine prostate.* Prostate, 2011. **71**(11): p. 1139-50.

39. Xie, Q., et al., *Dissecting cell-type-specific roles of androgen receptor in prostate homeostasis and regeneration through lineage tracing.* Nat Commun, 2017. **8**: p. 14284.

40. Karthaus, W.R., et al., *Regenerative potential of prostate luminal cells revealed by single-cell analysis.* Science, 2020. **368**(6490): p. 497-505.

41. Wang, Y., et al., *Cell differentiation lineage in the prostate.* Differentiation, 2001. **68**(4-5): p. 270-9.

42. Liu, J., et al., *Regenerated luminal epithelial cells are derived from preexisting luminal epithelial cells in adult mouse prostate.* Mol Endocrinol, 2011. **25**(11): p. 1849-57.

43. Chua, C.W., et al., *Differential requirements of androgen receptor in luminal progenitors during prostate regeneration and tumor initiation.* Elife, 2018. **7**.

44. Ammirante, M., et al., *An IKKalpha-E2F1-BMI1 cascade activated by infiltrating B cells controls prostate regeneration and tumor recurrence.* Genes Dev, 2013. **27**(13): p. 1435-40.

45. Henry, G., et al., *Molecular pathogenesis of human prostate basal cell hyperplasia.* Prostate, 2017. **77**(13): p. 1344-1355.

46. Wang, S., et al., *Pten deletion leads to the expansion of a prostatic stem/progenitor cell subpopulation and tumor initiation.* Proc Natl Acad Sci U S A, 2006. **103**(5): p. 1480-5.

47. Smith, B.A., et al., *A basal stem cell signature identifies aggressive prostate cancer phenotypes.* Proc Natl Acad Sci U S A, 2015. **112**(47): p. E6544-52.

48. Treuting, P.M., et al., *Comparative anatomy and histology a mouse and human atlas*. 2012, Elsevier,: London. p. 1 online resource (474 p.).

49. Kato, M., et al., *Activation of FGF2-FGFR signaling in the castrated mouse prostate stimulates the proliferation of basal epithelial cells.* Biol Reprod, 2013. **89**(4): p. 81.

50. Lai, K.P., et al., *Suppressed prostate epithelial development with impaired branching morphogenesis in mice lacking stromal fibromuscular androgen receptor.* Mol Endocrinol, 2012. **26**(1): p. 52-66.

51. Yu, S., et al., *Altered prostate epithelial development and IGF-1 signal in mice lacking the androgen receptor in stromal smooth muscle cells.* Prostate, 2011. **71**(5): p. 517-24.

52. Yu, S., et al., *Altered prostate epithelial development in mice lacking the androgen receptor in stromal fibroblasts.* Prostate, 2012. **72**(4): p. 437-49.

53. Luo, S., et al., *Chronic Inflammation: A Common Promoter in Tertiary Lymphoid Organ Neogenesis.* Front Immunol, 2019. **10**: p. 2938.

54. Di Carlo, E., et al., *The prostate-associated lymphoid tissue (PALT) is linked to the expression of homing chemokines CXCL13 and CCL21.* Prostate, 2007. **67**(10): p. 1070-80.

55. Vickman, R.E., et al., *Heterogeneity of human prostate carcinoma-associated fibroblasts implicates a role for subpopulations in myeloid cell recruitment.* Prostate, 2020. **80**(2): p. 173-185.

56. Giannoni, E., et al., *Reciprocal activation of prostate cancer cells and cancer-associated fibroblasts stimulates epithelial-mesenchymal transition and cancer stemness.* Cancer Res, 2010. **70**(17): p. 6945-56.

57. Bartsch, G., et al., *Light microscopic stereological analysis of the normal human prostate and of benign prostatic hyperplasia.* J Urol, 1979. **122**(4): p. 487-91.

58. Shapiro, E., et al., *The relative proportion of stromal and epithelial hyperplasia is related to the development of symptomatic benign prostate hyperplasia.* J Urol, 1992. **147**(5): p. 1293-7.

59. Foster, B.A., et al., *Enforced expression of FGF-7 promotes epithelial hyperplasia whereas a dominant negative FGFR2iiib promotes the emergence of neuroendocrine phenotype in prostate glands of transgenic mice.* Differentiation, 2002. **70**(9-10): p. 624-32.

60. Konno-Takahashi, N., et al., *Engineered FGF-2 expression induces glandular epithelial hyperplasia in the murine prostatic dorsal lobe.* Eur Urol, 2004. **46**(1): p. 126-32.

61. Kaplan-Lefko, P.J., et al., *Enforced epithelial expression of IGF-1 causes hyperplastic prostate growth while negative selection is requisite for spontaneous metastogenesis.* Oncogene, 2008. **27**(20): p. 2868-76.

62. Yoshio, Y., et al., *Effect of transforming growth factor alpha overexpression on urogenital organ development in mouse.* Differentiation, 2010. **80**(2-3): p. 82-8.

63. Robert, G., et al., *Inflammation in benign prostatic hyperplasia: a 282 patients' immunohistochemical analysis.* Prostate, 2009. **69**(16): p. 1774-80.

64. Theyer, G., et al., *Phenotypic characterization of infiltrating leukocytes in benign prostatic hyperplasia.* Lab Invest, 1992. **66**(1): p. 96-107.

65. Aloisi, F. and R. Pujol-Borrell, *Lymphoid neogenesis in chronic inflammatory diseases.* Nat Rev Immunol, 2006. **6**(3): p. 205-17.

66. Weinstein, A.M. and W.J. Storkus, *Therapeutic Lymphoid Organogenesis in the Tumor Microenvironment.* Adv Cancer Res, 2015. **128**: p. 197-233.

67. Tang, H., et al., *Lymphotoxin signalling in tertiary lymphoid structures and immunotherapy.* Cell Mol Immunol, 2017. **14**(10): p. 809-818.

68. Inamura, S., et al., *Appearance of High Endothelial Venule-Like Vessels in Benign Prostatic Hyperplasia is Associated With Lower Urinary tract Symptoms.* Prostate, 2017. **77**(7): p. 794-802.

69. Pitzalis, C., et al., *Ectopic lymphoid-like structures in infection, cancer and autoimmunity.* Nat Rev Immunol, 2014. **14**(7): p. 447-62.

70. Shipman, W.D., D.C. Dasoveanu, and T.T. Lu, *Tertiary lymphoid organs in systemic autoimmune diseases: pathogenic or protective?* F1000Res, 2017. **6**: p. 196.

71. Aydin, O., et al., *Immunohistological analysis of mast cell numbers in the intratumoral and peritumoral regions of prostate carcinoma compared to benign prostatic hyperplasia.* Pathol Res Pract, 2002. **198**(4): p. 267-71.

72. Globa, T., et al., *Mast cell phenotype in benign and malignant tumors of the prostate.* Pol J Pathol, 2014. **65**(2): p. 147-53.

73. Boehm, B.J., et al., *Acute bacterial inflammation of the mouse prostate.* Prostate, 2012. **72**(3): p. 307-17.

74. St Sauver, J.L., et al., *Longitudinal association between prostatitis and development of benign prostatic hyperplasia.* Urology, 2008. **71**(3): p. 475-9; discussion 479.

75. Krieger, J.N., S.O. Ross, and D.E. Riley, *Chronic prostatitis: epidemiology and role of infection.* Urology, 2002. **60**(6 Suppl): p. 8-12; discussion 13.

76. Roberts, R.O., et al., *Prevalence of a physician-assigned diagnosis of prostatitis: the Olmsted County Study of Urinary Symptoms and Health Status Among Men.* Urology, 1998. **51**(4): p. 578-84.

77. Done, J.D., et al., *Role of mast cells in male chronic pelvic pain.* J Urol, 2012. **187**(4): p. 1473-82.

78. Bharucha, A.E. and T.H. Lee, *Anorectal and Pelvic Pain.* Mayo Clin Proc, 2016. **91**(10): p. 1471-1486.

79. Alexander, R.B., F. Brady, and S. Ponniah, *Autoimmune prostatitis: evidence of T cell reactivity with normal prostatic proteins.* Urology, 1997. **50**(6): p. 893-9.

80. Siegel, R.L., K.D. Miller, and A. Jemal, *Cancer statistics, 2020.* CA Cancer J Clin, 2020. **70**(1): p. 7-30.

81. McNeal, J.E., *Regional morphology and pathology of the prostate.* Am J Clin Pathol, 1968. **49**(3): p. 347-57.

82. Fletcher, C.D.M., *Diagnostic histopathology of tumors*. 1995, Edinburgh ; New York: Churchill Livingstone.

83. Lawson, D.A., et al., *Prostate stem cells and prostate cancer.* Cold Spring Harb Symp Quant Biol, 2005. **70**: p. 187-96.

84. Zhang, D., et al., *Stem cell and neurogenic gene-expression profiles link prostate basal cells to aggressive prostate cancer.* Nat Commun, 2016. **7**: p. 10798.

85. Ao, M., et al., *Cross-talk between paracrine-acting cytokine and chemokine pathways promotes malignancy in benign human prostatic epithelium.* Cancer Res, 2007. **67**(9): p. 4244-53.

86. Kumar, M.P., et al., *Analysis of Single-Cell RNA-Seq Identifies Cell-Cell Communication Associated with Tumor Characteristics.* Cell Rep, 2018. **25**(6): p. 1458-1468 e4.

87. Cabello-Aguilar, S., et al., *SingleCellSignalR: inference of intercellular networks from single-cell transcriptomics.* Nucleic Acids Res, 2020. **48**(10): p. e55.

88. Lukacs, R.U., et al., *Isolation, cultivation and characterization of adult murine prostate stem cells.* Nat Protoc, 2010. **5**(4): p. 702-13.

89. Shi, X., et al., *Prostate progenitor cells proliferate in response to castration.* Stem Cell Res, 2014. **13**(1): p. 154-63.

90. Montgomery, R.B., et al., *Maintenance of intratumoral androgens in metastatic prostate cancer: a mechanism for castration-resistant tumor growth.* Cancer Res, 2008. **68**(11): p. 4447-54.

91. Ammirante, M., et al., *B-cell-derived lymphotoxin promotes castration-resistant prostate cancer.* Nature, 2010. **464**(7286): p. 302-5.

92. Shafi, A.A., A.E. Yen, and N.L. Weigel, *Androgen receptors in hormone-dependent and castration-resistant prostate cancer.* Pharmacol Ther, 2013. **140**(3): p. 223-38.

93. Koivisto, P., et al., *Androgen receptor gene and hormonal therapy failure of prostate cancer.* Am J Pathol, 1998. **152**(1): p. 1-9.

94. Grivennikov, S.I., F.R. Greten, and M. Karin, *Immunity, inflammation, and cancer.* Cell, 2010. **140**(6): p. 883-99.

95. Vital, P., P. Castro, and M. Ittmann, *Oxidative stress promotes benign prostatic hyperplasia.* Prostate, 2016. **76**(1): p. 58-67.

96. Kramer, G., D. Mitteregger, and M. Marberger, *Is benign prostatic hyperplasia (BPH) an immune inflammatory disease?* Eur Urol, 2007. **51**(5): p. 1202-16.

97. De Marzo, A.M., et al., *Proliferative inflammatory atrophy of the prostate: implications for prostatic carcinogenesis.* Am J Pathol, 1999. **155**(6): p. 1985-92.

98. De Marzo, A.M., Y. Nakai, and W.G. Nelson, *Inflammation, atrophy, and prostate carcinogenesis.* Urol Oncol, 2007. **25**(5): p. 398-400.

99. De Marzo, A.M., et al., *Inflammation in prostate carcinogenesis.* Nat Rev Cancer, 2007. **7**(4): p. 256-69.

100. Pages, F., et al., *Immune infiltration in human tumors: a prognostic factor that should not be ignored.* Oncogene, 2010. **29**(8): p. 1093-102.

101. Woo, J.R., et al., *Tumor infiltrating B-cells are increased in prostate cancer tissue.* J Transl Med, 2014. **12**: p. 30.

102. Nelson, B.H., *CD20+ B cells: the other tumor-infiltrating lymphocytes.* J Immunol, 2010. **185**(9): p. 4977-82.

103. Garcia-Hernandez, M.L., et al., *A Unique Cellular and Molecular Microenvironment Is Present in Tertiary Lymphoid Organs of Patients with Spontaneous Prostate Cancer Regression.* Front Immunol, 2017. **8**: p. 563.

104. Yamakoshi, Y., et al., *Immunological potential of tertiary lymphoid structures surrounding the primary tumor in gastric cancer.* Int J Oncol, 2020. **57**(1): p. 171-182.

105. Schupp, J., et al., *Targeting myeloid cells in the tumor sustaining microenvironment.* Cell Immunol, 2019. **343**: p. 103713.

106. Taverna, G., et al., *Mast cells as a potential prognostic marker in prostate cancer.* Dis Markers, 2013. **35**(6): p. 711-20.

107. Lee, S.W.H., E.M.C. Chan, and Y.K. Lai, *The global burden of lower urinary tract symptoms suggestive of benign prostatic hyperplasia: A systematic review and meta-analysis.* Sci Rep, 2017. **7**(1): p. 7984.

108. Nickel, J.C., et al., *The relationship between prostate inflammation and lower urinary tract symptoms: examination of baseline data from the REDUCE trial.* Eur Urol, 2008. **54**(6): p. 1379-84.

109. Barry, M.J., *Epidemiology and natural history of benign prostatic hyperplasia.* Urol Clin North Am, 1990. **17**(3): p. 495-507.

110. Izumi, K., et al., *Androgen receptor roles in the development of benign prostate hyperplasia.* Am J Pathol, 2013. **182**(6): p. 1942-9.

111. Vignozzi, L., et al., *Antiinflammatory effect of androgen receptor activation in human benign prostatic hyperplasia cells.* J Endocrinol, 2012. **214**(1): p. 31-43.

112. Cohen, P., et al., *Insulin-like growth factor axis abnormalities in prostatic stromal cells from patients with benign prostatic hyperplasia.* J Clin Endocrinol Metab, 1994. **79**(5): p. 1410-5.

113. Luo, J., et al., *Gene expression signature of benign prostatic hyperplasia revealed by cDNA microarray analysis.* Prostate, 2002. **51**(3): p. 189-200.

114. Vignozzi, L., et al., *Fat boosts, while androgen receptor activation counteracts, BPH-associated prostate inflammation.* Prostate, 2013. **73**(8): p. 789-800.

115. Nickel, J.C., *Prostatic inflammation in benign prostatic hyperplasia - the third component?* Can J Urol, 1994. **1**(1): p. 1-4.

116. Kramer, G. and M. Marberger, *Could inflammation be a key component in the progression of benign prostatic hyperplasia?* Curr Opin Urol, 2006. **16**(1): p. 25-9.

117. Delongchamps, N.B., et al., *Evaluation of prostatitis in autopsied prostates--is chronic inflammation more associated with benign prostatic hyperplasia or cancer?* J Urol, 2008. **179**(5): p. 1736-40.

118. Fibbi, B., et al., *Chronic inflammation in the pathogenesis of benign prostatic hyperplasia.* Int J Androl, 2010. **33**(3): p. 475-88.

119. Steiner, G., et al., *Phenotype and function of peripheral and prostatic lymphocytes in patients with benign prostatic hyperplasia.* J Urol, 1994. **151**(2): p. 480-4.

120. Norstrom, M.M., et al., *Progression of benign prostatic hyperplasia is associated with pro-inflammatory mediators and chronic activation of prostate-infiltrating lymphocytes.* Oncotarget, 2016. **7**(17): p. 23581-93.

121. Konig, J.E., et al., *Analysis of the inflammatory network in benign prostate hyperplasia and prostate cancer.* Prostate, 2004. **58**(2): p. 121-9.

122. Kramer, G., et al., *Increased expression of lymphocyte-derived cytokines in benign hyperplastic prostate tissue, identification of the producing cell types, and effect of differentially expressed cytokines on stromal cell proliferation.* Prostate, 2002. **52**(1): p. 43-58.

123. Handisurya, A., et al., *Differential expression of interleukin-15, a pro-inflammatory cytokine and T-cell growth factor, and its receptor in human prostate.* Prostate, 2001. **49**(4): p. 251-62.

124. Steiner, G.E., et al., *Cytokine expression pattern in benign prostatic hyperplasia infiltrating T cells and impact of lymphocytic infiltration on cytokine mRNA profile in prostatic tissue.* Lab Invest, 2003. **83**(8): p. 1131-46.

125. Steiner, G.E., et al., *Expression and function of pro-inflammatory interleukin IL-17 and IL-17 receptor in normal, benign hyperplastic, and malignant prostate.* Prostate, 2003. **56**(3): p. 171-82.

126. Penna, G., et al., *Human benign prostatic hyperplasia stromal cells as inducers and targets of chronic immuno-mediated inflammation.* J Immunol, 2009. **182**(7): p. 4056-64.

127. Colbeck, E.J., et al., *Tertiary Lymphoid Structures in Cancer: Drivers of Antitumor Immunity, Immunosuppression, or Bystander Sentinels in Disease?* Front Immunol, 2017. **8**: p. 1830.

128. Xu, W. and J. Banchereau, *The antigen presenting cells instruct plasma cell differentiation.* Front Immunol, 2014. **4**: p. 504.

129. Gordon, S. and P.R. Taylor, *Monocyte and macrophage heterogeneity.* Nat Rev Immunol, 2005. **5**(12): p. 953-64.

130. Martinez, F.O. and S. Gordon, *The M1 and M2 paradigm of macrophage activation: time for reassessment.* F1000Prime Rep, 2014. **6**: p. 13.

131. Orecchioni, M., et al., *Macrophage Polarization: Different Gene Signatures in M1(LPS+) vs. Classically and M2(LPS-) vs. Alternatively Activated Macrophages.* Front Immunol, 2019. **10**: p. 1084.

132. Mould, K.J., et al., *Single cell RNA sequencing identifies unique inflammatory airspace macrophage subsets.* JCI Insight, 2019. **4**(5).

133. Murphy, S.F., A.J. Schaeffer, and P. Thumbikat, *Immune mediators of chronic pelvic pain syndrome.* Nat Rev Urol, 2014. **11**(5): p. 259-69.

134. Wong, L., et al., *Experimental autoimmune prostatitis induces microglial activation in the spinal cord.* Prostate, 2015. **75**(1): p. 50-9.

135. Ou, Z., et al., *Infiltrating mast cells enhance benign prostatic hyperplasia through IL-6/STAT3/Cyclin D1 signals.* Oncotarget, 2017. **8**(35): p. 59156-59164.

136. Kim, J.H., et al., *Proliferation of Prostate Stromal Cell Induced by Benign Prostatic Hyperplasia Epithelial Cell Stimulated With Trichomonas vaginalis via Crosstalk With Mast Cell.* Prostate, 2016. **76**(15): p. 1431-44.

137. Sayed, B.A., et al., *The master switch: the role of mast cells in autoimmunity and tolerance.* Annu Rev Immunol, 2008. **26**: p. 705-39.

138. Walker, M.E., J.K. Hatfield, and M.A. Brown, *New insights into the role of mast cells in autoimmunity: evidence for a common mechanism of action?* Biochim Biophys Acta, 2012. **1822**(1): p. 57-65.

139. Strand, D.W., et al., *Isolation and analysis of discreet human prostate cellular populations.* Differentiation, 2016. **91**(4-5): p. 139-51.

140. Ittmann, M., et al., *Animal models of human prostate cancer: the consensus report of the New York meeting of the Mouse Models of Human Cancers Consortium Prostate Pathology Committee.* Cancer Res, 2013. **73**(9): p. 2718-36.

141. Berry, S.J., et al., *Development of canine benign prostatic hyperplasia with age.* Prostate, 1986. **9**(4): p. 363-73.

142. Steiner, M.S., et al., *The chimpanzee as a model of human benign prostatic hyperplasia.* J Urol, 1999. **162**(4): p. 1454-61.

143. Ittmann, M., *Anatomy and Histology of the Human and Murine Prostate.* Cold Spring Harb Perspect Med, 2018. **8**(5).

144. McAuley, E., et al., *Sox2 Expression Marks Castration-Resistant Progenitor Cells in the Adult Murine Prostate.* Stem Cells, 2019. **37**(5): p. 690-700.

145. Vykhovanets, E.V., et al., *Experimental rodent models of prostatitis: limitations and potential.* Prostate Cancer Prostatic Dis, 2007. **10**(1): p. 15-29.

146. Rudick, C.N., A.J. Schaeffer, and P. Thumbikat, *Experimental autoimmune prostatitis induces chronic pelvic pain.* Am J Physiol Regul Integr Comp Physiol, 2008. **294**(4): p. R1268-75.

147. Gao, Y., et al., *Chronic prostatitis alters the prostatic microenvironment and accelerates preneoplastic lesions in C57BL/6 mice.* Biol Res, 2019. **52**(1): p. 30.

148. Burcham, G.N., et al., *Impact of prostate inflammation on lesion development in the POET3(+)Pten(+/-) mouse model of prostate carcinogenesis.* Am J Pathol, 2014. **184**(12): p. 3176-91.

149. Rivero, V.E., et al., *Non-obese diabetic (NOD) mice are genetically susceptible to experimental autoimmune prostatitis (EAP).* J Autoimmun, 1998. **11**(6): p. 603-10.

150. Rivero, V., C. Carnaud, and C.M. Riera, *Prostatein or steroid binding protein (PSBP) induces experimental autoimmune prostatitis (EAP) in NOD mice.* Clin Immunol, 2002. **105**(2): p. 176-84.

151. Ramsey, C., et al., *Aire deficient mice develop multiple features of APECED phenotype and show altered immune response.* Hum Mol Genet, 2002. **11**(4): p. 397-409.

152. Stegle, O., S.A. Teichmann, and J.C. Marioni, *Computational and analytical challenges in single-cell transcriptomics.* Nat Rev Genet, 2015. **16**(3): p. 133-45.

153. AlJanahi, A.A., M. Danielsen, and C.E. Dunbar, *An Introduction to the Analysis of Single-Cell RNA-Sequencing Data.* Mol Ther Methods Clin Dev, 2018. **10**: p. 189-196.

154. Stoeckius, M., et al., *Simultaneous epitope and transcriptome measurement in single cells.* Nat Methods, 2017. **14**(9): p. 865-868.

155. Gao, S., *Data Analysis in Single-Cell Transcriptome Sequencing*. 2018, Springer New York. p. 311-326.

156. Stuart, T. and R. Satija, *Integrative single-cell analysis.* Nat Rev Genet, 2019. **20**(5): p. 257-272.

157. Stahl, P.L., et al., *Visualization and analysis of gene expression in tissue sections by spatial transcriptomics.* Science, 2016. **353**(6294): p. 78-82.

158. Ramilowski, J.A., et al., *A draft network of ligand-receptor-mediated multicellular signalling in human.* Nat Commun, 2015. **6**: p. 7866.

CHAPTER 2. INFLAMMATION AND CASTRATE PROSTATE AND ORGANOID MORPHOLOGY

Meaghan M Broman, Paula O Cooper, Hsing Hui Wang, Gregory M Cresswell, Timothy L Ratliff

2.1 Abstract

Inflammation is commonly associated with both benign prostatic hyperplasia (BPH) and prostate cancer (PCa) and has been associated with treatment failure in both conditions. Inflammation is hypothesized to contribute to the pathogenesis of BPH and PCa, although the means by which this may occur are not fully understood. It is hypothesized that inflammation-modulated epithelial progenitor cell alterations promote the development and resistance to treatment of both these conditions. In this study, we evaluate the impact of autoimmune-type inflammation on the morphology of the murine prostate and isolated basal progenitor cells under androgen deprived conditions to better understand the behavior of purported progenitor cells and their potential roles in PCa and BPH development and treatment resistance.

Utilizing the Prostate Ovalbumin Expressing Transgenic (POET)-3 mouse model of inducible autoimmune prostatitis, the impact of induced autoimmune inflammation and androgen deprivation on the histomorphology of whole prostates and tissue organoids generated from isolated Lin(CD45/CD31)$^{-}$Sca-1^{+}CD49f^{+} (LSC) basal epithelial cells containing basal progenitor cells was assessed.

Overall, prostatic inflammation promoted basal epithelial and stromal expansion in castrate prostates. Inflammation initially promoted LSC proliferation, which diminished over time. LSC from inflamed prostates generated larger and more organized tissue organoids and diminished the reduction in organoid growth resulting from androgen synthesis inhibition or androgen receptor signaling blockade.

These results indicate alterations in epithelial and stromal morphology and basal epithelial growth and differentiation programs by inflammation that persist for a time after resolution of the initial inflammatory insult or removal from the inflammatory microenvironment. Also, inflammation-

induced alterations promote basal epithelial cell proliferation in the face of androgen signaling blockade, suggesting a role for inflammation-induced alterations in anti-androgen treatment resistance and outgrowth in BPH and PCa.

2.2 Introduction

Prostatic disease is a common affliction among older men. Benign prostatic hyperplasia (BPH) affects approximately half of men over 50 and is the most common cause of lower urinary tract symptoms (LUTS) among older men [1]. Prostate cancer (PCa) is the commonly diagnosed non-cutaneous cancer and the second deadliest cancer type among men [2]. Both BPH and PCa develop under the influence of androgens, and androgen-targeted therapy is a component of treatment for both conditions [3, 4]. However, some patients will experience disease progression despite the diminished activity of androgens, indicating the influence of other factors in driving BPH and PCa cell growth [3, 4]. Inflammation is commonly observed in BPH and PCa lesions and has been associated with the development and progression of both conditions [5-7]. In BPH, where inflammatory infiltrates are commonly associated with the characteristic hyperplastic nodules, the degree of immune cell infiltration has been associated with both increased prostate size and LUTS severity in BPH patients [5, 6]. Also, studies exploring the link between prostatitis and prostate carcinogenesis have demonstrated that inflammation may induce genetic and epigenetic changes in epithelial progenitor cells that promote proliferation and carcinogenesis [8, 9].

The prostate is composed of branching glandular ducts lined by pseudostratified epithelium surrounded by dense fibromuscular stromal tissue [10]. The epithelial compartment is composed of three types of cells: luminal, basal, and rare neuroendocrine cells [10-12]. Secretory luminal cells expressing Keratin 8 (K8), Keratin 18 (K18), and androgen receptor (AR) are arranged in a single layer around the lumen and depend on androgen for their function and survival [12, 13]. A layer of basal epithelial cells expressing Keratin 5 (K5), Keratin 14 (K14), and low to no AR expression separates luminal cells from the epithelial basement membrane [12, 13]. Intermediate-type cells expressing both basal and luminal cell markers are observed in prostate epithelial cell cultures *in vitro* and *in vivo* during development, however they are not typically observed in the normal adult prostate [12, 14-16]. Rare neuroendocrine cells expressing the characteristic

neuroendocrine markers Chromogranin A and Synaptophysin are also present, although the precise function of these cells is unclear [11, 12].

Previous studies have indicated considerable cellular heterogeneity within the luminal and basal epithelial populations, including subsets with stem-like characteristics [17]. Under the influence of androgens, these cells maintain the prostate epithelium through normal cellular turnover and by repair following injury [18]. Lineage tracing studies have demonstrated that in the normal adult prostate, luminal and basal cells are each maintained by separate populations of unipotent progenitor cells [14, 19, 20]. However, basal progenitor cells have been previously shown to be capable of differentiating into luminal cells when luminal cells are lost under pathological conditions such as prostatitis, as well as in experimental conditions such as prostate regeneration assays [8, 21-24].

Normal prostate development, differentiation, function, and cellular turnover occur under the control of androgens [10]. Upon androgen deprivation, either by castration or anti-androgen therapy, the prostate undergoes dramatic involution and atrophy due predominately to extensive luminal cell apoptosis [25]. Basal epithelial cells, which do not require androgens for their maintenance, persist and the proportion of basal cells to luminal cells is increased following castration [26, 27]. Upon reintroduction of androgens, the luminal epithelium is replenished mainly by remaining castration-resistant luminal cells [18]. However, castration-resistant basal progenitor cells retain the ability to regenerate the entire epithelium upon repeated cycles of androgen deprivation and reintroduction [16, 24, 25]. These persisting cells are of special interest for their ability to survive androgen deprivation similar to treatment-resistant BPH cells and castration-resistant prostate cancer (CRPC) cells [14, 28]. As these conditions develop under the influence of androgens and are initially dependent on androgens for growth and survival, treatment typically involves androgen deprivation therapy (ADT) targeting androgen synthesis and/or AR signaling [29]. However, many BPH and PCa patients eventually fail anti-androgen therapy, resulting in the need for surgical intervention for symptomatic BPH or progression to lethal androgen-independent CRPC, respectively [30, 31].

In mice, a population of basal progenitor cells has been previously identified and enriched based on their lineage negative ($CD45/CD31^-$), Stem Cell Antigen-1 (Sca-1) positive CD49f-positive

(Lin$^-$Sca-1$^+$CD49$^+$, LSC) expression [19, 32, 33]. The capacity for self-renewal and differentiation of these cells has been assessed through their ability to form tissue organoids in 3D culture and form prostate tissue in prostate graft assays [24, 32]. Previous studies have demonstrated that less than 1% of enriched LSC have the ability to form organoids, indicating that these progenitor cells compose a small percentage of the epithelial cell population [24]. Additionally, the capacity of LSC for proliferation and self-renewal is enhanced by inflammation [33]. Previous studies have suggested the involvement of certain stem-like epithelial cell subtypes in the development of prostate disease, and it is hypothesized that increased cellular turnover in response to inflammation may contribute to BPH and PCa development by promoting epithelial cell hyperplasia and neoplastic transformation, respectively [8, 34, 35]. As chronic inflammation is commonly observed in BPH and PCa lesions and has been associated with the development and progression of both conditions, it has been hypothesized that inflammation may contribute to resistance to anti-androgen therapy, although how this may occur is not well understood [5, 6, 30, 36, 37]. It is hypothesized that inflammation may contribute to BPH and PCa by promoting progenitor cell survival, growth, and differentiation and resisting the reduction in cell growth and differentiation resulting from androgen synthesis or AR signaling inhibition.

To explore the relationship between prostatic inflammation and prostate disease, the Prostate Ovalbumin Expressing Transgenic (POET)-3 mouse model of inducible autoimmune prostatitis was previously developed [38]. In this model, ovalbumin is expressed under the control of a prostate-specific composite probasin promoter (ARR_2PB) [33, 38]. Prostatitis is induced through the injection of activated ovalbumin-specific T cells. This induces inflammation resembling the chronic abacterial inflammation observed in 90% of diagnosed cases of prostatitis in men [38]. In previous studies using this model, inflammation was shown to induce proliferation and expansion of the LSC population *in vivo* and *in vitro* culture of LSC isolated from inflamed prostates formed larger organoids, as well as a higher percentage of hollow tubule-like organoids compared to LSC from non-inflamed (naïve) prostates [33].

In this current study, we sought to further characterize the impact of *in vivo* inflammation on basal progenitor cell differentiation and growth under androgen deficient conditions in a model of androgen-targeted therapy of BPH and PCa by evaluation of whole prostate and prostate basal cell organoid histomorphology. To assess basal cell growth and differentiation under androgen-

deprived conditions, whole prostates were collected from castrate inflamed and naive POET-3 mice and LSC were isolated from inflamed and naïve POET-3 mouse prostates and cultured under androgen-free conditions. In addition, LSC were also cultured in the presence of the androgen receptor (AR) antagonist Enzalutamide (Enza) or the 5α reductase enzyme inhibitor (5αRI) Dutasteride (Duta) to assess the impact of androgen synthesis and AR inhibition on organoid morphology *in vitro*. Inhibition of androgen synthesis involves blocking the conversion of testosterone to its more active form dihydrotestosterone (DHT) through DHT synthesis pathway enzyme inhibition. 5αRI such as Dutasteride inhibit the activity of the 5αR enzymes Srd5a1, Srd5a2, and Srd5a3 in prostate cells [39]. The AR antagonist Enzalutamide has been used in the treatment of androgen-dependent PCa to block AR nuclear translocation and cellular signaling [40-42]. Overall, inflammation promoted basal epithelial cell hyperplasia and stromal expansion and inflammatory cell infiltration *in vivo* and promoted LSC growth and differentiation *in vitro* in the face of androgen blockade, suggesting a role for inflammation in resistance to ADT.

2.3 Materials and methods

2.3.1 Mice

Prostate ovalbumin expressing transgenic-3 (POET-3) mice (C57BL/6 background) were generated as previous described [38]. $Rag1^{-/-}Thy1.1^{+}$OT-I mice were generated by breeding C57BL/6 $Thy1.1^{+}$ mice (Jackson Laboratories, Bar Harbor, ME) with $Rag1^{-/-}$ mice (a gift from Dr.W.E. Heath, The Walter and Eliza Hall Institute of Medical Research, Melbourne, Australia). All animals were housed and maintained under pathogen free conditions with 12 hour-light/12 hour-dark cycles. All procedures involving mouse welfare have conformed to national rules and Purdue Animal Use and Committee (PACUC) approved protocols.

2.3.2 Induction of Inflammation

Inflammation was induced in POET-3 mice as previously described [38]. In summary, splenocytes were isolated from $Rag1^{-/-}Thy1.1^{+}$OT-I mice, activated by 1μg/mL SIINFEKL (Ova peptide 257-264, American Peptide, Sunnyvale, CA; ovalbumin (chicken) acetate salt H-7738.1000, Bachem, Torrance, CA) and cultured for 48 hours *in vitro*. Activated $Thy1.1^{+}CD8^{+}$ T cells were collected

and purified by Ficoll gradient (Atlanta Biologicals, Lawrenceville, GA). A total of $5x10^6$ purified OT-I cells were transferred into POET-3 mice intravenously to induce inflammation.

2.3.3 Generation of castrate mouse prostates

Prostatitis was induced in 8-12 week-old male POET-3 mice as described above. Mice were castrated 5 days-post-induction of inflammation, along with naïve (non-inflamed) control mice. Whole prostates were harvested at 5, 14, or 28 days post-castration and fixed in 10% neutral buffered formalin (NBF). Fixed prostates were embedded in paraffin and sectioned for hematoxylin and eosin (H&E) and immunohistochemistry (IHC) or immunofluorescence (IF) staining.

2.3.4 In vivo BrdU staining

Inflamed and naïve mice were castrated as described above and injected intraperitoneally with 100ul bromodeoxyuridine (BrdU) (BD Pharmingen, Franklin Lakes, NJ) at 5, 14, or 28 days post-castration. Prostates were harvested 2 hours post-BrdU injection, digested, and processed to a single cell suspension as described above. Cells were stained with Zombie NIR Viability Dye (BioLegend) and antibodies for LSC surface markers using the following antibodies: FITC-CD45 (clone 30-F11, BioLegend), BV605-Sca-1 (clone E13-161.7, BioLegend), PE-CD49f (clone GoH3, BioLegend). Stained samples were fixed in 10% NBF then stained for BrdU using an APC BrdU Flow Kit (BD Pharmingen) according to manufacturer protocols. Stained samples were run on a BD LSR Fortessa Flow Cytometer and analyzed with FloJo software.

2.3.5 Isolation of murine LSC population

LSC population were isolated as previously described (H. H. Wang et al., 2015). In summary, prostates were harvested from male 8-12 week-old naïve and inflamed POET-3 mice, digested and processed to a single cell suspension as described above. To enrich LSC, cells were incubated with the following fluorescence conjugated specific antibodies for 5-10 minutes at 1:100 dilution: APC-Sca-1(clone E13-161.7, BioLegend,), PE-CD49f (clone GoH3, BioLegend), FITC-CD45 (clone 30-F11, BioLegend), and FITC-CD31 (clone MEC13.3, BioLegend). The antibody cocktail included Zombie Violet Viability Dye (BioLegend) at a 1:100 dilution. Live cell sorting was

performed on the BD FACS Aria (BD Biosciences, Franklin Lakes, NJ) under sterile conditions. Isolated cells were then cultured or lysed in TRK lysis buffer for RNA isolation and cDNA synthesis.

2.3.6 LSC culture and organoid forming assay

Enriched prostate basal cells were cultured as previously described (H. H. Wang et al., 2015). Dissociated and sorted $Lin^{-}Sca\text{-}1^{+}$ $CD49f^{+}$ prostate cells were suspended in 2:1 Matrigel (Corning, Corning, NY) and PrEGM (Lonza, Basel, Switzerland) and plated in 12-well plates at a density of 10,000 cells per well. Cells were then cultured for 7-10 days in PrEGM with 10nM Enzalutamide (Selleckchem, Houston, TX) or 250nM Dutasteride (Selleckchem). Each treatment included 1:1000 DMSO cultured cells as controls. Organoids were released from Matrigel by incubation in 1 mg/ml Dispase in PrEGM for one hour at 37ºC, then fixed in 10% NBF for 30 minutes, followed by 70% ethanol. Fixed organoids were embedded in Histogel (Thermo Fisher Scientific) then embedded in paraffin prior to sectioning and H&E and IHC or IF staining.

2.3.7 Immunohistochemistry and immunofluorescence

Following paraffin block sectioning and deparaffinization, antigen retrieval was performed in a BioCare decloaking chamber (Biocare Medical, Pacheco, CA) at 95C for 20 minutes. Slides were cooled and transferred to TRIS buffer with Tween 20 detergent (TBST). Slides were stained in a BioCare Intellipath stainer (BioCare Medical) at room temperature. Primary antibodies for IF or IHC included anti-Keratin 5 (1:500, clone, Biolegend), anti-Keratin 8 (1:1000, clone, Biolegend), anti-p63 (1:2400, clone, Abcam, Cambridge, UK), anti-AR (1:500, polyclonal, Abcam).Slides were either digitized using a using a Leica Versa8 whole-slide scanner (Leica, Wetzlar, Germany) or imaged on an Olympus BX51 microscope and Olympus DP80 camera (Olympus Corporation, Tokyo, Japan) and analyzed using ImageScope software (Leica) or ImageJ software (NIH).

2.3.8 RNA isolation, cDNA synthesis and qPCR

RNA was isolated from TRK buffer-lysed cell samples using the Promega Total RNA Kit (Promega, Madison, WI) per manufacturer protocols. cDNA was synthesized using reverse transcriptase (New England Biolabs, Ipswich, MA). qPCR was performed using Quanta PerfeCTa

FastMix II (QuantaBio, Beverly, MA) and commercial probes (Integrated DNA Technologies, Coralville, IA) for the following genes: *Srd5a1*, *Srd5a2*, *Srd5a3*.

2.3.9 Statistical analysis

Statistical analyses were performed using GraphPad Prism v6 software (GraphPad Software Inc., San Diego, CA). A two-tailed student's T test was performed on murine organoid size and type data and for IF quantification of measurements taken from histologic images of inflamed and naïve control and Enza and Duta-treated LSC organoid images. P values less than 0.05 were considered significant.

2.4 Results

2.4.1 Castrate prostate morphology

The POET-3 mouse expresses ovalbumin under the control of the prostate epithelium-specific probasin promoter [38]. Prostatic inflammation is induced through the adoptive transfer of ovalbumin-specific $CD8^+$ T cells (OT-1) isolated from the spleens of $Rag1^{-/-}Thy1.1^+$OT-I mice and activated and expanded *in vitro* by culture with synthetic ovalbumin MHC Class I peptide (SINFEKL) (Fig. 2.1 A) [38]. Through this method, the POET-3 generates reproducible prostate-specific T cell dominant chronic autoimmune-type inflammation that mimics the characteristics of inflammation in most human prostatitis cases and BPH inflammation [37, 38]. To explore the impact of inflammation and castration on prostate morphology, inflammation was induced in POET-3 mice as described above, the mice were castrated and then prostates were examined histologically at 5, 14, or 28 days post-castration.

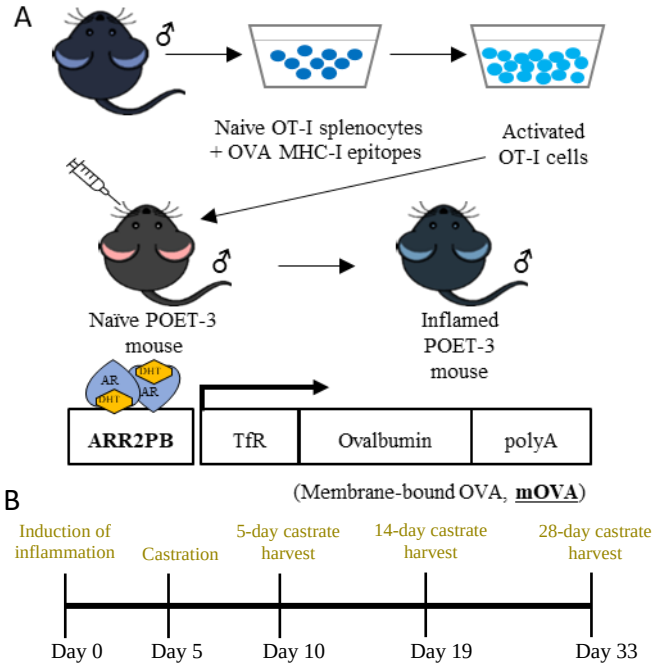

Figure 2.1 (A) Induction of prostatic inflammation in the POET-3 mouse. (B) Schedule of inflammation, castration, and harvest of inflamed and naïve POET-3 mice.

Previous studies in the intact POET-3 mouse model indicate that induced inflammation peaks around 6 days post- OTI injection and declines steadily thereafter [38]. Histologically, induction of inflammation results in infiltration of lymphoid and myeloid cells into the ventral, anterior, and dorsolateral prostate lobes [33, 38]. At 6 days post-injection, the epithelium of intact mouse prostates was thickened and epithelial cells were enlarged with round pale nuclei and abundant cytoplasm (Fig. 2.3). Basal cells expressing the basal epithelial marker K5 were rounded and crowded along the basement membrane (Fig. 2.3). The stromal compartment was expanded by fibroblasts and infiltrated by a mix of lymphoid and myeloid immune cells (Fig. 2.3) [38]. In contrast, epithelial cells of naïve prostates were arranged in a single orderly layer with small dark nuclei (Fig. 2.3). $K5^{+}$ basal cells were small and spaced out along the basement membrane (Fig. 2.3). Consistent with previous studies, these findings indicate that inflammation induces epithelial cell growth and hypertrophy as well as stromal expansion [38].

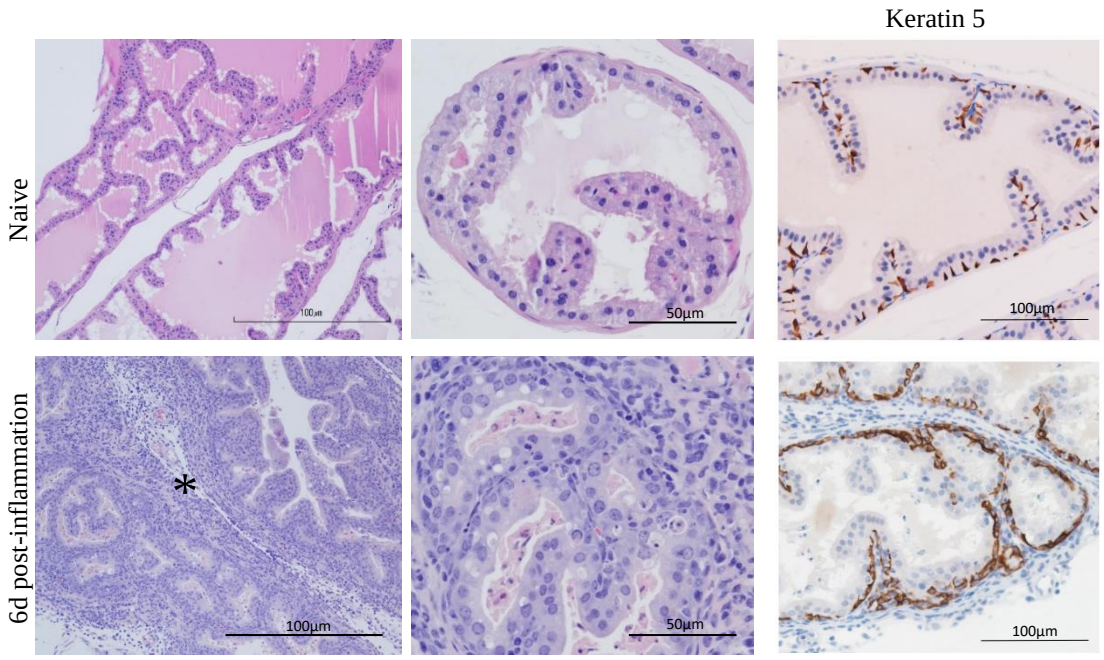

Figure 2.2 Photomicrographs of naïve (top) POET-3 mouse prostate and POET-3 mouse prostate 6 days post OT-I injection (bottom) showing expansion and infiltration of stroma (asterisk) by inflammatory cells (left) and enlargement of epithelial cells (center). Keratin 5-positive basal cells (right) are rounded and prominent in inflamed prostate compared to naïve prostate.

At 5 days post-castration, luminal cells had begun to take on a low columnar to cuboidal shape in contrast to the taller columnar cells of intact mice (Fig. 2.3). In naive prostates, K5-positive basal cells were small and angular with small dark nuclei, while in inflamed prostates basal cells were rounded and prominent with larger rounded nuclei (Fig. 2.3). At 14 days post-castration, the basal layer of inflamed mice remained more pronounced with larger rounded nuclei compared to naïve prostates (Fig. 2.4 A). The stromal compartment of naïve prostates was condensed with immune cells typically arranged in small periglandular and perivascular clusters composed of small lymphocytes and plasma cells, which occasionally formed larger lymphoid aggregates (Fig. 2.4 B). In contrast, the stroma of inflamed castrate mice was relatively hypercellular and expanded by fibroblasts and collagen and infiltrated lymphocytes, plasma cells and myeloid cells (Fig 2.4). These immune cells were generally widely distributed within the stroma or in small periglandular or perivascular lymphoid aggregates (Fig. 2.4). At 28 days post-castration, differences in epithelial and stromal morphology between naïve and inflamed were less prominent (Fig. 2.5). The stroma of inflamed prostates was slightly thickened in some areas, and immune cells in both naïve and

inflamed were generally arranged in small perivascular aggregates with few scattered larger stromal aggregates (Fig. 2.5).

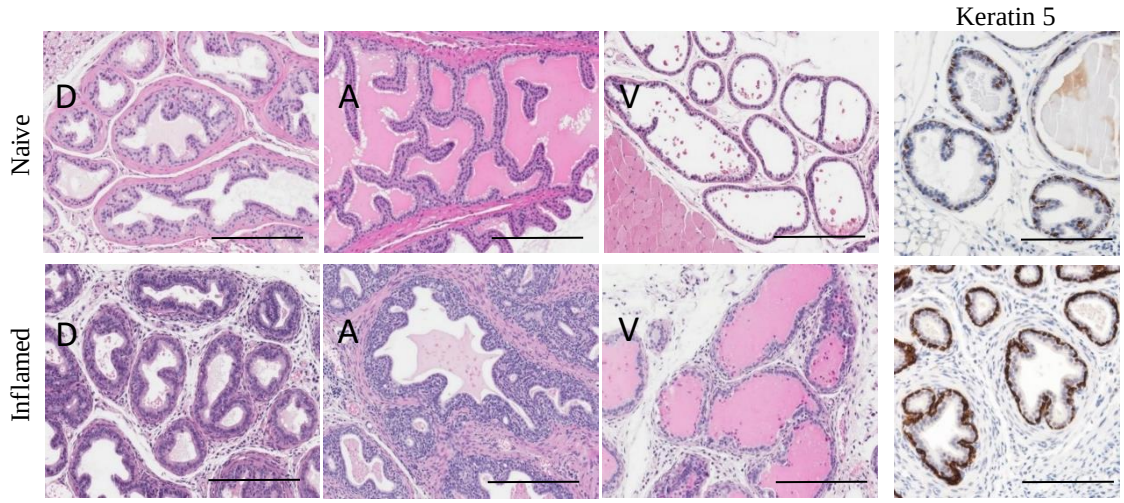

Figure 2.3. H&E and Keratin 5 IHC photomicrographs of naïve (top) and inflamed (bottom) POET-3 mouse prostates 5 days post-castration. D: dorsal lobe, A: Anterior lobe, V: ventral lobe. Scale bar=100µm.

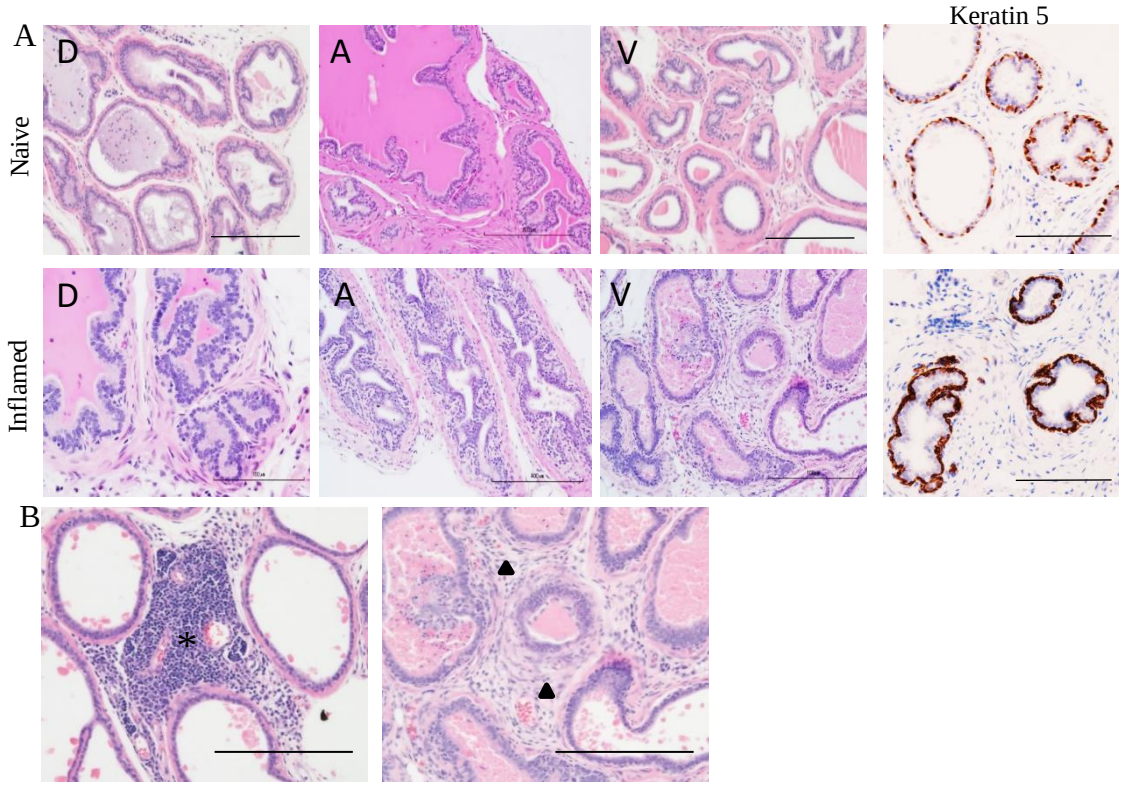

Figure 2.4. (A) H&E and Keratin 5 IHC photomicrographs of naïve (top) and inflamed (bottom) POET-3 mouse prostates 14 days post-castration. D: dorsal lobe, A: Anterior lobe, V: ventral lobe. (B) Naïve (left) and inflamed (right) 14-day castrate prostates showing lymphoid aggregate (asterisk) in naïve prostate and expanded stroma in inflamed prostate (arrowheads). Scale Bar=100µm.

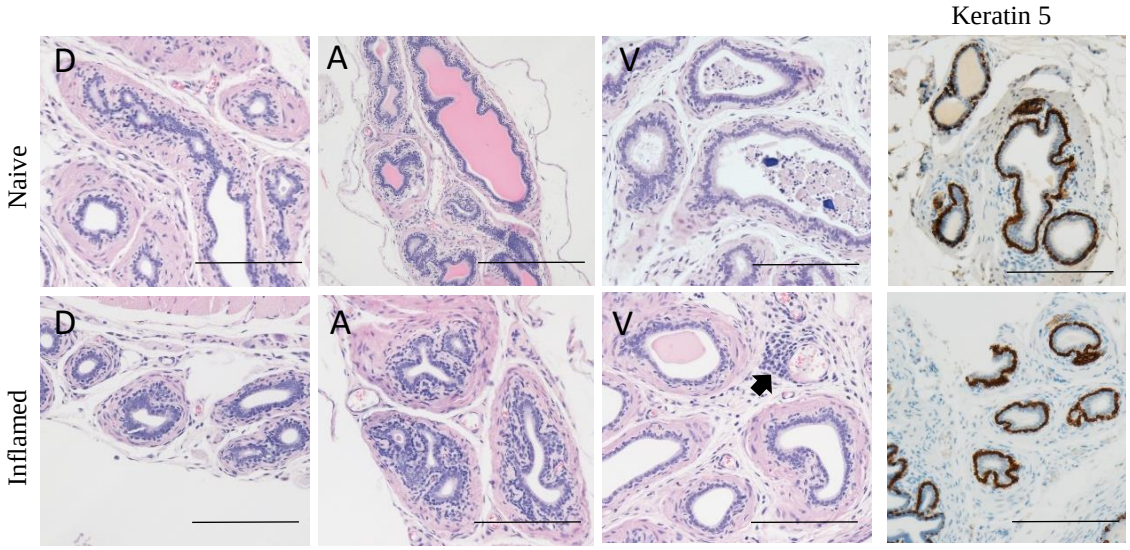

Figure 2.5. H&E and Keratin 5 IHC photomicrographs of naïve (top) and inflamed (bottom) POET-3 mouse prostates 28 days post-castration. The stroma of inflamed prostates was slightly thickened and immune cells were often arranged in small perivascular aggregates (arrow). D: dorsal lobe, A: Anterior lobe, V: ventral lobe. Scale bar=100μm.

Previous studies have shown that induction of inflammation resulted in increased LSC proliferation in intact POET-3 mice as demonstrated by BrdU incorporation [33]. It was hypothesized that induction of inflammation prior to castration would promote LSC proliferation under castrate conditions, as well. To determine the impact of inflammation on LSC proliferation, inflamed and naïve castrate mice were injected with BrdU 2 hours prior to harvest. $BrdU^{+}$ LSC were increased in inflamed 5-day castrate mice compared to naïve 5-day castrate mice, although this increase was not statistically significant (Fig. 2.7). This increase was slightly diminished at 14 days post-castration and further diminished at 28 days post-castration. These findings indicate that induction of inflammation initially boosts LSC proliferation compared to naïve prostates, which is consistent with previous findings in intact POET-3 mice [33]. This effect is diminished over time, suggesting that the initial inflammatory insult largely resolves, consistent with the resolving inflammation

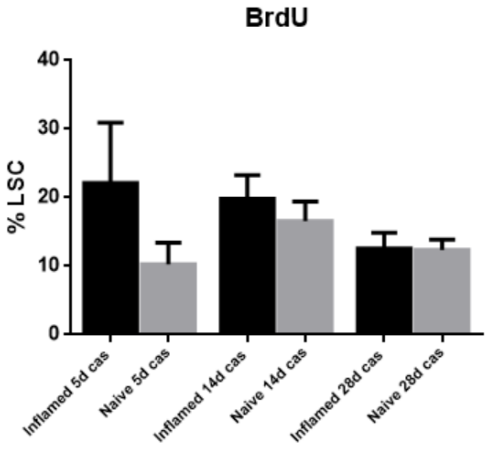

Figure 2.6 . Percentage of BrdU+ LSC in inflamed and naive castrate prostates at 5, 14, and 28 days post-castration.

observed in intact POET-3 mice [38]. However, while LSC proliferation is not significantly different between inflamed and naïve castrate mice at the 14-day post-castration timepoint, alterations in basal morphology were still apparent histologically in inflamed prostates. Epithelial and stromal morphology was generally similar between inflamed and naïve castrate prostates at 28-day post-castration. Few small perivascular lymphoid aggregates were present in the stroma of inflamed and naïve prostates. Overall, these findings indicate that LSC proliferation is initially increased by inflammation and diminishes over time to the level of naïve prostates by 28 days post-castration. Also, inflammation initially alters basal epithelial and stromal morphology which persists at two weeks post-castration and eventually diminishes until inflamed prostates largely resemble naïve prostates by 28 days post-castration. This is indicative of effective resolution of inflammation.

2.4.2 In vivo inflammation promotes in vitro growth of isolated basal cells

Given the impact of induced inflammation on basal epithelial cell morphology *in vivo* as well as previous studies demonstrating expansion and enhanced *in vitro* growth of basal LSC from inflamed POET-3 mice, we sought to further evaluate the impact of *in vivo* inflammation on the growth and differentiation of isolated LSC *in vitro* under androgen deficient conditions [33]. It is hypothesized that prostatic inflammation may promote basal cell growth and basal-to-luminal differentiation in the absence of androgen, modeling basal cell growth and differentiation in the context of anti-androgen therapy. To test this, LSC were isolated from the prostates of inflamed and naïve POET-3 mice and cultured in a 3D Matrigel matrix for 7-10 days under androgen-free conditions to assess organoid morphology and expression of markers associated with basal and luminal differentiation. Previous studies in this mouse model have shown marked expansion of the $Lin^{-}Sca\text{-}1^{+}CD49f^{+}$ LSC basal epithelial population concurrent with an increased $CD45^{+}$ leukocyte population and loss of $Lin^{-}Sca\text{-}1^{+}CD49f^{-}$ luminal cells [33]. Isolated LSC from both inflamed and naïve prostates produced organoids that were typically round or occasionally slightly ovoid (Fig. 2.9). Overall, organoids grown from inflamed LSC were significantly larger in diameter than those from naïve LSC (Fig. 2.10). Both inflamed and naïve LSC generate a mixture of solid and hollow tubule-like organoids, with inflamed LSC generating a significantly higher percentage of hollow type organoids (Fig. 2.10). The tubule-like organoids typically consisted of a variably defined outer layer of basal-like cells and one or multiple layers of large luminal-like

cells surrounding a central lumen (Fig. 2.8 A). The lumina of hollow organoids often contained brightly eosinophilic proteinaceous secretory material (Fig. 2.8 A). The outer basal-type cells were typically cuboidal to slightly flattened with round nuclei and surrounded layers of larger polygonal luminal type cells with usually larger open round to ovoid nuclei with one or more prominent nucleoli and variable amounts of pale eosinophilic cytoplasm (Fig. 2.8 A).

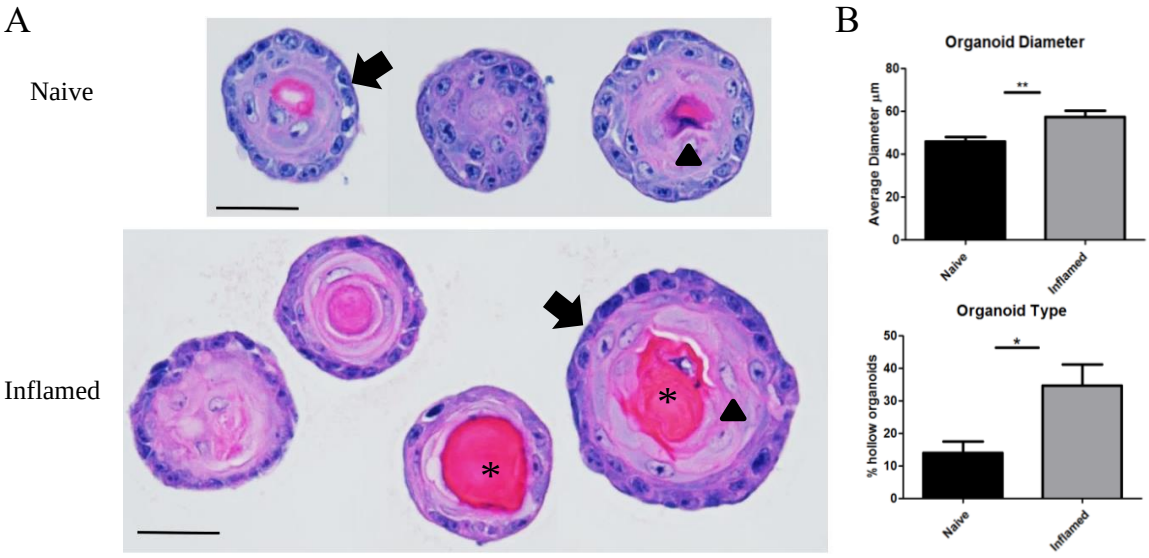

Figure 2.7. (A) Morphology of naïve (top) and inflamed (bottom) LSC organoids, with an outer basal-like layer (arrows) surrounding larger luminal-like cells (arrowheads). Hollow-type organoids formed basal and liminal-like cell layers surrounding a central lumen often containing eosinophilic proteinaceous material (asterisk). (B) Inflamed organoids were significantly larger and formed significantly more hollow-type organoids.

Consistent with previous observations, culture of LSC from inflamed mice resulted in an overall greater proportion of hollow tubule-type organoids to solid-type organoids compared to naïve LSC cultures (Fig. 2.8 B) [33]. Inflamed organoids usually had a more distinct basal-like cell layer around the outer edge and larger luminal-type cells with abundant cytoplasm toward the center (Fig. 2.8 A). In contrast, naïve organoids were overall significantly smaller (P=0.0007) with a significantly greater proportion of solid organoids (P=0.0166) (Fig. 2.8 B). The basal-like cell layer was generally less distinct compared to inflamed organoids (Fig. 2.8 A). Expression of the basal cell marker p63 was consistently seen in both naïve and inflamed organoids (Fig. 2.9 A). p63 staining was strongest among basal-type cells at the periphery of organoids, and generally present throughout solid organoids but diminished or lost in luminal-type cells at the centers of larger or hollow-type organoids (Fig. 2.9 A). Co-immunofluorescence staining with the basal K5 and the luminal K8 found that both naïve and inflamed organoids variably expressed both K5 and

K8, reminiscent of a basal/luminal intermediate transit amplifying cell (TAC) phenotype (Fig. 2.9 A) [12]. While average K5 expression did not differ significantly between naïve and inflamed organoids, there was a significant (P=0.0412) increase in average K8 expression among inflamed organoids (Fig. 2.9, B). Previous studies by Cooper (2020) showed that AR is induced by inflammation in the POET-3 mouse model and demonstrated increased nuclear AR staining in inflamed LSC organoids compared to naïve (manuscript in preparation) [43]. This indicates that AR is active in inflamed organoids and is likely driving the enhanced differentiation of inflamed organoids in the absence of androgen in culture [43].

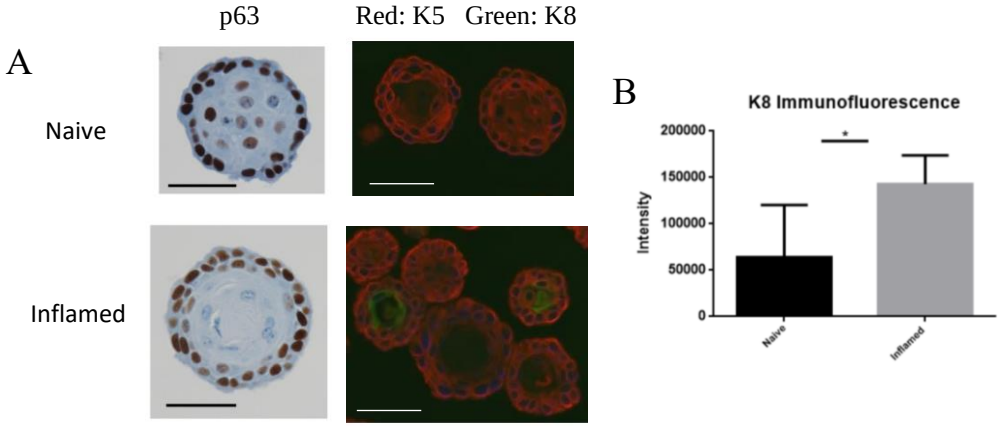

Figure 2.8. (A) p63 IHC and Keratin 5 (K5) and Keratin 8 (K8) immunofluorescence in naïve (top) and inflamed (bottom) LSC organoids. Scale bar=50μm. (B) Quantification of K8 immunofluorescence.

Overall, *in vivo* inflammation promoted the formation of multilayered organoids from isolated LSC reminiscent of the *in vivo* prostate glandular organization and promoted differentiation into cells with luminal-like morphology expressing the luminal marker K8 and loss of basal marker p63 expression. K8-expressing cells generally retained some K5 expression suggesting that full basal-to luminal differentiation is not complete, which may relate to diminished AR signaling required for luminal cell differentiation [27]. These findings indicate that induction of inflammation *in vivo* alters basal progenitor cells in a manner that promotes expansion and differentiation that persists even after these cells are removed from the inflammatory prostate microenvironment.

2.4.3 In vivo inflammation promotes basal cell organoid growth following androgen receptor signaling and androgen synthesis inhibition

To assess the impact of *in vivo* inflammation on basal cell organoid morphology in the face of AR signaling inhibition, isolated LSC were cultured with the AR antagonist Enza. To initiate AR signaling, AR binds to testosterone or DHT in the cytoplasm then translocates to the nucleus where it binds to androgen response elements in the DNA and activates gene transcription [40]. Enza inhibits DHT binding to AR and subsequent nuclear translocation and DNA binding [41]. LSC were sorted and plated as described previously with the addition of 10uM Enzalutamide starting at day 1 of culture and continuing for 7-10 days. Consistent with previous studies, Enza treatment reduced organoid formation, although this difference did not reach statical significance in this study (Fig. 2.10 A) [43]. Enza treatment resulted in significantly smaller organoids from naïve LSC compared to inflamed LSC, with an average 23.0% decrease in diameter in inflamed vs 30.1% decrease in naïve Enza-treated LSC compared to untreated controls. The percentage of hollow organoids generated from inflamed LSC varied but was overall higher, although not significantly different from naïve Enza-treated LSC organoids (Fig. 2.10 A).

Morphologically, the basal-like cell layer of naïve Enza-treated organoids was usually present, although generally less distinct compared to inflamed Enza-treated organoids which more often had more distinct basal-type and luminal-type cell layers (Fig. 2.10 B). Similar to untreated organoids, all organoids expressed p63, particularly in the outer basal-like layer with diminished expression in the central luminal-type cells (Fig. 2.10 C). Inflamed Enza-treated organoids variably expressed weak nuclear AR staining while AR staining was absent in naïve Enza-treated organoids, suggesting AR activity in inflamed organoids (Fig. 2.10 C). Similar to control organoids, naïve and inflamed Enza-treated organoids demonstrated similar K5 expression by IF but significantly ($p=0.0263$) higher K8 expression in inflamed organoids compared to naïve (Fig. 2.10 D). Also, Enza treatment resulted in an average 30.3% decrease in K8 IF intensity in naïve organoids and an average 3.1% reduction in inflamed organoids compared to DMSO controls, although the differences in K8 IF intensity between naïve treated and nontreated organoids and between inflamed treated and non-treated organoids did not reach statistical significance due to limited organoid numbers following Enza treatment (Fig. 2.10 E). Overall, inflammation partially abrogated the growth reduction induced by Enza treatment. Also, the presence of AR staining in

Enza-treated organoids suggests that inflammation can promote AR nuclear localization and possibly activity despite AR antagonism.

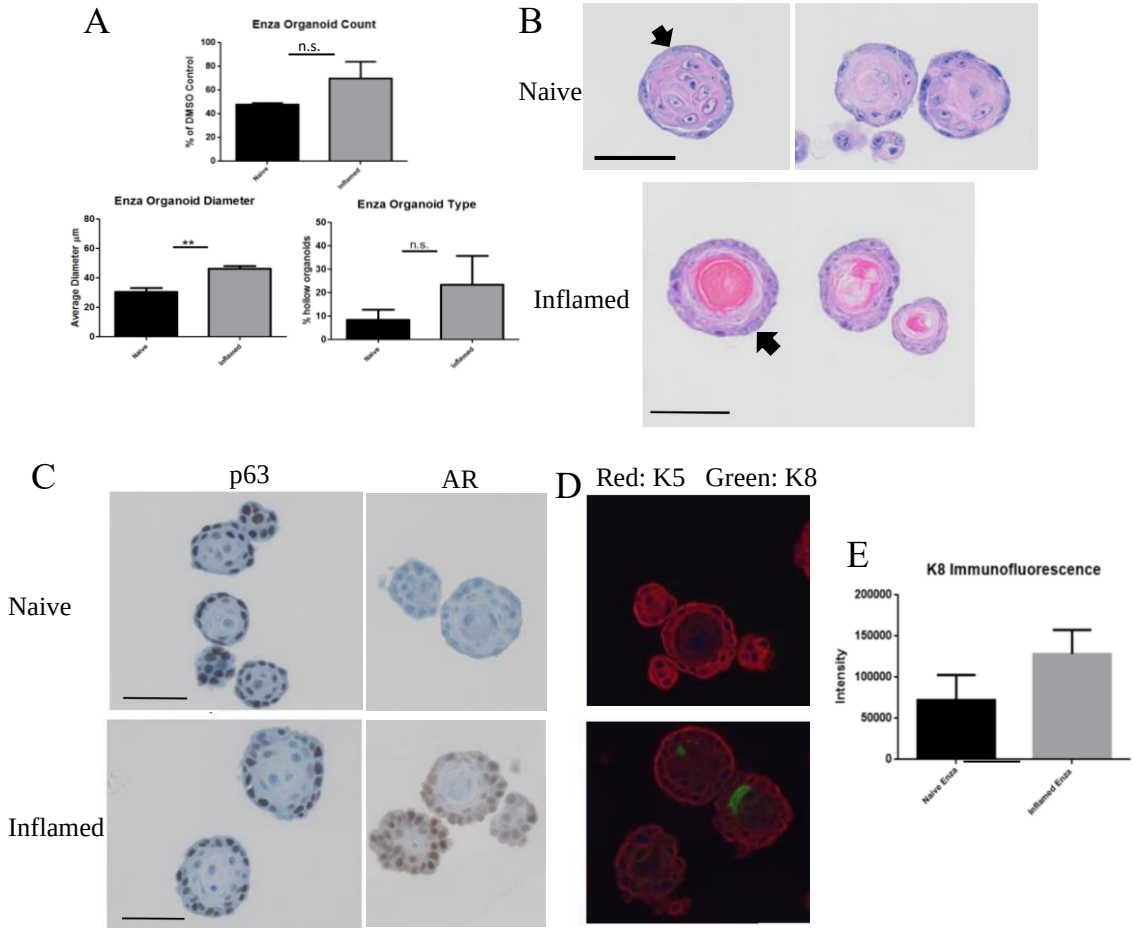

Figure 2.9. (A) Comparison of organoid number, diameter, and type between Enza-treated LSC organoids. (B) Organoids derived from naïve (top) and inflamed (bottom) LSC treated with Enza. Inflamed organoids formed more prominent basal-like layers (arrows). (C) p63 and AR and (D) K5 and K8 expression in naïve and inflamed Enza-treated LSC organoids. (E) Quantification of K8 immunofluorescence.

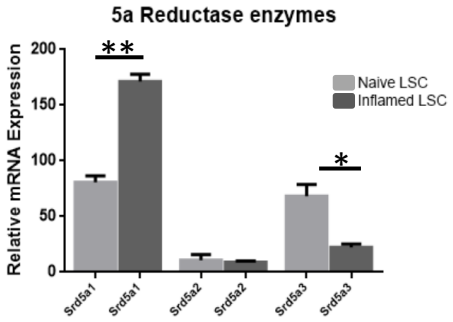

Figure 2.10 . Expression of 5αR enzyme genes in isolated naïve and inflamed LSC.

To assess the impact of *in vivo* inflammation on basal cell organoid morphology following androgen synthesis inhibition, LSC were cultured in the presence of the 5αRI Duta, which inhibits the activity of three 5αR enzymes (*Srd5a1, Srd5a2, Srd5a3*) of the DHT synthesis pathway [39]. Gene expression of *Srd5a1* was significantly (P=0.0093) elevated in inflamed LSC

compared to naïve (Fig. 2.11). Interestingly, expression of *Srd5a3* was significantly (P=0.0496) reduced in inflamed LSC. *Srd5a1* expression is typically associated with the epithelium, and its expression in epithelial basal progenitor cells appears to be preferentially enhanced by inflammation.

LSC were sorted and plated as described previously with the addition of 250nM Duta starting at day 1 of culture and continuing for 7-10 days. As with Enza treatment, Duta reduced the overall number of organoids formed in culture. While Duta-treated inflamed and naïve organoids were not significantly different in diameter, Duta treatment significantly reduced the overall number of hollow-type organoids produced from naïve LSC (P=0.0325) (Fig. 2.12 A). Also, while hollow-type organoids were reduced among inflamed LSC, this reduction was not statistically significant (Fig. 2.12 A). Morphologic differences were similar to those observed with Enza treatment, with a more distinct cuboidal basal-like layer in inflamed vs naïve organoids (Fig. 2.12 B). Both inflamed and naïve Duta-treated LSC organoids expressed p63 and variably had weak nuclear AR expression (Fig. 2.12 C).

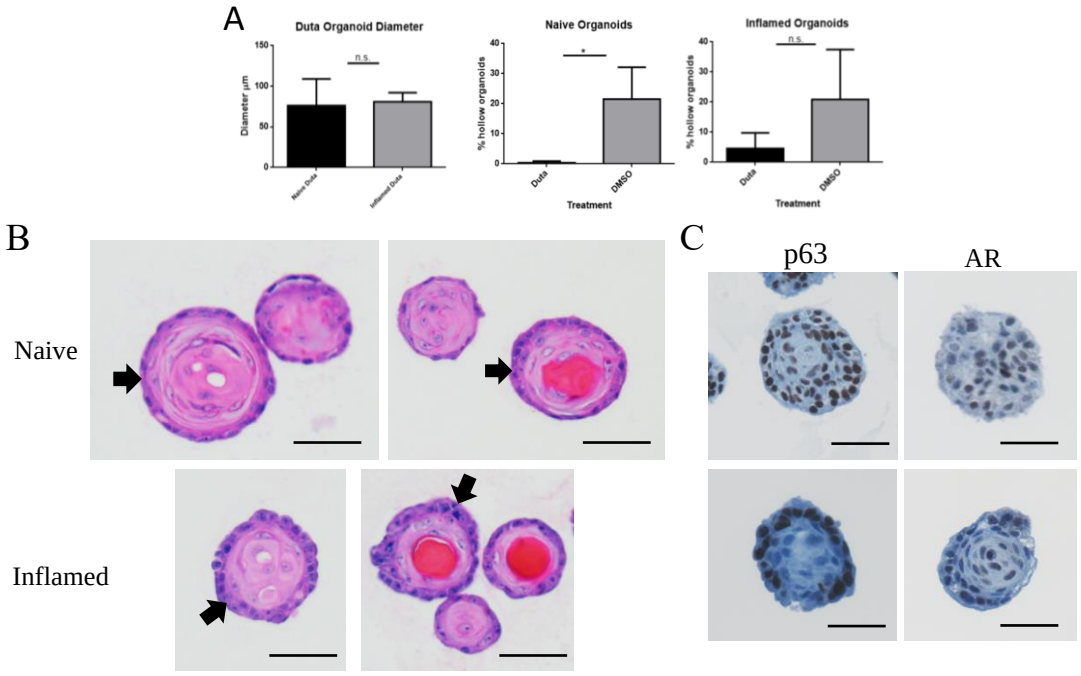

Figure 2.11. (A) Diameter of naïve and inflamed Duta treated LSC organoids was not significantly different, and Duta treatment significantly reduced naïve hollow-type organoids but reduction in inflamed hollow-type organoids was not statistically significant. (B) Organoids derived from naïve (top) and inflamed (bottom) LSC cultured with 250nM Duta. Inflamed LSC produced organoids with more prominent basal-like layers (arrows). (C) All organoids had strong p63 staining in outer basal-like cells and often diminished staining in central luminal-like cells. (D) Both naïve and inflamed Duta-treated organoids expressed weak nuclear AR. Scale bar=50µm.

Overall, Enza treatment reduced LSC expansion and growth resulting in smaller organoids compared to DMSO controls, and this reduction was partially counteracted in inflamed LSC. Also, expression of the luminal marker K8 was increased in inflamed LSC-derived organoids. Both Enza and Duta treatment also reduced the formation of hollow-type organoids by naïve LSC. These findings suggest that inflammation may promote an LSC growth program that partially abrogates the decrease in growth and differentiation that occurs following androgen deprivation or AR signaling blockade. This occurrence may mimic the outgrowth of prostate epithelial cells through ADT, suggesting a role for prostatic inflammation in the development of ADT resistance and disease progression.

2.5 Discussion

The purpose of the current study is to evaluate the impact of autoimmune-type inflammation on the growth and morphology of basal epithelial LSC *in vivo* and *in vitro* under androgen deficient conditions mimicking ADT in a mouse model of resolving autoimmune-type prostatic inflammation. Prostate basal epithelial progenitor cells are a hypothesized to contribute to the development of BPH and PCa, both of which develop and progress under the influence of androgens [14, 28, 35, 44, 45]. Previous studies have demonstrated the impact of inflammation on the expansion and differentiation of prostate basal epithelial progenitor cells [8, 33]. As both BPH and PCa develop and progress under the influence of androgens, and current treatment of both conditions typically involves inhibition of androgen synthesis and/or signaling activity [29]. While many patients will initially respond to androgen-targeted treatment, many will eventually progress and require alternative treatment strategies [30, 31]. And while the mechanisms by which therapeutic resistance develops in BPH and PCa are not clear, it is hypothesized that inflammation may contribute to therapeutic resistance.

Cellular turnover and replacement is typically a slow process in the normal adult prostate [13]. However, under certain pathological conditions such as prostatitis, cellular turnover and proliferation may be significantly increased, and this increased turnover may contribute to prostate cell hyperplasia and carcinogenesis [24, 33, 34]. Previous studies by this lab in the POET-3 mouse model described the morphologic changes in the intact mouse prostate following induction of autoimmune-type inflammation, as well as the impact of *in vivo* inflammation on the formation of

tissue organoids generated from isolated $Lin^{-}Sca\text{-}1^{+}CD49f^{+}$ LSC in *in vitro* culture [33, 38, 43]. The purpose of the current study was to evaluate and describe the impact of chronic autoimmune-type inflammation on prostate cellular morphology, differentiation, and growth *in vivo* and *in vitro* following androgen deprivation and androgen signaling blockade. As inflammation is hypothesized to contribute to epithelial cell resistance to androgen deprivation therapy in BPH and PCa, we sought to further explore the impact of inflammation on prostate morphology and on basal epithelial cell survival, growth, and differentiation capabilities in the absence of androgen through histologic evaluation of castrate prostates and isolated basal epithelial cell-derived tissue organoids.

Induction of inflammation prior to castration resulted in increased LSC proliferation and altered basal cell and stromal morphology that persisted after the resolution of the initial inflammatory insult. While differences in LSC proliferation were not apparent between inflamed and naïve prostates by 14 days post-castration, morphologic differences were still apparent, with enlarged and prominent basal epithelial cells and expanded stroma. At 28 days post-castration, morphologic differences were less notable between inflamed and naïve prostates. inflamed and naïve prostates were less notable at 28 days post-castration. These observations are consistent with the resolution of inflammation in the POET-3 mouse, which generally peaks around 6-7 days post-induction and resolves after approximately 14 days in intact mice. Interestingly, while both inflamed and naïve castrate prostates contained small, scattered aggregates of lymphoid cells within the stromal compartment, some 14-day naïve castrate prostates also contained larger, more prominent lymphoid aggregates, some of which resembled organizing lymphoid structures. Lymphoid aggregates and organized lymphoid structures outside of primary and secondary lymphoid organs, referred to as tertiary lymphoid or ectopic lymphoid structures, may arise in response to chronic antigenic stimulation and have been observed in multiple tissues, including the normal aged adult human prostate and in association with BPH and PCa [46, 47]. The precise function and impact of these lymphoid aggregates and structures in either normal or diseased prostates is not fully understood [46, 47]. These structures have been observed in association with various chronic inflammatory conditions such as allograft rejection, autoimmunity, and cancer [47, 48].

Consistent with the previous study by Wang et al (2015), organoids derived from inflamed LSC were significantly larger than those generated from naïve LSC, indicative of increased proliferative capacity and organoid forming efficiency of inflamed LSC [33]. Also, inflamed LSC formed a

greater proportion of hollow tubule-like organoids to solid organoids, suggesting enhanced capacity for differentiation and organization into prostate glandular-like structures [33]. In this study, we observed that in addition to forming overall larger and more hollow-type organoids, inflamed LSC generally formed organoids with more distinct outer basal-like and inner luminal-like cell layers and more highly expressed the luminal marker K8, suggesting an increased differentiation capacity and ability to recapitulate the prostate acinar structure. Additionally, Cooper et al (2020) demonstrated that AR expression was increased in inflamed LSC and inflamed LSC organoids showed increased nuclear AR expression compared to naïve [43]. As AR is required for luminal to basal differentiation, K8 expression along with increased nuclear AR expression by IHC indicate that the maintenance of AR activity is enhanced in the inflamed organoids despite androgen deprivation and AR inhibition. In all, these findings suggest that the enhanced proliferative and differentiation capacity of inflamed LSC is due at least in part to the impact of inflammation on AR expression and activity. Currently, the mechanism by which inflammation drives AR expression and nuclear localization is not yet known. While the mechanisms which drive nuclear localization in the absence of androgen have not been fully identified, previous studies have suggested various adaptive pathways in CRPC that may promote anti-androgen treatment failure [49, 50]. For example, studies have indicated roles for specific AR domains and co-factor interactions in directing AR localization in CRPC [49]. Other proposed mechanisms include emergence of AR splice variants or AR mutations. Another potential mechanism observed in CRPC is stabilization of the AR protein, which has previously been demonstrated in inflamed POET-3 LSC [43, 50]. The precise mechanisms by which inflammation promotes AR stability and nuclear localization have yet to be elucidated.

Following *in vitro* treatment with the androgen receptor antagonist Enzalutamide, LSC capacity for proliferation and growth was diminished as demonstrated by overall smaller and often less well-organized organoids lacking central lumina. Inflamed LSC again generated significantly larger organoids with significantly greater expression of K8. Previous studies have suggested that castration-resistant tumors may escape ADT through intratumoral expression of androgen synthesis enzymes [39, 51, 52]. Increased expression of *Srd5a1* in inflamed LSC may suggest that inflammation drives DHT enzyme upregulation which may contribute to ADT resistance. The reduction in hollow-type organoids generated from naive LSC following Duta treatment suggests

that increased *Srd5a1* expression and DHT synthesis by inflamed LSC may be partly responsible for enhanced differentiation of inflamed LSC organoids.

Isolated prostate epithelial cells from luminal and basal lineages have been previously shown to generate morphologically distinct organoids [19]. Kwon et al (2016) generated organoids from isolated murine prostate epithelial lineages in culture medium containing specific growth factors with and without DHT and observed that epithelial progenitor cells from different lineages produced distinct organoid types, which were classified into four types (Type I-Type IV) based on morphology and AR, K8, K5, and p63 staining [19]. In that study, naïve basal cells produced predominately $AR^{+}K5^{+}K8^{+}p63^{+}$ Type I organoids and a small fraction of Type II organoids with an outer layer of $K5^{+}$ cells and inner $K8^{+}$ cells around a lumen [19]. These organoids also expressed nuclear AR, which was diminished in organoids cultured in the absence of DHT [19]. In this current study, organoids produced from isolated LSC most resembled a combination of Type I and Type II-like organoids with a greater proportion of the more stratified Type II-like organoids from inflamed LSC compared to naïve LSC. While *in vitro* androgen deprivation diminished organoid nuclear AR expression, inflamed LSC organoids and Duta-treated organoids variably expressed low levels of nuclear AR. It should be noted that in addition to DHT, the culture medium used in the Kwon study included multiple specific growth factors (Noggin, EGF 50 ng/mL, R-spondin1, TGF-β/Alk inhibitor A83-01, and Y-27632), which were not included in the PrEGM medium used in the current study. Therefore, morphologic comparison between the previous and current studies is not exact [19, 33].

The prostate epithelium displays significant heterogeneity beyond the general luminal and basal identities and include subsets with properties of epithelial progenitor cells [17]. While prostate basal epithelial cells are generally identified by their $K5^{+}K14^{+}p63^{+}AR^{low/-}$ expression, basal progenitor cell subsets have been identified by various markers in various studies, including Sca-1 and CD49f [16, 19, 21, 25, 32-34]. Sca-1 is expressed by various murine cell types in many tissues and has been used in combination with other markers for the enrichment of stem and progenitor cells from various tissue types [53]. In mice, Sca-1 has been used to identify both basal and luminal progenitor cells in the adult prostate [19, 21, 33, 34, 54]. CD49f, also known as Integrin α6, has been previously identified in various epithelial and mesenchymal stem cell populations [55]. CD49f is also a conserved stem cell marker between rodents and humans, as

well as various other mammalian species [55]. While Sca-1 is expressed by both basal and luminal progenitors, CD49f expression is associated with basal epithelial progenitors [19, 21, 33]. In the human prostate where Sca-1 is not expressed, a population of basal progenitor cells considered equivalent to murine LSC has been identified and enriched based on their expression of epithelial cell adhesion molecule (EpCAM) and CD49f and negative expression of luminal cell marker CD26 [56]. Various studies have identified markers that have been used to identify and isolate prostate basal stem/progenitor populations, including the pro-survival apoptosis regulator B-cell lymphoma 2 (Bcl-2), the cell surface glycoprotein CD44, Trop2, CD133, c-kit/CD117, and Zeb1 [16, 25, 34, 45, 57, 58]. L. Wang et al (2015) proposed a four-marker set which included Sca-1, CD133, CD44, and c-kit/CD117 for the isolation of basal progenitor cells [34]. Also, various other markers such as Nkx3.1, Lrg5, and the transcription factor Sox2 have been associated with populations of castration-resistant prostate epithelial cells [59-61].

It has been hypothesized that populations of castration-resistant progenitor cells are responsible for prostate epithelial regeneration following post-castration androgen reintroduction, and previous studies have shown that populations of luminal and basal progenitor cells persist and retain the ability to regenerate the epithelium upon restoration of androgen stimulation [16, 24, 25]. Some progenitor cells may also proliferate following castration [57]. More recently, Karthaus et al. (2020) identified subpopulations of luminal cells with enhanced regenerative abilities that persisted following androgen deprivation and suggested that these cells were largely responsible for regeneration of luminal cells following androgen reintroduction [18]. These findings suggest that epithelial regeneration and maintenance may be a more complex process than once thought and are significantly impacted by microenvironmental factors such as inflammation and androgen status, with likely implications for the cellular origins and pathogenesis of BPH and PCa.

The mechanisms by which therapeutic resistance develops in BPH and PCa are not clear. Potential mechanisms proposed by previous studies include AR mutations or gene amplification, emergence of AR splice variants, alternate AR-dependent gene activation, or intracrine androgen production by tumor cells [31, 39, 62, 63]. Inflammatory mediators released by immune cells may drive production of cytokines, chemokines, growth factors, and reactive oxygen and nitrogen species which in turn may promote cellular proliferation and transformation as well as recruit additional immune cells to the microenvironment [64-67]. Previous studies have shown that the capacity of

basal progenitor cells for proliferation and self-renewal is enhanced by inflammation, and it is hypothesized that chronic prostatic inflammation may contribute to BPH and/or PCa treatment resistance by promoting epithelial progenitor proliferation and survival in the face of androgen deprivation and AR signaling inhibition [8, 24, 33, 34].

This study describes the impact of inflammation on castrate prostate and isolated basal progenitor cells in a mouse model of autoimmune-type prostatitis [38]. Several mouse models have been developed to investigate the relationship of prostatic inflammation to prostate disease, many of which involve bacterial inoculation to induce inflammation [8, 34]. However, in most human prostatitis cases, a bacterial cause is not identified, and the inflammatory process is suspected to be autoimmune in nature [33, 38]. Thus, the POET-3 mouse model was developed to more closely mimic the abacterial chronic autoimmune-type inflammation observed in most human prostatitis patients [38]. With this model, the impact of autoimmune-type inflammation on various prostate epithelial, stromal, and immune cell populations can be investigated [33, 38, 68]. The findings of this study and previous studies by this lab using the POET-3 mouse indicate that autoimmune-type inflammation can promote basal cell proliferation *in vivo*, and this enhanced growth capacity persists even when the initial inflammatory insult has resolved or when these cells are removed from the inflammatory microenvironment, indicating a lasting alteration in the basal epithelial cell growth program [33]. Also, while reduction in AR signaling by treatment with either the AR antagonist Enzalutamide or the 5αRI Dutasteride diminished LSC growth capacity *in vitro*, prior *in vivo* inflammation can partially abrogate this effect, suggesting a role for inflammation in resistance to anti-androgen treatment.

One limitation to the POET-3 mouse in modeling BPH inflammation is that unlike the resolving inflammation in this model, the inflammation of BPH fails to resolve and often progresses over time. Similarly, the impact on cell proliferation and morphology induced in the POET-3 mouse also is diminished in conjunction with resolution of inflammation, while in BPH prostatic enlargement and cellular expansion progress. It is hypothesized that the continued inflammatory stimulation of prostate epithelial and stromal cells would promote continued proliferation and progressive prostatic enlargement despite androgen-targeted therapy intended to limit cell growth. The results of the current study demonstrate the promotion of basal epithelial cell proliferation and differentiation by a single inflammatory insult, and it is surmised that repeated or continuous

inflammatory stimulation would further promote these effects potentially involving AR. The precise mechanisms by which inflammation promotes cell proliferation, differentiation, and therapeutic resistance in BPH and PCa are not yet fully elucidated, and further studies are needed to uncover the molecular mechanisms connecting chronic inflammation and BPH and PCa.

2.6 References

1. Fibbi, B., et al., *Chronic inflammation in the pathogenesis of benign prostatic hyperplasia.* Int J Androl, 2010. **33**(3): p. 475-88.

2. Siegel, R.L., K.D. Miller, and A. Jemal, *Cancer statistics, 2020.* CA Cancer J Clin, 2020. **70**(1): p. 7-30.

3. Nicholson, T.M. and W.A. Ricke, *Androgens and estrogens in benign prostatic hyperplasia: past, present and future.* Differentiation, 2011. **82**(4-5): p. 184-99.

4. Izumi, K., L. Li, and C. Chang, *Androgen receptor and immune inflammation in benign prostatic hyperplasia and prostate cancer.* Clin Investig (Lond), 2014. **4**(10): p. 935-950.

5. Nickel, J.C., et al., *Chronic Prostate Inflammation is Associated with Severity and Progression of Benign Prostatic Hyperplasia, Lower Urinary Tract Symptoms and Risk of Acute Urinary Retention.* J Urol, 2016. **196**(5): p. 1493-1498.

6. Robert, G., et al., *Inflammation in benign prostatic hyperplasia: a 282 patients' immunohistochemical analysis.* Prostate, 2009. **69**(16): p. 1774-80.

7. St Sauver, J.L., et al., *Longitudinal association between prostatitis and development of benign prostatic hyperplasia.* Urology, 2008. **71**(3): p. 475-9; discussion 479.

8. Kwon, O.J., et al., *Prostatic inflammation enhances basal-to-luminal differentiation and accelerates initiation of prostate cancer with a basal cell origin.* Proc Natl Acad Sci U S A, 2014. **111**(5): p. E592-600.

9. Kwon, O.J. and L. Xin, *Prostate epithelial stem and progenitor cells.* Am J Clin Exp Urol, 2014. **2**(3): p. 209-18.

10. Toivanen, R. and M.M. Shen, *Prostate organogenesis: tissue induction, hormonal regulation and cell type specification.* Development, 2017. **144**(8): p. 1382-1398.

11. Shen, M.M. and C. Abate-Shen, *Molecular genetics of prostate cancer: new prospects for old challenges.* Genes Dev, 2010. **24**(18): p. 1967-2000.

12. Karthaus, W.R., et al., *Identification of multipotent luminal progenitor cells in human prostate organoid cultures.* Cell, 2014. **159**(1): p. 163-175.

13. Schalken, J.A. and G. van Leenders, *Cellular and molecular biology of the prostate: stem cell biology.* Urology, 2003. **62**(5 Suppl 1): p. 11-20.

14. Choi, N., et al., *Adult murine prostate basal and luminal cells are self-sustained lineages that can both serve as targets for prostate cancer initiation.* Cancer Cell, 2012. **21**(2): p. 253-65.

15. Hudson, D.L., et al., *Epithelial cell differentiation pathways in the human prostate: identification of intermediate phenotypes by keratin expression.* J Histochem Cytochem, 2001. **49**(2): p. 271-8.

16. Wang, Y., et al., *Cell differentiation lineage in the prostate.* Differentiation, 2001. **68**(4-5): p. 270-9.

17. Crowley, L., et al., *A single-cell atlas of the mouse and human prostate reveals heterogeneity and conservation of epithelial progenitors.* Elife, 2020. **9**.

18. Karthaus, W.R., et al., *Regenerative potential of prostate luminal cells revealed by single-cell analysis.* Science, 2020. **368**(6490): p. 497-505.

19. Kwon, O.J., L. Zhang, and L. Xin, *Stem Cell Antigen-1 Identifies a Distinct Androgen-Independent Murine Prostatic Luminal Cell Lineage with Bipotent Potential.* Stem Cells, 2016. **34**(1): p. 191-202.

20. Liu, J., et al., *Regenerated luminal epithelial cells are derived from preexisting luminal epithelial cells in adult mouse prostate.* Mol Endocrinol, 2011. **25**(11): p. 1849-57.

21. Lawson, D.A., et al., *Isolation and functional characterization of murine prostate stem cells.* Proc Natl Acad Sci U S A, 2007. **104**(1): p. 181-6.

22. Toivanen, R., A. Mohan, and M.M. Shen, *Basal Progenitors Contribute to Repair of the Prostate Epithelium Following Induced Luminal Anoikis.* Stem Cell Reports, 2016. **6**(5): p. 660-667.

23. Xin, L., D.A. Lawson, and O.N. Witte, *The Sca-1 cell surface marker enriches for a prostate-regenerating cell subpopulation that can initiate prostate tumorigenesis.* Proc Natl Acad Sci U S A, 2005. **102**(19): p. 6942-7.

24. Xin, L., et al., *Self-renewal and multilineage differentiation in vitro from murine prostate stem cells.* Stem Cells, 2007. **25**(11): p. 2760-9.

25. Goldstein, A.S., et al., *Trop2 identifies a subpopulation of murine and human prostate basal cells with stem cell characteristics.* Proc Natl Acad Sci U S A, 2008. **105**(52): p. 20882-7.

26. Wu, C.T., et al., *Increased prostate cell proliferation and loss of cell differentiation in mice lacking prostate epithelial androgen receptor.* Proc Natl Acad Sci U S A, 2007. **104**(31): p. 12679-84.

27. Xie, Q., et al., *Dissecting cell-type-specific roles of androgen receptor in prostate homeostasis and regeneration through lineage tracing.* Nat Commun, 2017. **8**: p. 14284.

28. Wang, S., et al., *Pten deletion leads to the expansion of a prostatic stem/progenitor cell subpopulation and tumor initiation.* Proc Natl Acad Sci U S A, 2006. **103**(5): p. 1480-5.

29. Izumi, K., et al., *Androgen receptor roles in the development of benign prostate hyperplasia.* Am J Pathol, 2013. **182**(6): p. 1942-9.

30. Vital, P., P. Castro, and M. Ittmann, *Oxidative stress promotes benign prostatic hyperplasia.* Prostate, 2016. **76**(1): p. 58-67.

31. Shafi, A.A., A.E. Yen, and N.L. Weigel, *Androgen receptors in hormone-dependent and castration-resistant prostate cancer.* Pharmacol Ther, 2013. **140**(3): p. 223-38.

32. Lukacs, R.U., et al., *Isolation, cultivation and characterization of adult murine prostate stem cells.* Nat Protoc, 2010. **5**(4): p. 702-13.

33. Wang, H.H., et al., *Characterization of autoimmune inflammation induced prostate stem cell expansion.* Prostate, 2015. **75**(14): p. 1620-31.

34. Wang, L., et al., *Expansion of prostate epithelial progenitor cells after inflammation of the mouse prostate.* Am J Physiol Renal Physiol, 2015. **308**(12): p. F1421-30.

35. Wang, Z.A., et al., *Lineage analysis of basal epithelial cells reveals their unexpected plasticity and supports a cell-of-origin model for prostate cancer heterogeneity.* Nat Cell Biol, 2013. **15**(3): p. 274-83.

36. Kramer, G., D. Mitteregger, and M. Marberger, *Is benign prostatic hyperplasia (BPH) an immune inflammatory disease?* Eur Urol, 2007. **51**(5): p. 1202-16.

37. Theyer, G., et al., *Phenotypic characterization of infiltrating leukocytes in benign prostatic hyperplasia.* Lab Invest, 1992. **66**(1): p. 96-107.

38. Haverkamp, J.M., et al., *An inducible model of abacterial prostatitis induces antigen specific inflammatory and proliferative changes in the murine prostate.* Prostate, 2011. **71**(11): p. 1139-50.

39. Chang, K.H., et al., *Dihydrotestosterone synthesis bypasses testosterone to drive castration-resistant prostate cancer.* Proc Natl Acad Sci U S A, 2011. **108**(33): p. 13728-33.

40. Feng, Q. and B. He, *Androgen Receptor Signaling in the Development of Castration-Resistant Prostate Cancer.* Front Oncol, 2019. **9**: p. 858.

41. Ito, Y. and M.D. Sadar, *Enzalutamide and blocking androgen receptor in advanced prostate cancer: lessons learnt from the history of drug development of antiandrogens.* Res Rep Urol, 2018. **10**: p. 23-32.

42. Penning, T.M., *Androgen biosynthesis in castration-resistant prostate cancer.* Endocr Relat Cancer, 2014. **21**(4): p. T67-78.

43. Cooper, P.O., *The impacts of inflammation on adult prostate stem cells* in *Comparative Pathobiology*. 2020, Purdue University.

44. Henry, G., et al., *Molecular pathogenesis of human prostate basal cell hyperplasia.* Prostate, 2017. **77**(13): p. 1344-1355.

45. Smith, B.A., et al., *A basal stem cell signature identifies aggressive prostate cancer phenotypes.* Proc Natl Acad Sci U S A, 2015. **112**(47): p. E6544-52.

46. Di Carlo, E., et al., *The prostate-associated lymphoid tissue (PALT) is linked to the expression of homing chemokines CXCL13 and CCL21.* Prostate, 2007. **67**(10): p. 1070-80.

47. Garcia-Hernandez, M.L., et al., *A Unique Cellular and Molecular Microenvironment Is Present in Tertiary Lymphoid Organs of Patients with Spontaneous Prostate Cancer Regression.* Front Immunol, 2017. **8**: p. 563.

48. Pitzalis, C., et al., *Ectopic lymphoid-like structures in infection, cancer and autoimmunity.* Nat Rev Immunol, 2014. **14**(7): p. 447-62.

49. Dar, J.A., et al., *The N-terminal domain of the androgen receptor drives its nuclear localization in castration-resistant prostate cancer cells.* J Steroid Biochem Mol Biol, 2014. **143**: p. 473-80.

50. Lakshmana, G. and A. Baniahmad, *Interference with the androgen receptor protein stability in therapy-resistant prostate cancer.* Int J Cancer, 2019. **144**(8): p. 1775-1779.

51. Attard, G., et al., *Antitumor activity with CYP17 blockade indicates that castration-resistant prostate cancer frequently remains hormone driven.* Cancer Res, 2009. **69**(12): p. 4937-40.

52. Uemura, M., et al., *Novel 5 alpha-steroid reductase (SRD5A3, type-3) is overexpressed in hormone-refractory prostate cancer.* Cancer Sci, 2008. **99**(1): p. 81-6.

53. Holmes, C. and W.L. Stanford, *Concise review: stem cell antigen-1: expression, function, and enigma.* Stem Cells, 2007. **25**(6): p. 1339-47.

54. Kwon, O.J., et al., *The Sca-1(+) and Sca-1(-) mouse prostatic luminal cell lineages are independently sustained.* Stem Cells, 2020. **38**(11): p. 1479-1491.

55. Krebsbach, P.H. and L.G. Villa-Diaz, *The Role of Integrin alpha6 (CD49f) in Stem Cells: More than a Conserved Biomarker.* Stem Cells Dev, 2017. **26**(15): p. 1090-1099.

56. Strand, D.W., et al., *Isolation and analysis of discreet human prostate cellular populations.* Differentiation, 2016. **91**(4-5): p. 139-51.

57. Shi, X., et al., *Prostate progenitor cells proliferate in response to castration.* Stem Cell Res, 2014. **13**(1): p. 154-63.

58. Wang, X., et al., *Identification of a Zeb1 expressing basal stem cell subpopulation in the prostate.* Nat Commun, 2020. **11**(1): p. 706.

59. McAuley, E., et al., *Sox2 Expression Marks Castration-Resistant Progenitor Cells in the Adult Murine Prostate.* Stem Cells, 2019. **37**(5): p. 690-700.

60. Wang, B.E., et al., *Castration-resistant Lgr5(+) cells are long-lived stem cells required for prostatic regeneration.* Stem Cell Reports, 2015. **4**(5): p. 768-79.

61. Chua, C.W., et al., *Single luminal epithelial progenitors can generate prostate organoids in culture.* Nat Cell Biol, 2014. **16**(10): p. 951-61, 1-4.

62. Montgomery, R.B., et al., *Maintenance of intratumoral androgens in metastatic prostate cancer: a mechanism for castration-resistant tumor growth.* Cancer Res, 2008. **68**(11): p. 4447-54.

63. Koivisto, P., et al., *Androgen receptor gene and hormonal therapy failure of prostate cancer.* Am J Pathol, 1998. **152**(1): p. 1-9.

64. Thapa, D. and R. Ghosh, *Chronic inflammatory mediators enhance prostate cancer development and progression.* Biochem Pharmacol, 2015. **94**(2): p. 53-62.

65. Grivennikov, S.I., F.R. Greten, and M. Karin, *Immunity, inflammation, and cancer.* Cell, 2010. **140**(6): p. 883-99.

66. Steiner, G.E., et al., *Cytokine expression pattern in benign prostatic hyperplasia infiltrating T cells and impact of lymphocytic infiltration on cytokine mRNA profile in prostatic tissue.* Lab Invest, 2003. **83**(8): p. 1131-46.

67. Kramer, G., et al., *Increased expression of lymphocyte-derived cytokines in benign hyperplastic prostate tissue, identification of the producing cell types, and effect of differentially expressed cytokines on stromal cell proliferation.* Prostate, 2002. **52**(1): p. 43-58.

68. Burcham, G.N., et al., *Impact of prostate inflammation on lesion development in the POET3(+)Pten(+/-) mouse model of prostate carcinogenesis.* Am J Pathol, 2014. **184**(12): p. 3176-91.

CHAPTER 3. IMMUNE HISTOLOGY AND SINGLE CELL RNA SEQUENCING ANALYSIS IN BPH

Meaghan M Broman, Nadia A Lanman, Renee E Vickman, Gregory M Cresswell, Juan Sebastian Paez Paez, Susan Crawford, Simon W Hayward, Gervaise Henry, Douglas Strand, Timothy L Ratliff

3.1 Abstract

Benign Prostatic Hyperplasia (BPH) is a common prostatic disease among older men. Lymphoid aggregates and organizing lymphoid structures termed tertiary lymphoid structures (TLS) are commonly observed in mucosal tissues and sites of chronic inflammation, including the prostate; however, a potential role for these lymphoid structures in BPH is not known. Here we evaluate the morphologic and gene expression characteristic of lymphoid structures and lymphoid cell populations in BPH prostates.

Whole mounts of 5 small "early-stage" and 12 large "late-stage" BPH specimens were examined by histology and immunohistochemistry (IHC) to characterize the morphology and cellular composition of lymphoid aggregates and structures. Single cell RNA Sequencing (scRNA-Seq) was performed on $CD45^{+}EpCAM^{-}CD200^{-}$ immune cells were isolated from 10 small and 3 large BPH prostate tissue samples to identify immune cell types and signaling pathways based on differential gene expression (DGE) patterns. Findings in BPH prostates were compared with histologic and scRNA-Seq analyses of normal non-BPH prostates.

Histologic evaluation of small (n=5) and large (n=12) BPH and normal prostate (n=2) specimens found that BPH immune cell populations were distributed within stromal, intraepithelial, and intraluminal areas. Stromal lymphoid cells were arranged in loose and dense aggregates and rarely dense follicle-like structures resembling TLS. scRNA-Seq data indicate that immune cell subsets present in small and large BPH and normal prostates cluster in a similar manner, and were predominately composed of lymphoid cells, particularly T cells. Expression of several chemokine genes associated with lymphoid cell recruitment and chemotaxis and associated with TLS formation and maintenance were increased in BPH lymphoid cells compared to normal prostate

immune cell populations. Also, International Prostate Symptom Score (IPSS) and prostate volume were positively correlated with the proportion of Cluster 0 $CD8^+$ T cells in BPH patients.

These findings describe the composition, distribution, and gene expression of BPH lymphoid cell populations and lymphoid structures resembling TLS suggest a role for T cells in BPH pathogenesis. However, further studies are needed to determine the clinical significance of TLS in BPH.

3.2 Introduction

Benign prostatic hyperplasia (BPH) is a common urologic condition among older men, affecting approximately half of men by age 50 and nearly 80% by age 80 [1]. The normal non-BPH adult prostate is defined as having a volume at or below 20 cc from men 18-24 years of age [2]. As men age, cellular proliferation and progressive expansion of the prostate glandular and stromal compartments within the periurethral transitional zone results in increased prostate volume [3, 4]. BPH nodules typically consist of both epithelial and stromal proliferation and expansion, although one may predominate over the other [1]. Often, the fibromuscular stroma predominates within these hyperplastic nodules, with a decreased ratio of glandular epithelium to stroma compared to the normal prostate [1, 5, 6]. Immune cell infiltrates are commonly observed in association with BPH nodules and are hypothesized to contribute to the pathogenesis of the disease; however, definitive data linking the two are lacking. [1, 2, 7].

The normal non-BPH adult prostate is defined as having a volume at or below 20 cc from men 18-24 years of age [2]. The immune cell population in the normal prostate is generally small and consists of both lymphoid and myeloid subtypes [7, 8]. The lymphoid component is typically the most abundant immune tissue in the prostate. T cells usually predominate with smaller populations of B cells, macrophages, natural killer (NK) cells, mast cells, and plasma cells [7, 8]. As men age, the overall immune cell component of the prostate increases [7].

Lymphoid cells reside in both the intraepithelial and stromal compartments [8]. Intraepithelial lymphoid cells consist predominately of $CD8^+$ T cells, while stromal lymphoid cells consist of a mix of $CD4^+$ T cells, $CD8^+$ T cells, B cells, and plasma cells [7, 8]. Stromal lymphoid cells may be arranged in loose aggregates or dense follicular structures with or without a germinal center [8].

These aggregates and follicles are most commonly located in periglandular areas but may be distributed in other areas within the stroma [8]. Similar organized lymphoid structures have been observed in many tissues and have been referred to as tertiary lymphoid structures (TLS), tertiary lymphoid organs, or ectopic lymphoid structures [8]. TLS develop in response to chronic inflammation or infection and have been observed in association with chronic allograft rejection, autoimmunity, and various tumor types including prostate cancer [9-11]. TLS and other mucosa-associated lymphoid tissue are one component of the lymphoid immune system. Primary lymphoid organs (PLO) include the bone marrow and the thymus. Secondary lymphoid organs (SLO) include lymph nodes, splenic white pulp, the human appendix, tonsils, and Peyer's patches [11]. SLO also includes mucosal-associated lymphoid tissues (MALT) which can be found in mucosal tissues including the lung and intestine [11]. PLO and SLO originate during embryological development, and MALT develops in the postnatal period [11]. Inflammatory mediators produced by immune cells such as CCL3 and CCL4 stimulate stromal cells to produce chemokines and adhesion molecules that promote lymphoid recruitment and TLS formation [12]. Chronic stimulation by lymphoid-derived inflammatory mediators, including the TNF family members TNFα, lymphotoxin α (LTα) and lymphotoxin β (LTβ), further promote TLS formation and maintenance through the stimulation of adhesion molecule expression by endothelial cells [13-16].

The function of TLS appears to vary among tissue types and disease states. They have been shown to be involved in a protective immune response to various infectious agents and have generally been considered a positive prognostic indicator and potential immunotherapy target in various cancers [9, 17-21]. However, these structures have also been associated with tissue damage in chronic allograft rejection [22]. In the prostate, TLS have been observed in prostate tumors and have been suggested to enhance antitumor immunity [9]. These structures have also been observed in the prostates of aged men in the absence of BPH or PCa and their formation appears to coincide with the overall increase in immune cells that occurs with age; however, the function of TLS in the prostate is unclear and their role in BPH is not known [8].

In this study, we sought to characterize and compare the immune cell populations of early-stage and late-stage BPH and normal prostates to identify potential immune-related mechanisms of BPH progression. To do this, we combined morphologic analyses of tissue sections with single cell

RNA sequencing (scRNA-Seq) analysis of immune cells from BPH and normal prostate specimens. BPH prostates were obtained from patients undergoing surgery for low Gleason grade prostate tumors that also has evidence of BPH and from patients undergoing surgery for symptomatic BPH. The prostates were classified as small (less than 60 grams) prostates representing "early-stage" BPH or large (greater than 70 grams) prostates representing advanced "late-stage" BPH. Fixed tissues from each specimen were stained with specific immune cell markers to localize immune cell types within the tissue and compare to scRNA-Seq classifications. $CD45^+$ immune cells were isolated from each specimen and analyzed by single-cell RNA sequencing (scRNA-Seq) and Cellular Indexing of Transcriptomes and Epitopes by Sequencing (CITE-Seq) labelling to identify immune cell subtypes based on differentially expressed genes (DEG) and cell surface markers, respectively, compared to known immune cell phenotypes. Finally, these data were compared to previously published scRNA-Seq data and histologic sections of normal non-BPH prostates. Similar to previous studies, lymphoid cells predominate in the BPH prostate. Intraepithelial lymphocytes were predominately $CD8^+$ T cells, while stromal lymphocytes were predominately $CD4^+$ T cells mixed with B cells and fewer $CD8^+$ T cells. Stromal lymphoid cells were arranged in loose aggregates or follicle-like structures, a few of which formed germinal center-like areas. Overall, few $FoxP3^+$ regulatory T cells (Treg) were present in lymphoid aggregates. Also, expression of inflammatory mediators associated with lymphocyte recruitment were elevated in BPH T cell populations compared to normal prostates. Overall, BPH immune cell composition and gene expression are indicative of a chronic mixed inflammatory process that may contribute to additional immune cell recruitment and stimulation.

3.3 Methods

3.3.1 Human prostate tissues

BPH prostatic tissues were obtained from BPH patients undergoing simple prostatectomy (SP) or robot-assisted laparoscopic prostatectomy (RALP) surgery for symptomatic BPH or prostate cancer (PCa), respectively, and were divided into small BPH representing "early-stage" BPH and large BPH representing "late-stage" BPH based on prostate size. Small BPH samples were obtained from patients undergoing surgery for the treatment of small organ-confined peripheral zone (PZ) PCa of Gleason grade 6 (3+3) or 7 (3+4 or 4+3) and with a prostatic weight of 60 grams

or less. Large BPH samples were obtained from patients undergoing surgery for symptomatic BPH and had a prostatic weight over 70 grams. Other patient criteria include no history of chronic prostatitis or uncontrolled diabetes, and no prior placement of an indwelling catheter. Clinical data for BPH sample patients is summarized in Table 3.1. Normal non-BPH prostate (n=2) sections (kindly provided by Dr. Douglas Strand, University of Texas Southwestern, Dallas, TX) were made from archived prostate specimens obtained at autopsy from young men with no known clinical history or histologic evidence of BPH. All human tissue procurement was done in accordance with protocols approved by the Institutional Review Boards of each institution.

Table 3.1 Summary of clinical data from small BPH and large BPH patients.

Patient Sample	Age	BMI	IPSS	Prostate Weight (g)
Small 003	67	24.92	6	38.0
Small 004	61	25.13	1	52.0
Small 006	74	25.52	2	47.0
Small 007	61	26.55	5	45.0
Small 008	68	22.58	0	48.0
Small 009	63	27.18	2	45.0
Small 010	68	27.76	2	45.0
Small 013	69	27.34	6	38.0
Small 1144	61	26.16	14	46.0
Small 1196	71	27.22	3	56.0
Large 012	67	26.26	30	71.0
Large 1157	76	24.30	17	82.0
Large 1195	63	29.03	8	124.0

3.3.2 Prostate histology and immunohistochemistry

Full thickness cross sections of small BPH and large BPH prostate were fixed in 10% neutral buffered formalin (NBF) for histology. Formalin fixed prostate tissues were embedded in paraffin, sectioned, and stained with hematoxylin and eosin (H&E). For immunohistochemical staining, additional sections from 3 small BPH and 3 large BPH specimens were deparaffinized and stained for immunohistochemistry with the following antibodies: CD8a (clone C8/144B, Abcam), CD4 (clone EPR6855, Abcam), CD79a (clone SP18, Invitrogen), CD11b (clone ERP1344, Abcam), CD68 (clone EPR20545, Abcam), CD163 (clone OTI2G12, Abcam), NCAM1 (CD56) (clone

EP2567Y, Abcam), CD138 (polyclonal, Abcam), FoxP3 (polyclonal, Novus Biologicals). Additionally, 2 normal prostate specimens (kindly provided by Dr. Douglas Strand, University of Texas Southwestern, Dallas, TX) were stained with H&E.

3.3.3 BPH tissue processing and sorting for scRNA-Seq

Transitional zone (TZ) tissue was excised from small BPH (n=10) and large BPH (n=3) prostates then minced and digested in 200 U/ml Collagenase I (Thermo Fisher) in Hank's balanced salt solution (HBSS) (Fisher) at 37^{o}C with agitation at 190-200 RPM for two hours. Digested samples were spun down at 250 x g at room temperature (RT) for 7 minutes and the supernatant aspirated. Samples were incubated in 5 ml TrypLE dissociation reagent (Thermo Fisher) at 37^{o}C with agitation at 200 RPM for 5-10 minutes. TrypLE was neutralized with 10 ml complete RPMI (Sigma Aldrich) then passed through a 10 ml pipette, followed by a 5 ml pipette, followed by an 18G syringe 5 times. Samples were filtered through a 100um and then a 70um cell strainer, rinsed with PBS and spun down at 200 RPM for 7 minutes. Samples were incubated in ammonium-chloride-potassium (ACK) lysis buffer for 3 minutes at RT to lyse red blood cells then rinsed in PBS and spun twice. Samples were incubated with 5ul Human TruStain Fx Blocking reagent (Biolegend) and 0.5ul Zombie Viability Dye (Biolegend) in 100ul PBS per sample for 10-15 minutes at RT in the dark, filtered and spun, then incubated with an antibody cocktail of CD45-PE (clone HI30, Biolegend) pan-leukocyte marker, EpCAM-APC (clone 9C4, Biolegend) epithelial cell marker, and CD200-PE/Cy7 (clone OX-104, Biolegend) endothelial cell marker or single antibodies for compensation controls (if necessary) for 30 minutes at 4^{o}C. Samples were washed with PBS spun down then resuspended in complete RPMI for live cell sorting on the BD FACS ARIA II (BD Biosciences, San Jose, CA) to isolate $CD45^{+}EpCAM^{-}CD200^{-}$ immune cells. Prior to loading, some BPH cell preps were labeled with TotalSeq-B Antibodies (Biolegend) CD3 (clone UCHT1), CD4 (clone RPA-T4), CD8 (clone RPA-T8), CD11b (clone ICRF44), and CD19 (clone HIB19) per manufacturer instructions.

3.3.4 Single-cell RNA-Seq

scRNA-Seq of BPH samples was performed utilizing the 10X Chromium v3 (10X Genomics, Pleasanton, CA). Sorted $CD45^{+}EpCAM^{-}CD200^{-}$ immune cells from each BPH sample were

counted, prepped and loaded into the 10X chip for a 5000 target cell recovery per 10X Genomics protocols. cDNA synthesis and clean-up steps were performed per manufacturer protocols. cDNA content and quality were assessed via Agilent Bioanalyzer (Agilent Technologies, Santa Clara, CA). Sample library preparation was performed per 10X Genomics protocols prior to sequencing. The resulting data was combined with previously published scRNA-Seq data from three normal prostates from young men aged 18 to 31 years [32].

3.3.5 Sample sequencing and data analysis

BPH samples were sequenced by the Purdue Genomics Core using a NovaSeq S4 flow cell on a NovaSeq 6000 platform (Illumina, San Diego, CA). Paired-end, 2x150 base-pair reads were sequenced to a depth of 50,000 reads per cell. TotalSeq-B antibody libraries for quantification of cell surface proteins were sequenced at a depth of 5,000 reads per cell. The estimated number of cells along with mean reads per cell and mean number of genes per cell for each sample are listed in Table 3.2. Distinct immune cell clusters were identified based on gene expression patterns and marker genes, as well as using the protein expression observed from the CD3, CD4, CD8, CD11b, and CD19 CITE-seq data and subsequently classified based on known immune phenotypes.

Table 3.2 List of human BPH samples included in the scRNA-Seq analysis with estimated number of cells, mean reads per cell, and median genes per cell from each sample.

Sample	Sample Type	CD45+ cells	Mean reads/cell	Median genes/cell
003	Small BPH	6,388	68,457	1,692
004	Small BPH	4,163	64,080	1,599
006	Small BPH	6,427	40,164	1,628
007	Small BPH	4,427	172,916	1,958
008	Small BPH	5,053	109,389	1,652
009	Small BPH	3,659	98,901	1,740
010	Small BPH	3,750	65,500	1,576
013	Small BPH	5,230	75,242	1,476
1144	Small BPH	600	65,637	1,662
1196	Small BPH	4,554	49,264	1,489
012	Large BPH	5,826	51,084	1,526
1157	Large BPH	6,816	44,585	1,525
1195	Large BPH	5,377	84,624	1,591

Sequencing reads from the Chromium system were de-multiplexed, adapters removed, and read trimmed using the CellRanger pipeline v3.0.0 (10x Genomics). FASTQ files were generated using CellRanger mkfastq. Parameters specified were that dual indices were to be ignored, no mismatches were allowed within barcodes, and the flag "—use-bases-mask=Y26n*,I8n*,n*,Y98n" was set. CellRanger count (chemistry version "SC3Pv2") was used for read filtering, alignment to the ENSEMBL human reference genome version GrCh38, barcode counting, and unique molecular identifier (UMI) counting. All reads were aligned to reference genome using the STAR aligner v2.5.4[1].

R version 3.5.1 and Bioconductor version 3.8 were used for all statistical and bioinformatic analyses. Cells with fewer than 1,000 or greater than 10,000 observed genes were removed from further analysis. Cells with 22% or more of all reads mapping to mitochondrial genes were also excluded. The Seurat toolkit for single-cell analyses, version 3.1.3 was used for data scaling and normalization, cell clustering based on gene expression, and identification of marker genes[X, Y] [24]. Data were normalized using scTransform v.0.3.1 and cell cycle scoring was performed using cell cycle-related genes [25]. Scaling was performed, regressing out cell cycle scores, mitochondrial reads, and UMI counts using linear models to remove heterogeneity due to these variables.

After scaling, dimensionality reduction was performed, followed by unsupervised clustering of cells. The 300 most variable genes were then selected, and the scaled and normalized data for these genes were used to perform a principal component analysis (PCA). The first 30 principal components, which account for the vast majority of the variability in the data, were used for downstream analysis. Unsupervised clustering was then performed using graph-based approaches to first construct K-nearest neighbor graphs (with K = 30). Clusters were identified using the Louvain method for community detection, as implemented in Seurat. A resolution of 0.2 was selected, which was determined primarily using clustering trees via the clustree R package v 0.4.3, selecting a resolution that provides stable clusters [26]. P-values were corrected for multiple testing using the Benjamini-Hochberg method [27]. Biomarkers were considered statistically significant at a 1% false discovery rate (FDR) using the Wilcoxon rank sum test. Differentially expressed genes between small and large sample groups were identified using the edgeR

Bioconductor package, v 3.31 with an FDR cutoff of 5%. Both raw and processed scRNA-seq data are available on GEO under accession number GSE164695.

3.3.6 Mouse prostate inflammation models

POET-3 mouse prostates were inflamed as previously described [28, 29]. In summary, splenocytes were isolated from Rag1$^{-/-}$Thy1.1^{+}OT-I mice, activated by 1μg/mL SIINFEKL (Ova peptide 257-264, American Peptide, Sunnyvale, CA; ovalbumin (chicken) acetate salt H-7738.1000, Bachem, Torrance, CA) and cultured for 48 hours *in vitro*. Activated Thy1.1^{+}CD8^{+} T cells were collected and purified by Ficoll gradient (Atlanta Biologicals, Lawrenceville, GA). A total of 5x10^{6} purified OT-I cells were transferred into POET-3 mice intravenously to induce inflammation. POET-3 prostates were harvested at 6 days post-inflammation. Aire KO mouse prostates were inflamed by subcutaneous injection of 200 ug mouse prostate antigen in Complete Freud's Adjuvant (Sigma Aldritch, S. Louis, MO) boosted with Incomplete Freud's Adjuvant (Sigma Aldritch). Aire KO prostates were harvested 2 weeks post-booster. Prostates were fixed in 10% NBF and processed for histology and CD8 (clone 4SM15, Thermo Fisher) IHC as described above.

3.4 Results

3.4.1 BPH immune cell histology indicates a chronic inflammatory microenvironment

Previous studies have described the immune cell populations using histology and immunohistochemistry (IHC) [7, 30]. BPH prostate sections were evaluated histologically to determine the immune cell composition and distribution. While the extent of immune cell infiltration varied among samples, the distribution of immune cells was generally similar within the intraluminal, intraepithelial, and stromal areas. Glandular lumina contained variable numbers of large macrophages and few neutrophils (Fig. 3.1). Similar to previous studies, the bulk of the immune cell infiltrate was composed of lymphocytes within the periglandular stroma and epithelium [7]. Intraepithelial lymphocytes were predominately CD8^{+} T cells and fewer CD4^{+} T cells (Fig. 3.2). Stromal lymphocytes were predominately CD4^{+} T cells mixed with B cells and CD8^{+} T cells (Fig. 3.2, 3.3). CD4^{+} T cells and B cells often formed aggregates and organizing lymphoid structures intermixed with fewer CD8^{+} T cells (Fig. 3.3). CD8^{+} T cells were also

distributed throughout the stroma, either scattered or associated with other lymphoid cells (Fig. 3.2, 3.3)

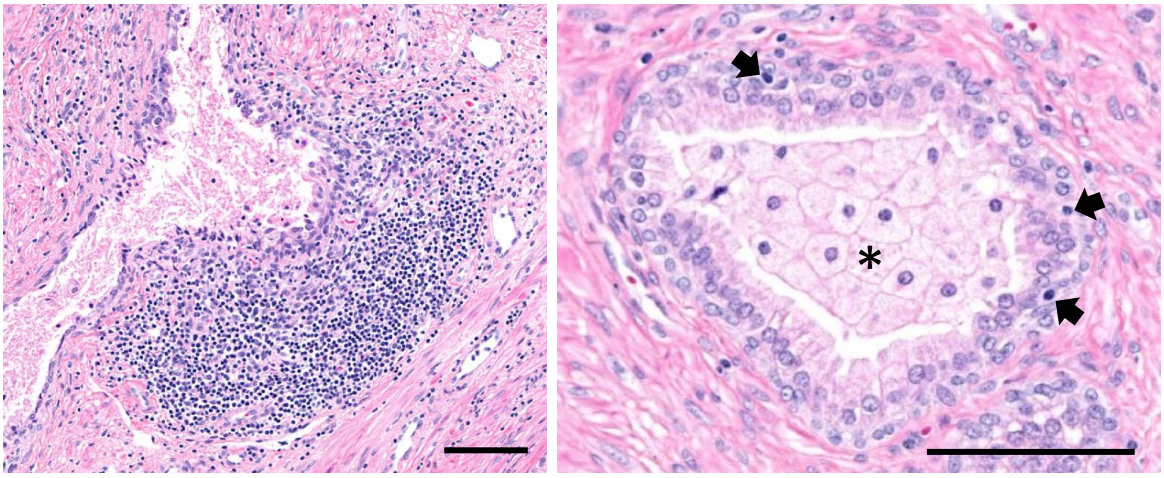

Figure 3.1 H&E sections of human BPH prostate showing a periglandular lymphoid aggregate (left) and gland (right) with intraluminal macrophages (asterisk) and intraepithelial leukocytes (arrows). Scale bars=100um.

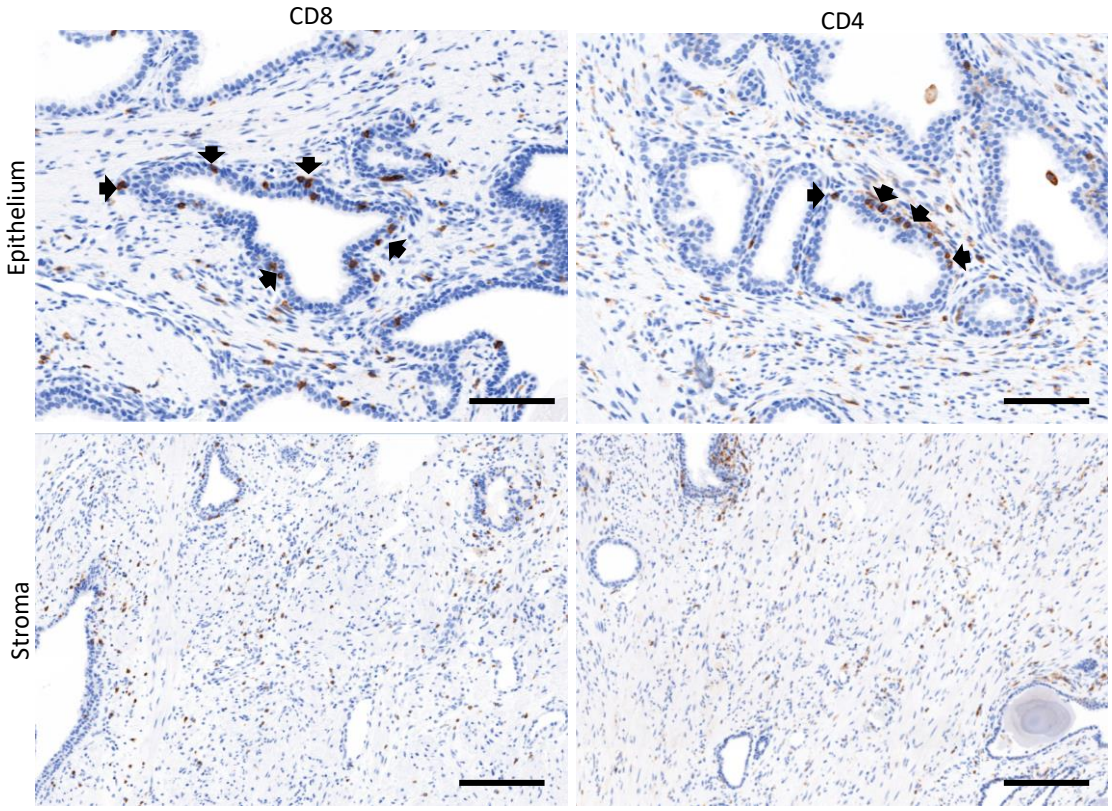

Figure 3.2 IHC sections of human BPH epithelium (top) and stroma (bottom) showing distribution of CD8+ (left) and CD4+ (right) T cells within the epithelium (arrows) and in the stroma. Scale bars=200μm.

The organization of stromal lymphoid cells in BPH specimens varied from loose aggregates to dense aggregates and occasionally organizing follicle-like structureswhich in rare instances formed areas resembling germinal center (Fig. 3.3). The loose aggregates were composed mostly of $CD4^+$ T cells intermixed with $CD79a^+$ B cells, $CD8^+$ T cells, and few $NCAM^+$ (CD56) natural killer (NK) cells (Fig. 3.3 A). Follicle-like structures were composed mostly of densely packed $CD79a^+$ B cells surrounded by $CD4^+$ T cells (Fig. 3.3 A). Fewer $CD8^+$ T cells were mixed with the $CD4^+$ T cells. Small numbers of $FoxP3^+$ T cells were present within some lymphoid aggregates (Fig. 3.3 B). Scattered $CD138^+$ plasma cells were distributed within the stroma and often in periglandular areas (Fig. 3.3 B). Larger lymphoid aggregates and organizing structures described here were not observed in sections from two normal prostates, although one specimen had scattered small periglandular groupings of lymphocytes as well as local infiltration of lymphoid cells adjacent to the urethra. In all, the presence of organizing B and T cell structures suggest a robust localized B and T cell adaptive immune response [8].

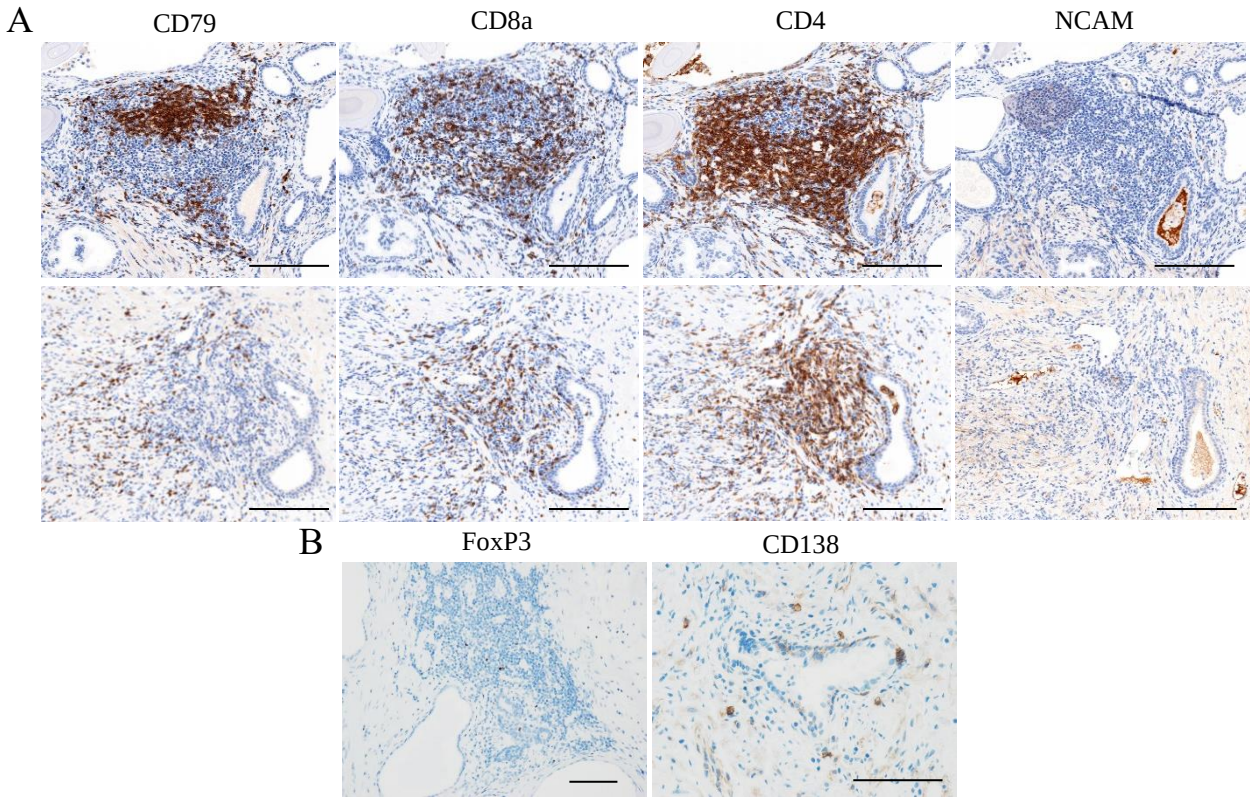

Figure 3.3 (A) human BPH prostate IHC of dense follicle-like (top) and loose lymphoid aggregates (bottom) showing the distribution of CD79a+ B cells, CD8+ T cells, CD4+ T cells, and NCAM+ NK cells within lymphoid structures. Scale bars=200μm. (B) IHC of FoxP3+ Treg (left) within lymphoid aggregate and CD138+ plasma cells (right) surrounding a gland (asterisk). Scale bars=100μm.

In addition to lymphoid populations, macrophages were present within the stroma and epithelium. Cells expressing the macrophage marker $CD68^{+}$ were present in intraluminal, stromal, and periglandular areas and occasionally within the epithelium (Fig. 3.4). Macrophages expressing the M2 macrophage-associated marker $CD163^{+}$ were distributed throughout the stromal and often closely associated with lymphoid structures (Fig. 3.4) [31]. Neutrophils were generally rare to absent in most samples, which is consistent with previous studies and also may be related to the patient selection criteria of no diagnosis of active prostatitis or use of an indwelling catheter [8]. When present, neutrophils were observed within the lumens of intact and disrupted glands often mixed with cell debris (Fig. 3.5). In some areas near disrupted glands, the adjacent epithelium and stroma were locally infiltrated by low numbers of intact and intact and degenerate neutrophils and lymphocytes (Fig. 3.5).

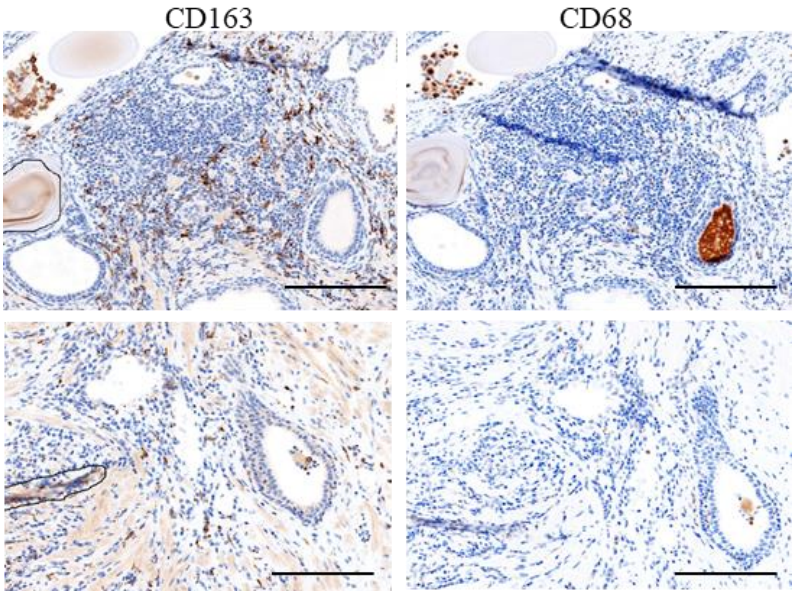

Figure 3.4. Human BPH prostate IHCof macrophage marker CD68 (left) M2 macrophage marker CD163 (right) in dense follicle-like (top) and loose aggregate (bottom) lymphoid structures. Scale bars=200μm.

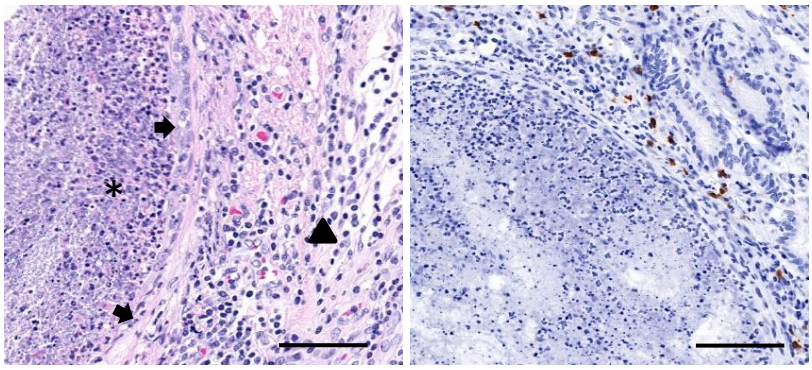

Figure 3.5. H&E (left) and CD8a IHC (right) sections of human BPH prostate. Left, gland with disrupted epithelium (arrows) and neutrophils and cell debris within the glandular lumen (asterisk). The periglandular stroma is infiltrated by lymphocytes (arrowhead). Right, $CD8^+$ T cell infiltration adjacent to disrupted glandular epithelium. Scale bars=100μm.

In contrast to BPH specimens, normal prostates had overall few immune cells and lacked the prominent lymphoid aggregates and follicular structures observed in BPH specimens. One specimen had moderate lymphoid infiltration adjacent to the urethra, but organizing lymphoid structures were not observed. Overall, the composition and distribution of immune cells is consistent with previous studies of the BPH prostate. It is also similar to the composition and distribution described by Di Carlo et al (2007) in prostates from aged men without histologic evidence of BPH [8]. However, these structures have not been previously described in the prostates of young men, nor were they observed in the young donor prostate specimens examined in this study. These findings suggest that lymphoid structures may be an age-related development independent of BPH; however, larger studies involving age-matched non-BPH and BPH specimens would be needed to explore a potential link between them.

3.4.2 scRNA-Seq identifies prostate immune cell populations and DEG patterns

Histologic and immunohistologic evaluation provided an overview of the general immune cell populations and their anatomic distribution using known immune cell markers. However, this evaluation is limited in uncovering the full heterogeneity of lymphoid cell populations. To further define the heterogeneity and gene expression profiles of BPH immune cells and also to identify expression of genes associated with lymphoid recruitment and organization, immune cells isolated from BPH specimens were analyzed by scRNA-Seq. scRNA-Seq data were obtained from $CD45^+EpCam^-CD200^-$ immune cells isolated from TZ tissues from 10 small (<60 grams) "early-stage" BPH prostates and 3 large (>70 grams) "late-stage" BPH prostates from patients undergoing

prostatectomy surgery for low Gleason score (≤7) PZ prostate tumors or symptomatic BPH, respectively. Resulting scRNA-Seq data from small and large BPH specimens were combined with scRNA-Seq data of immune cells from three normal non-BPH prostates. In a previous study conducted by Henry et al. (2018), normal non-BPH prostates were obtained from three healthy donors aged 18 to 31 years and whole cell suspensions from each prostate were analyzed by scRNA-Seq on the 10X Chromium platform [32]. Data from all samples were combined and analyzed together so that similar immune cell subtypes could be clustered and compared between sample types (Fig. 3.6 A). Unsupervised clustering separated the leukocyte population into clusters based on DEG patterns and CITE-seq markers for cell surface markers associated with specific immune cell populations (Fig. 3.6 B, C). While the number of clusters determined for each individual sample varied between 10 and 14, most cells from each sample clustered in a generally similar manner, with two main groupings of individual clusters and multiple smaller distinct clusters (Fig. 3.6 B, C). Clusters comprised of closely related immune cell subtypes grouped together, with more distinct subtypes separated into discrete clusters. When data from all samples were combined, immune cells were separated into 11 clusters representing the immune cell subtypes in the combined samples (Fig. 3.6 B, C).

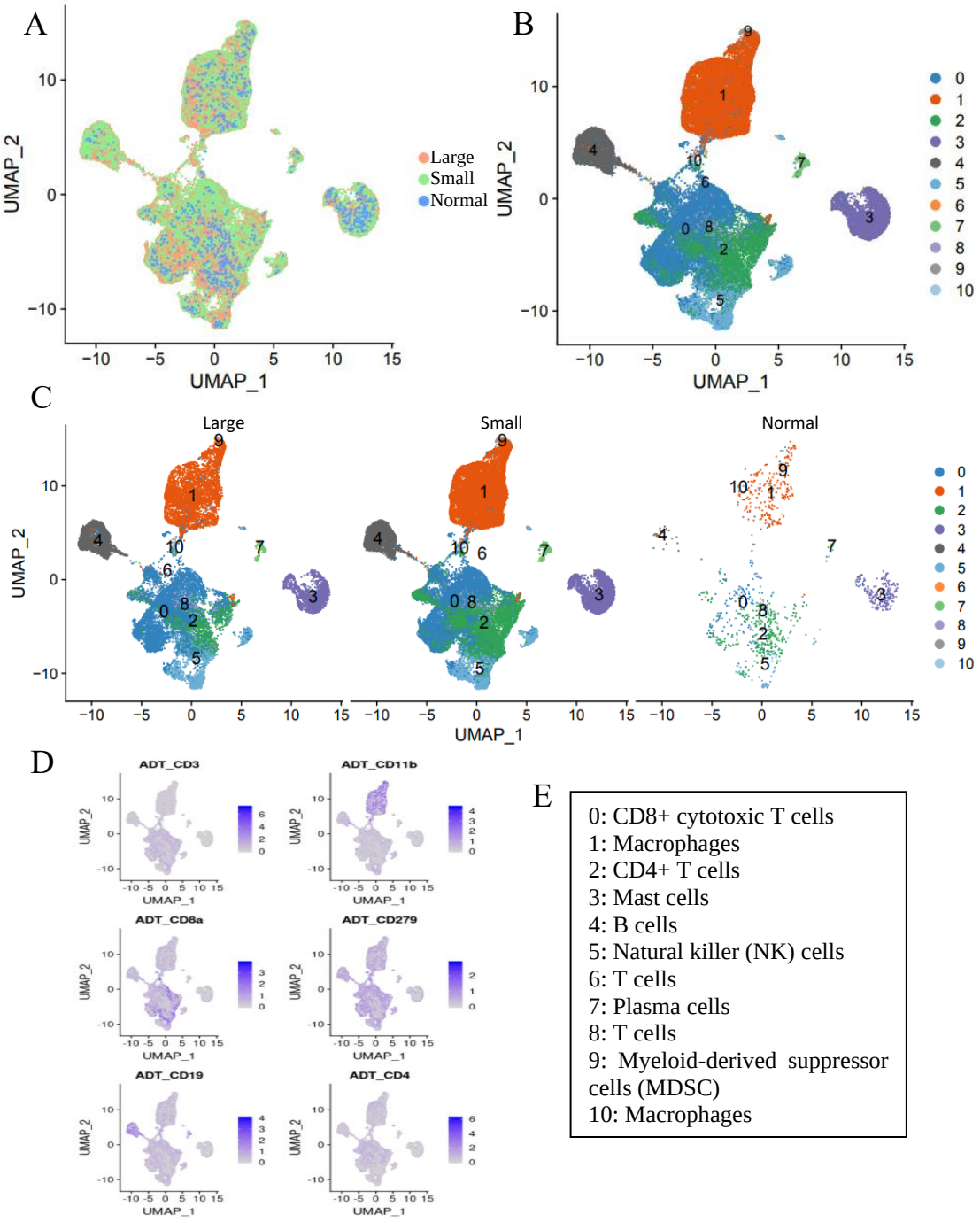

Figure 3.6. (A) Distribution of cells from large BPH (red), small BPH (green) and normal (blue) sample types among clusters. (B) Clustering analysis separated combined sample cells into 11 clusters. (C) Contribution of cells from each sample type to the clusters. (D) Distribution of CITE-Seq antibody staining among the clusters. (E) Cell type identification of 11 clusters identified by CITE-Seq and DGE analyses.

The initial cell type identification was performed using singleR referencing the Human Primary Cell Atlas. singleR identifies cell types by comparing their transcriptional profile to reference transcriptomes of known cell types. This analysis identified 37 cell types among all clusters. It should be noted that the Human Primary Cell Atlas data does not include all cell types, so certain immune cell types known to be present in the prostate such as plasma cells and mast cell were not specifically identified by this method. When this occurred, cell types were identified by characteristic markers in the gene expression data. Cluster identities were narrowed down based on differential gene expression (DGE) of known immune cell markers and labelling with CITE-Seq markers. CITE-Seq markers included T cell markers (CD3, CD4, CD8), NK marker NCAM (CD56), B cell marker CD19, and myeloid/macrophage marker CD11b. CD11b is a general marker of myeloid/macrophage cells that includes $CD68^+$ and $CD163^+$ macrophages. As CITE-Seq antibodies were not included in all samples, not every cell expressing the specific markers used in the CITE-Seq analysis was detected. However, this method aided in identification of clusters by indicating the clustering of cells expressing known immune cell surface markers.

Consistent with previous studies and with the histologic evaluation, lymphoid cells comprised the majority of immune cells, followed by myeloid/macrophage populations [7, 30]. The largest grouping of clusters (Clusters 0, 2, 5, 6, and 8) within each sample was identified as various T cell and NK cell subtypes (Fig. 3.6 B, D, E). Further characterization of the T cell subset indicated that Cluster 2 contained predominately $CD4^+$ T helper cells, while Cluster 0 was predominately $CD8^+$ cytotoxic T cells (CTC). T cells differentially expressing $FoxP3^+$ indicative of Treg were not initially identified in the full clustering analysis. When T cell clusters were combined and analyzed without the other subtypes, a subcluster (subcluster 7) differentially expressing FoxP3 was identified (Fig. 3.7).

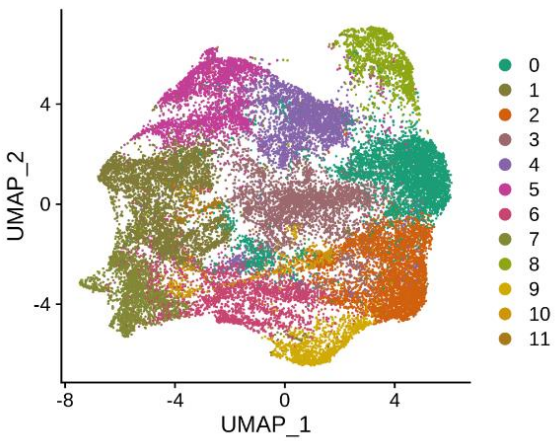

Figure 3.7. UMAP of combined T cell and NK cell subclustering. Subcluster 7 differentially expressed FoxP3.

The next largest cluster grouping was composed of myeloid/macrophage subtypes (Fig. 3.6 B, D, E). The majority of CD11b myeloid/macrophage cells were in Cluster 1. This cluster also differentially expressed CD163 and CD68.

Myeloid/macrophage Cluster 10 also differentially expressed CD68 and CD163, although CD163 expression was lower than in Cluster 1, indicating that most M2 macrophages segregate into Cluster 1. B cell marker $CD19^+$ cells were in Cluster 4. Cluster 3 was identified as mast cells based on DGE of mast cell-associated genes such as TPSAB1, CPA3, and KIT [33]. Cluster 7 plasma cells were identified by their differential expression of several immunoglobulin genes. Overall, individual samples and sample types clustered in a generally similar manner, indicating that similar immune cell types are present in both BPH and normal prostates, although BPH tissue had much higher numbers of infiltrating leukocytes. Also, these findings are consistent with histologic findings and previous studies indicating a predominance of T cells in BPH tissues [7, 8]. Subclustering analysis demonstrates the heterogeneity of prostate T cell populations and suggests certain subsets of T cells may promote TLS formation in BPH.

3.4.3 BPH lymphoid populations differentially express TLS-associated chemokine genes

Various lymphoid-derived chemokines have been associated with the formation and maintenance of TLS, either directly through immune cell recruitment or indirectly though stimulation of stromal cells. To identify expression of inflammatory mediator genes that may be involved in lymphoid recruitment and organization in BPH lymphoid populations, DEG in lymphoid clusters were compared between BPH and normal samples. Few or no genes were found to be differentially expressed between some clusters from normal and BPH samples due to these clusters having too few cells for comparison, particularly in normal prostate samples. In both large and small BPH, several chemokine and inflammatory mediator genes associated with lymphoid homing and organization were differentially expressed in T lymphocyte populations (Table 3.3). Large BPH and Small BPH Cluster 2 cells differentially expressed CXCR3, which is highly expressed on effector and memory T cells and involved in their recruitment to inflammatory sites [34] (Table 3.3 B). Expression of CCL20, which has been associated with Th17 T cell infiltration in TLS, was also increased in Cluster 2 $CD4^+$ T cells and Cluster 0 T cells in Large BPH [35] (Table 3.3 A, B). Cluster 2 $CD4^+$ T cells in Small BPH samples differentially expressed CCR7, the receptor for the lymphoid chemokines CCL19 and CCL21. CCL19 and CCL21 are produced by prostate stromal cells and are involved in lymphocyte recruitment to the prostate stromal compartment [8] (Table 3.3. B). Additionally, genes for mediators associated with stromal activation in TLS formation were also differentially expressed. TNFα been associated with stromal activation and TLS

formation, and TNF was upregulated in Large and Small BPH $CD4^+$ T cells (Table 3.3 B). Expression of CCL4, which promotes stromal cell activation and production of lymphoid chemokines CCL21 and CXCL13, were increased in Large BPH Cluster 0 $CD8^+$ T cells and Cluster 2 $CD4^+$ T cells and in Small BPH Cluster 2 $CD4^+$ T cells compared to normal prostate [12] (Table 3.3. A, B). Expression of CCL3, also associated with stromal activation, was also slightly increased in Large BPH Cluster 0 (Table 3.3 A). Also, LTB, which is associated with TLS maintenance, was differentially expressed in Large BPH $CD4^+$ T cells compared to Small BPH (Table 3.3 B). Overall, increased expression of genes associated with lymphoid cell recruitment and stromal activation compared to normal prostates suggest that T cells in the BPH prostate directly and indirectly promote further lymphoid cell recruitment and formation of TLS in BPH prostates. Also, expression of these mediators increased in $CD8^+$ T cells from Large BPH prostates compared to normal but not Small BPH $CD8^+$ T cells compared to normal, suggesting that $CD8^+$ T cells may play a relatively greater role in immune cell recruitment and TLS formation in late-stage symptomatic BPH than in early-stage non-symptomatic BPH.

Table 3.3. DGE of TLS-associated chemokine genes in Cluster 0 $CD8^+$ T cells (top) and Cluster 2 $CD4^+$ T cells(bottom) between sample types.

Cluster 0	**Fold Change**		
Gene	*Large BPH vs Normal*	*Small BPH vs Normal*	*Large BPH vs Small BPH*
CCL20	4.377714	-	0.737085
TNF	5.256931	-	0.297721
CCL4	2.100786	-	-
CCL3	0.342205	-	-
Cluster 2	**Fold Change**		
Gene	*Large BPH vs Normal*	*Small BPH vs Normal*	*Large BPH vs Small BPH*
CXCR3	4.48254	3.904588	0.577951
TNF	2.862653	3.405487	-0.54283
CCL5	2.103035	-	-
CCL4	1.557003	1.897514	-0.34051
CCL20	1.274667	-	-
CCR7	-	3.898129	-
LTB	-	-	0.894589

3.4.4 Correlation between clusters and clinical data

To determine if immune cell populations identified in the clustering analysis correlated with patient clinical data, we compared scRNA-Seq clustering data with International Prostate Symptom Score (IPSS), prostate volume, and body mass index (BMI) for each patient. We also compared the proportion of cells within each cluster with other clusters. Previous studies have linked T cell infiltration and the production of lymphocyte-derived inflammatory mediators to symptomatic BPH [36]. However, this does not rule out the possibility that the activation states and interactions of specific immune cell subtypes such as macrophages rather than the proportions of these cells play a role in driving BPH progression and symptoms.

The proportion of cells from each sample type assigned to each cluster varied among the sample types. $CD8^+$ T cells from large BPH specimens made up the largest proportion of Cluster 0 but the smallest proportion of $CD4^+$ T cells in Cluster 2 (Fig. 3.8 A). Some previous studies have observed an increased proportion of $CD4^+$ T cells to $CD8^+$ T cells in BPH samples, while others have observed a predominance of $CD8^+$ T cells [7, 30, 36]. This difference between studies may be related to various study factors such as sample size or tissue sampling and evaluation approaches, as well as variability in immune cell proportions among individual patient samples.

As expected, IPSS was significantly positively correlated with prostate volume (Fig. 3.8 B). Neither IPSS nor prostate volume were significantly correlated with BMI (Fig. 3.8 B). IPSS and prostate volume were positively correlated with the proportions of T cell clusters except for Cluster 2 $CD4^+$ T cells (Fig. 3.8 B). Also, the proportion of Cluster 2 $CD4^+$ T cells was negatively correlated with the proportion of Cluster 0 $CD8^+$ T cells, indicative of altered $CD4^+$ to $CD8^+$ T cell ratios in BPH specimens reported in previous studies [7, 30]. The proportion of B cells was significantly positively correlated with BMI (Fig. 3.8 B). These results suggest that increased proportions of T cells other than $CD4^+$ T cells play a role in driving prostate expansion and related symptoms.

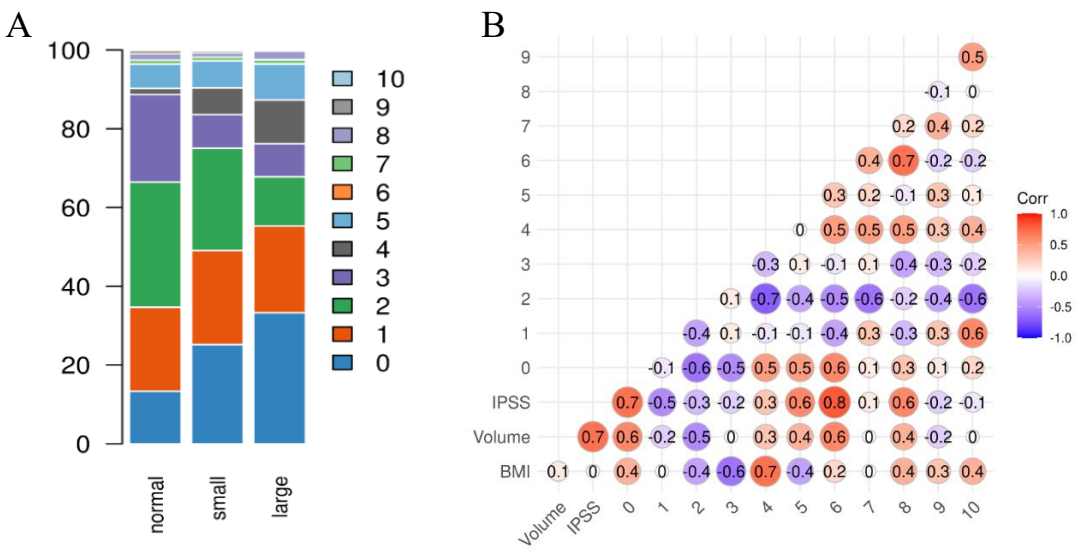

Figure 3.9. (A) Proportion of cells contributing to each cluster from the three sample types. (B) Correlation of the proportion of clusters with other clusters and with clinical parameters (IPSS, prostate volume, BMI). Values ≥ 0.6 or ≤ -0.6 were considered significant.

3.4.5 Mouse model of chronic immune prostatitis

Despite the anatomic differences between human and rodent prostates, mouse models have been invaluable in elucidating the mechanisms of prostate disease. Several rodent models of immune prostatitis have been previously developed [37]. In this study, we compared the morphology of two inducible immune prostatitis mouse models: the POET-3 model and the Aire KO model. POET-3 mice express ovalbumin in prostate epithelial cells under the control of the probasin promoter [29]. Inflammation is induced by adoptive transfer of activated ovalbumin-specific T cells which home to the prostate. Previous studies described the infiltration by myeloid and lymphoid cells accompanied by epithelial and stromal proliferation that follows induction of inflammation in this mouse model (Chapter 2, Fig. 2.3) [28, 29]. These studies have indicated that immune cell populations are initially predominately myeloid and shift to predominantly lymphoid over time, consistent with a chronic inflammatory process [29]. The resulting inflammation peaks around 6-7 days post-induction and steadily declines thereafter [29].

In contrast to the resolving prostatitis of the POET-3 mouse, the Aire KO mouse develops persistent immune prostatitis following induction. In this model, mice developed prostatitis following injection of mouse prostate antigen plus Complete Freud's Adjuvant and boosting with

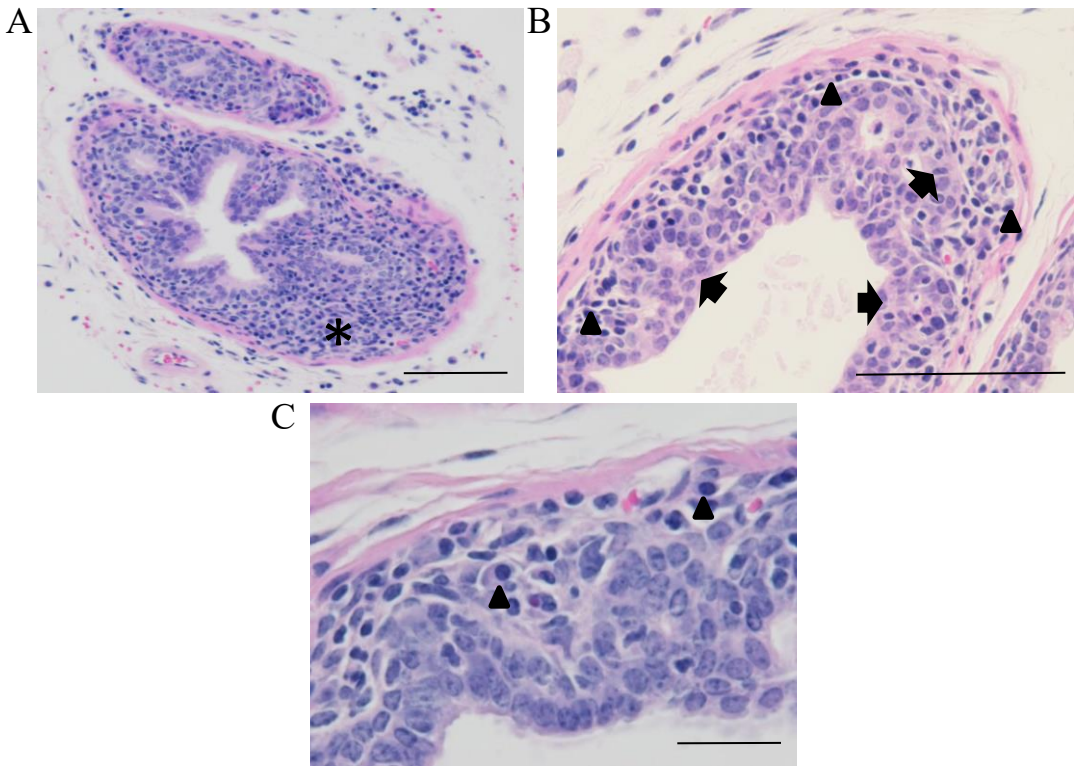

Figure 3.10. (A) Gland from an inflamed Aire KO mouse with subepithelial immune cell infiltrates (asterisk). (B) Subepithelial infiltrates consist of lymphoid cells (arrowheads) adjacent to the thickened epithelium (arrows). Scale bar=100μm. (C) Subepithelial infiltrates consist of lymphocytes and plasma cells (arrowheads). Scale bar=50μm.

Incomplete Freud's Adjuvant. While inflammation in POET-3 prostates begins to decline after about one week, robust immune cell infiltration persisted for at least 3 weeks post-booster injection in Aire KO mice. Immune cell infiltrates were predominately lymphocytic to lymphoplasmacytic and were observed in multiple lobes. Myeloid cells were relatively rare. Multifocally, the subepithelial connective tissue was expanded by immune cell infiltration composed of small lymphocytes and plasma cells (Fig. 3.9). Within the stroma, lymphocytes formed variably sized aggregates and organizing lymphoid structures resembling TLS which occasionally formed germinal centers (Fig. 3.10). $CD8^+$ T cells were present within the parafollicular zones of the follicle-like structures (Fig. 3.10 C). The formation of stromal lymphoid aggregates and organizing lymphoid structures closely resembles the distribution and composition of the lymphoid populations observed in BPH specimens. Evidence of lymphoid infiltration was not observed in sections of pancreas, liver, kidney, or lung, indicating that this induced inflammation

is prostate-specific. The inflammation induced in prostate antigen-immunized Aire KO mice is consistent with a chronic non-resolving immune-mediated inflammatory process.

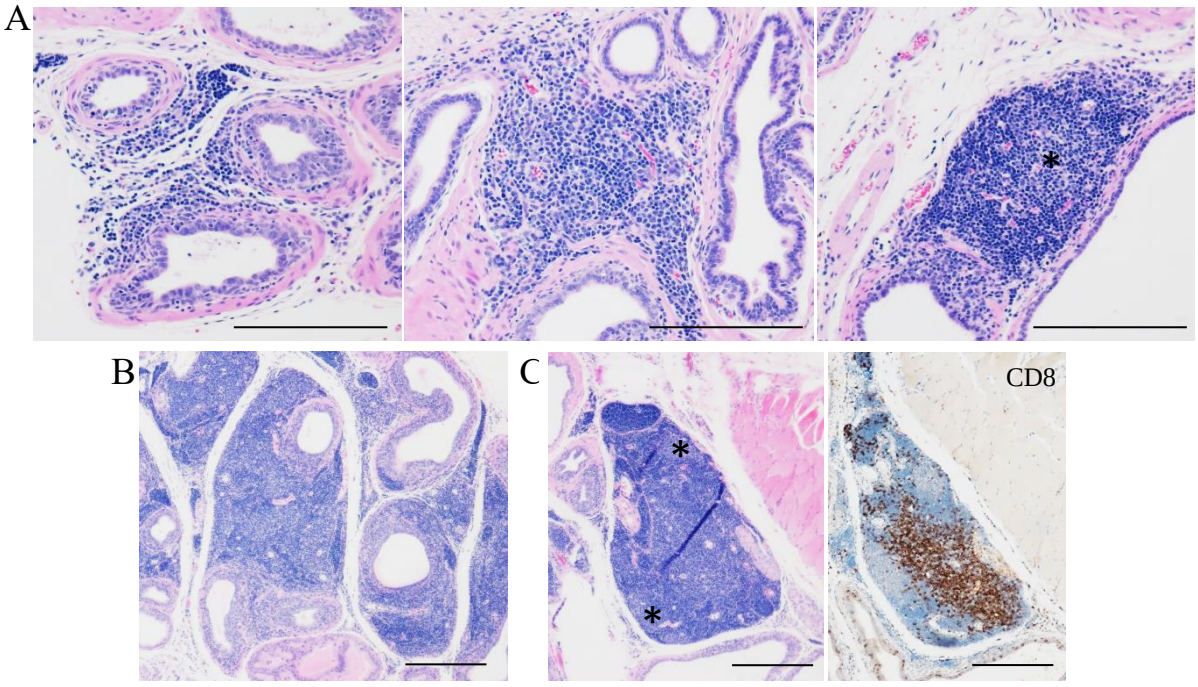

Figure 3.11. (A) Lymphoid aggregates and organizing structures within the stroma of inflamed Aire KO mice forming germinal center-like areas (asterisk). (B) Larger organizing lymphoid structures formed within the stroma and included numerous $CD8^+$ T cells in parafollicular T zones. Scale bar=100μm.

3.5 Discussion

While immune cells make up a relatively small proportion of all the cells of the prostate, they have a significant impact on the growth and function of other prostate cell populations through cellular interactions and the production of cytokines, chemokines, and growth factors [38, 39]. This study examined the morphology, composition, and gene expression of BPH prostate immune cells, in particular organizing stromal lymphoid structures resembling TLS. Overall, this study was consistent with previous studies with regard to the composition and distribution of immune cells in the prostate, particularly the lymphoid component. Histologically, the bulk of these immune cells, particularly lymphoid cells, resided in the stromal compartment, although immune cells were observed in intraepithelial and intraluminal areas as well. This is consistent with the scRNA-Seq clustering analysis, in which $CD4^+$ and $CD8^+$ T cells were the most abundant immune cell types, with smaller populations of macrophages, B cells, mast cells, and plasma cells. Intraepithelial T

cells were predominately $CD8^+$, while $CD4^+$ T cells were located mostly in the periglandular stroma. These $CD4^+$ T cells were often arranged in loose aggregates and organizing lymphoid structures in association with B cells, $CD8^+$ T cells, few $FoxP3^+$ Treg, and macrophages. Organizing follicular structures composed of germinal center-like areas of B cells surrounded by $CD4^+$ T cells were also occasionally observed, resembling the TLS previously described in the non-BPH prostate and PCa specimens [8, 9]. Gene expression of several inflammatory mediators previously associated with lymphocyte recruitment and TLS was increased in BPH lymphoid cells compared to normal prostates, suggesting enhanced lymphoid recruitment and activation in the BPH microenvironment. Overall, the presence of lymphoid aggregates and organizing follicular structures in the BPH prostate suggests a role for mucosa-associated TLS in the persistence of prostate inflammation [8].

The prostate is composed of glandular and stromal compartments. While the proportions of glandular epithelial cells and stromal smooth muscle cells and fibroblasts may change in the BPH prostate compared to the normal prostate, these cell types represent the majority of cells within the normal and diseased prostate [40-42]. The inflammatory cell population in the normal prostate is generally small, consisting of low numbers of T lymphocytes (predominately $CD8^+$ cytotoxic T cells), B lymphocytes and macrophages within the periglandular stroma [2, 7, 30]. In contrast, BPH specimens have increased numbers of $CD45^+$ leukocytes compared to normal prostates [30]. Previous studies noted that $CD3^+$ lymphocytes comprised the majority of infiltrating $CD45^+$ leukocytes in BPH specimens, and some studies have observed a shift in the ratio of $CD8^+$ T cells to $CD4^+$ T cells in favor of $CD4^+$ T cells in BPH compared to normal prostates, although this finding has not been consistent across all studies and may be influenced by sample size and histologic evaluation methods [7, 30, 38]. Theyer et al (1992) also noted an increase in HLA-DR expression in $CD45^+$ leukocytes in BPH compared to normal prostate [30]. Also, previous studies have shown a positive association between lymphocytic infiltration and mRNA expression of specific inflammatory cytokines including IFNγ, IL2, IL13, TGFβ, and IL4 [38]. Furthermore, T cell infiltration and production of lymphocyte-derived inflammatory mediators have been associated with symptomatic BPH [36]. These studies suggest roles for lymphoid populations in BPH; however, the potential roles of organizing lymphoid structures BPH have not been previously explored. In the current study, the presence of these structures in BPH tissues and the expression of TLS-associated chemokine genes by BPH lymphoid populations suggest a role for

these structures in immune cell recruitment and the maintenance and potentially progression of prostatic inflammation in BPH. TLS develop in response to chronic or repeated inflammatory insults including infection, allograft rejection, autoimmunity, and cancer [10, 11]. Inflammatory mediators including CCL3, CCL4, TNFα, and lymphotoxin produced by immune cells stimulate stromal cells to produce the homeostatic chemokines CCL21, CCL19, and CXCL13 and adhesion molecules that promote lymphoid recruitment and TLS formation and maintenance [12-15, 43] In the current study, scRNA-Seq indicates several TLS-associated chemokines and TNF family members are differentially expressed by T cell populations in BPH compared to T cells from normal prostates. Additionally, the correlation of IPSS and prostate volume indicates that specific lymphoid clusters, particularly the positive correlation with T cell clusters with the exception of $CD4^+$ T cells, are associated with the clinical manifestations of BPH. Larger studies regarding the proportions of specific T cell populations and clinical parameters may provide insights into the roles of these cells in clinical BPH and potentially reveal targets for treatment of BPH symptoms.

In the prostate, TLS have been previously observed in association with prostate cancer but also in the normal prostates of aged men [8, 9]. Di Carlo et al (2007) histologically evaluated prostate tissue obtained from men ranging from 62 to 70 years of age and without a histological diagnosis of BPH or PCa [8, 9]. They observed the distribution of lymphoid cells within prostate tissue, including the formation of follicular structures with germinal centers [8]. This study also reported many $FoxP3^+$ Treg associated with these lymphoid aggregates and structures [8]. In the current study, relatively few $FoxP3^+$ Treg were observed within some lymphoid aggregates and structures and a small T cell subcluster differentially expressing FoxP3 was identified by scRNA-Seq. This may suggest a reduction in Treg in BPH specimens, and potentially reflect a failure of regulatory T cell-mediated control of prostate inflammation in BPH. However, this difference may potentially be attributed at least in part to sample staining differences between the previous and current studies, so it is difficult to determine its significance based on these studies alone. A side-by-side age-matched comparison of BPH and non-BPH prostate specimens would aid in determining if there are differences in the Treg number or distribution between BPH and non-BPH prostates.

While lymphoid structures appear to be common in the prostates of older men, they are generally not observed in normal prostates from young men. These observations may suggest that TLS are

more of an age-related phenomenon that develop in response to inflammatory insults over the course of years and not necessarily directly related to BPH. However, as BPH is also associated with age and is hypothesized to be a chronic immune-mediated condition, it is possible that the development of both BPH and TLS is stimulated by similar factors.

Rodent models are the most commonly used animal models in prostate research, and several spontaneous and inducible prostatitis models have been developed. However, marked differences in rodent prostate anatomy mean that rodent models do not completely encompass the anatomic, morphologic and clinical aspects of human prostate disease [44]. Antigen-induced models using prostate homogenates have been used as inducible autoimmune prostatitis models in various mouse strains. Once such model, the Aire KO mouse, develops chronic lymphocytic to lymphoplasmacytic subepithelial and stromal inflammation, occasionally forming lymphoid follicles with germinal centers reminiscent of those observed in aged human prostates. It is anticipated that this mouse model may be useful in elucidating the conditions under which TLS form and their impact on other prostate cell types.

The combination of scRNA-Seq data and histologic examination allows for attempts to correlate morphologic features with gene expression, and potentially provide insights into the relationship between gene expression and immune cell activities in the BPH prostate. While this current study focused on the immune cell populations of BPH prostates and did not include analyses of other cell populations such as stromal cells which are known to be involved in immune cell recruitment and TLS formation, previous studies have explored the roles of other prostate cell types in the immune landscape of BPH. For example, Penna et al (2009) demonstrated that BPH stromal cells can produce pro-inflammatory cytokines and chemokines to recruit immune cells to the prostate and may also act as antigen presenting cells to induce cytokine secretion by $CD4^+$ T cells [3]. Also, CCL21 and CXCL13 produced by prostate stromal cells attract T and B cells via CCR7 and CXCR5, respectively, in the formation of TLS [8]. Although stromal cells were not included in the current scRNA-Seq analysis, scRNA-Seq data published by Strand et al (2019) from whole cell preparations from normal and BPH prostates indicate that CXCL13 expression is increased in BPH fibroblasts, and that CCL21 expression is increased in BPH endothelial cells [45].

The underlying causes of increased immune cell infiltration and the development of lymphoid structures in the prostates of aged men and in BPH is not fully understood. Previous bacterial infection, autoantigens, or hormone-associated immune changes that occur with age have been proposed as possible contributors [46, 47]. Systemic conditions such as obesity, metabolic syndrome and diabetes have also been suggested to impact prostatic inflammation [48]. Also, whether TLS are involved in BPH pathogenesis or develop independent of BPH is not clear. Future studies involving a comparison of TLS from age-matched BPH and non-BPH prostates and spatial transcriptomics techniques may provide further insights into the morphology and gene expression of lymphoid structures and their potential role in BPH.

3.6 References

1. Fibbi, B., et al., *Chronic inflammation in the pathogenesis of benign prostatic hyperplasia.* Int J Androl, 2010. **33**(3): p. 475-88.

2. Kramer, G., D. Mitteregger, and M. Marberger, *Is benign prostatic hyperplasia (BPH) an immune inflammatory disease?* Eur Urol, 2007. **51**(5): p. 1202-16.

3. Penna, G., et al., *Human benign prostatic hyperplasia stromal cells as inducers and targets of chronic immuno-mediated inflammation.* J Immunol, 2009. **182**(7): p. 4056-64.

4. De Nunzio, C., et al., *The controversial relationship between benign prostatic hyperplasia and prostate cancer: the role of inflammation.* Eur Urol, 2011. **60**(1): p. 106-17.

5. Park, H., et al., *Stromal nodules in benign prostatic hyperplasia: morphologic and immunohistochemical characteristics.* Prostate, 2014. **74**(14): p. 1433-43.

6. Deering, R.E., et al., *Morphometric quantitation of stroma in human benign prostatic hyperplasia.* Urology, 1994. **44**(1): p. 64-70.

7. Robert, G., et al., *Inflammation in benign prostatic hyperplasia: a 282 patients' immunohistochemical analysis.* Prostate, 2009. **69**(16): p. 1774-80.

8. Di Carlo, E., et al., *The prostate-associated lymphoid tissue (PALT) is linked to the expression of homing chemokines CXCL13 and CCL21.* Prostate, 2007. **67**(10): p. 1070-80.

9. Garcia-Hernandez, M.L., et al., *A Unique Cellular and Molecular Microenvironment Is Present in Tertiary Lymphoid Organs of Patients with Spontaneous Prostate Cancer Regression.* Front Immunol, 2017. **8**: p. 563.

10. Pitzalis, C., et al., *Ectopic lymphoid-like structures in infection, cancer and autoimmunity.* Nat Rev Immunol, 2014. **14**(7): p. 447-62.

11. Colbeck, E.J., et al., *Tertiary Lymphoid Structures in Cancer: Drivers of Antitumor Immunity, Immunosuppression, or Bystander Sentinels in Disease?* Front Immunol, 2017. **8**: p. 1830.

12. Luo, S., et al., *Chronic Inflammation: A Common Promoter in Tertiary Lymphoid Organ Neogenesis.* Front Immunol, 2019. **10**: p. 2938.

13. Weinstein, A.M. and W.J. Storkus, *Therapeutic Lymphoid Organogenesis in the Tumor Microenvironment.* Adv Cancer Res, 2015. **128**: p. 197-233.

14. Schneider, K., K.G. Potter, and C.F. Ware, *Lymphotoxin and LIGHT signaling pathways and target genes.* Immunol Rev, 2004. **202**: p. 49-66.

15. Tang, H., et al., *Lymphotoxin signalling in tertiary lymphoid structures and immunotherapy.* Cell Mol Immunol, 2017. **14**(10): p. 809-818.

16. Ruddle, N.H., *Lymphoid neo-organogenesis: lymphotoxin's role in inflammation and development.* Immunol Res, 1999. **19**(2-3): p. 119-25.

17. Sautes-Fridman, C., et al., *Tertiary Lymphoid Structures in Cancers: Prognostic Value, Regulation, and Manipulation for Therapeutic Intervention.* Front Immunol, 2016. **7**: p. 407.

18. Dieu-Nosjean, M.C., et al., *Tertiary lymphoid structures, drivers of the anti-tumor responses in human cancers.* Immunol Rev, 2016. **271**(1): p. 260-75.

19. Chiavolini, D., et al., *Bronchus-associated lymphoid tissue (BALT) and survival in a vaccine mouse model of tularemia.* PLoS One, 2010. **5**(6): p. e11156.

20. Slight, S.R., et al., *CXCR5(+) T helper cells mediate protective immunity against tuberculosis.* J Clin Invest, 2013. **123**(2): p. 712-26.

21. Rangel-Moreno, J., et al., *Pulmonary expression of CXC chemokine ligand 13, CC chemokine ligand 19, and CC chemokine ligand 21 is essential for local immunity to influenza.* Proc Natl Acad Sci U S A, 2007. **104**(25): p. 10577-82.

22. Koenig, A. and O. Thaunat, *Lymphoid Neogenesis and Tertiary Lymphoid Organs in Transplanted Organs.* Front Immunol, 2016. **7**: p. 646.

23. Henry, G., et al., *Molecular pathogenesis of human prostate basal cell hyperplasia.* Prostate, 2017. **77**(13): p. 1344-1355.

24. Macosko, E.Z., et al., *Highly Parallel Genome-wide Expression Profiling of Individual Cells Using Nanoliter Droplets.* Cell, 2015. **161**(5): p. 1202-1214.

25. Hafemeister, C. and R. Satija, *Normalization and variance stabilization of single-cell RNA-seq data using regularized negative binomial regression.* Genome Biol, 2019. **20**(1): p. 296.

26. Zappia, L. and A. Oshlack, *Clustering trees: a visualization for evaluating clusterings at multiple resolutions.* Gigascience, 2018. **7**(7).

27. Benjamini, Y., Hochberg, Y., *Controlling the false discovery rate: a practical and powerful approach to multiple testing.* Journal of the Royal Atatistical Society Series B 57, 1995: p. 289-300.

28. Wang, H.H., et al., *Characterization of autoimmune inflammation induced prostate stem cell expansion.* Prostate, 2015. **75**(14): p. 1620-31.

29. Haverkamp, J.M., et al., *An inducible model of abacterial prostatitis induces antigen specific inflammatory and proliferative changes in the murine prostate.* Prostate, 2011. **71**(11): p. 1139-50.

30. Theyer, G., et al., *Phenotypic characterization of infiltrating leukocytes in benign prostatic hyperplasia.* Lab Invest, 1992. **66**(1): p. 96-107.

31. Barros, M.H., et al., *Macrophage polarisation: an immunohistochemical approach for identifying M1 and M2 macrophages.* PLoS One, 2013. **8**(11): p. e80908.

32. Henry, G.H., et al., *A Cellular Anatomy of the Normal Adult Human Prostate and Prostatic Urethra.* Cell Rep, 2018. **25**(12): p. 3530-3542 e5.

33. Globa, T., et al., *Mast cell phenotype in benign and malignant tumors of the prostate.* Pol J Pathol, 2014. **65**(2): p. 147-53.

34. Groom, J.R. and A.D. Luster, *CXCR3 in T cell function.* Exp Cell Res, 2011. **317**(5): p. 620-31.

35. Nerviani, A. and C. Pitzalis, *Role of chemokines in ectopic lymphoid structures formation in autoimmunity and cancer.* J Leukoc Biol, 2018. **104**(2): p. 333-341.

36. Norstrom, M.M., et al., *Progression of benign prostatic hyperplasia is associated with pro-inflammatory mediators and chronic activation of prostate-infiltrating lymphocytes.* Oncotarget, 2016. **7**(17): p. 23581-93.

37. Vykhovanets, E.V., et al., *Experimental rodent models of prostatitis: limitations and potential.* Prostate Cancer Prostatic Dis, 2007. **10**(1): p. 15-29.

38. Steiner, G.E., et al., *Cytokine expression pattern in benign prostatic hyperplasia infiltrating T cells and impact of lymphocytic infiltration on cytokine mRNA profile in prostatic tissue.* Lab Invest, 2003. **83**(8): p. 1131-46.

39. Kramer, G., et al., *Increased expression of lymphocyte-derived cytokines in benign hyperplastic prostate tissue, identification of the producing cell types, and effect of differentially expressed cytokines on stromal cell proliferation.* Prostate, 2002. **52**(1): p. 43-58.

40. Karthaus, W.R., et al., *Identification of multipotent luminal progenitor cells in human prostate organoid cultures.* Cell, 2014. **159**(1): p. 163-175.

41. Shen, M.M. and C. Abate-Shen, *Molecular genetics of prostate cancer: new prospects for old challenges.* Genes Dev, 2010. **24**(18): p. 1967-2000.

42. Treuting, P.M., et al., *Comparative anatomy and histology a mouse and human atlas*. 2012, Elsevier,: London. p. 1 online resource (474 p.).

43. Jing, F. and E.Y. Choi, *Potential of Cells and Cytokines/Chemokines to Regulate Tertiary Lymphoid Structures in Human Diseases.* Immune Netw, 2016. **16**(5): p. 271-280.

44. Ittmann, M., et al., *Animal models of human prostate cancer: the consensus report of the New York meeting of the Mouse Models of Human Cancers Consortium Prostate Pathology Committee.* Cancer Res, 2013. **73**(9): p. 2718-36.

45. Strand, D.W. *Single-Cell RNA-sequencing Data-Strand Lab*. 2019; Available from: https://dev.strandlab.net/sc.data/.

46. Vignozzi, L., et al., *Antiinflammatory effect of androgen receptor activation in human benign prostatic hyperplasia cells.* J Endocrinol, 2012. **214**(1): p. 31-43.

47. Neyt, K., et al., *Tertiary lymphoid organs in infection and autoimmunity.* Trends Immunol, 2012. **33**(6): p. 297-305.

48. Vignozzi, L., et al., *Fat boosts, while androgen receptor activation counteracts, BPH-associated prostate inflammation.* Prostate, 2013. **73**(8): p. 789-800.

CHAPTER 4. IMMUNE CELL INTERACTIONS IN BENIGN PROSTATIC HYPERPLASIA

Meaghan M Broman, Nadia A Lanman, Renee E Vickman, Gregory M Cresswell, Juan Sebastian Paez Paez, Susan Crawford, Simon W Hayward, Gervaise Henry, Douglas Strand, Timothy L Ratliff

4.1 Abstract

Benign Prostatic Hyperplasia (BPH) is the most common prostatic disease among older men. While chronic inflammation is frequently associated with BPH, the role of interactions between and within immune cell populations in BPH development and progression is unclear. Single cell RNA sequencing (scRNA-seq) is used to identify cell types and signaling pathways in healthy and diseased tissues and, more recently, identify ligand-receptor interactions within tumors. Here we further develop and apply these methods to identify and predict immune cell ligand-receptor pairs to elucidate the potential roles of immune cell interactions in BPH.

scRNA-Seq data from immune cells isolated from small early-stage BPH and large late-stage BPH were combined with scRNA-Seq data from three normal prostates and immune cell subtypes were identified based on marker gene expression profiles. Ligand-receptor interaction scores were then calculated based on ligand and receptor gene expression and cell number referencing databases of known ligand-receptor pairs. Median ligand-receptor scores were compared between BPH and normal prostate samples.

Bioinformatic analysis of combined sample scRNA-Seq data identified 11 immune cell clusters. DGE patterns and pathway analyses among myeloid/macrophage subsets suggest a mixed inflammatory microenvironment in BPH. Comparison of ligand-receptor interaction scores between sample types indicate that immune cell interactions, particularly specific interactions involved in immune cell migration, adhesion, and activity, are altered between BPH and normal prostates and between early-stage and late-stage BPH, suggesting that these interactions may contribute to the perpetuation of BPH inflammation.

These results indicate that interactions between and among immune cell populations perpetuate the non-resolving inflammatory microenvironment of BPH. This study identifies potential

immune-related disease mechanisms and targets for further validation and study and also highlights the utility of scRNA-Seq and bioinformatic analysis techniques in identification and comparison of cellular interactions in diseased and normal tissues.

4.2 Introduction

Prostatitis is a common urologic condition with an estimated overall prevalence from 2% to 16% [5-7]. The National Institutes of Health (NIH) divides prostatic inflammation into four categories: acute bacterial prostatitis (Type I), chronic bacterial prostatitis (Type II), chronic prostatitis/chronic pelvic pain syndrome (CP/CPPS) (Type III), and asymptomatic inflammatory prostatitis (Type IV) [8, 9]. Around 90% of diagnosed prostatitis cases in men are categorized as CP/CPPS [8]. The pathogenesis of CP/CPPS is unclear, as no infectious cause is identified [8]. A role for immune cells in the development and progression of BPH was first proposed by Moore in 1937 [10]. High prostate inflammatory cell infiltration has been associated with increased International Prostate Symptom Score (IPSS) and LUTS [3, 11]. Also, a study by St. Sauver et al (2008) suggested that men diagnosed with prostatitis were at a higher risk of developing symptoms related to BPH as well as being more likely to eventually require medical or surgical treatment for BPH [5].

Immune cell signaling and cytokine production are known to modulate the microenvironment of the normal and diseased prostate. Several studies have characterized the composition and cytokine profile of immune cells in the normal and BPH prostate [3, 12-15]. As discussed in Chapter 2, the overall immune cell population is small in the normal prostate and consists predominately of $CD8^+$ T lymphocytes, B cells and macrophages and small numbers of other immune cell types such as mast cells and plasma cells (Chapter 2) [3, 12]. As men age, the overall number of immune cells increases [3, 13, 16]. In BPH, immune cells are commonly associated with hyperplastic nodules and consist predominately of activated $CD4^+$ memory T cells [3, 13, 16-18]. Immune cell recruitment and activation occur under the influence of various cytokines produced by multiple prostate cell types. Pro-inflammatory cytokines such as interleukin 15 (IL-15) produced by stromal smooth muscle cells and interferon γ (IFNγ) from T cells recruit $CD4^+$ T lymphocytes [13, 19]. Also, immune cell-derived cytokines may promote stromal and epithelial cell activation and proliferation [14, 20]. One important feature of BPH inflammation is its progressive and non-

resolving nature. Unlike most tissue inflammation following injury which eventually wanes and resolves, BPH inflammation continues and often worsens over time. It is hypothesized that immune-mediated mechanisms may underlie the failure of BPH inflammation to resolve as well as the development and progression of cellular hyperplasia and LUTS, and that immune cells and their interactions may represent potential BPH therapeutic targets [13, 21]. However, the means by which various immune cell populations may contribute to BPH and the perpetuation of associated inflammation are not fully understood [13].

Advances in scRNA-Seq methods over the past decade have elucidated the extent of gene expression, regulation and signaling networks in cells from normal and diseased tissues [22-24]. scRNA-Seq has been previously used to identify and define cell types and subtypes by differential gene expression (DGE) patterns within various tissues and cell populations, as well as to identify and compare cellular signaling pathway activation [22-24]. scRNA-Seq has been increasingly used to characterize cellular populations in various normal and diseased tissues, including the prostate (Chapter 2) [25]. More recently, methods to predict ligand-receptor interactions among cell types using scRNA-Seq data have been developed and published [24, 26]. Cell-cell communications via ligand-receptor interactions play a vital role in cellular function and homeostasis, cell differentiation, and tissue and organ development [23]. Perturbations in cell-cell communications contribute to the development of disease states such as autoimmune disease and cancer [23]. Some specific ligand-receptor pairs between prostate cell types are known to impact immune cells in the prostate [12]. For example, CXCL13 expressed by follicular dendritic cells (FDC) promotes CXCR5-expressing B cell migration and organization, and CCL21 produced by endothelial cells recruits CCR7-expressing T cells [12]. However, the roles of receptor-ligand interactions between various cell types in healthy and diseased prostates is largely unclear. BPH has been hypothesized to be an immune-mediated disease, however the potential roles of immune cell subtypes in the initiation and progression of BPH are not clear [13]. Similarly, immune cell ligand-receptor interactions and the roles they may play in BPH are also not fully elucidated. As discussed in Chapter 2, gene expression of multiple chemokines known to be involved in immune cell recruitment and activation through interactions with specific stromal cell receptors was increased in BPH lymphocytes compared to normal prostates, suggesting that interactions between inflammatory mediators and their receptors may be altered in BPH (Chapter 2). It is hypothesized

that alterations in ligand-receptor interactions between and among immune cell populations contribute to the perpetuation and progression of BPH inflammation.

The aim of this current study is to further develop scRNA-Seq analysis methods to further characterize immune cell populations and to predict and compare ligand-receptor interactions among immune cells in small early-stage BPH, large late-stage BPH tissues and normal non-BPH prostate tissues. Overall, results indicate a mixed inflammatory microenvironment perpetuated by interactions between myeloid/macrophage and $CD8^+$ T cell populations. It is anticipated that this study will further clarify the immune landscape of the prostate and contribute to our understanding of the roles of immune cells in the initiation and progression of BPH.

4.3 Methods

4.3.1 Human prostate samples

BPH prostatic tissues were obtained from BPH patients undergoing simple prostatectomy (SP) or robot-assisted laparoscopic prostatectomy (RALP) surgery for symptomatic BPH or prostate cancer (PCa) as described in detail in Chapter 3, Section 3.3.1. In summary, transitional zone tissues from 10 Small BPH (<60g) and 3 Large BPH (>70g) were collected and processed for scRNA-Seq. Sections from each prostate were fixed in 10% NBF for histology and immunohistochemistry.

4.3.2 BPH tissue processing, sorting and isolation of BPH prostate cell populations

BPH tissues were processed for scRNA-Seq as described in Chapter 3, Section 3.3.2 and 3.3.3. In summary, transition zone tissues from each sample were digested and processed to a single cell suspension. Samples were incubated with 5ul Human TruStain Fx Blocking reagent (Biolegend) and 0.5ul Zombie Viability Dye (Biolegend) in 100ul PBS per sample then incubated with an antibody cocktail of CD45-PE (clone HI30, Biolegend) pan-leukocyte marker, EpCAM-APC (clone 9C4, Biolegend) epithelial cell marker, and CD200-PE/Cy7 (clone OX-104, Biolegend) endothelial cell marker or single antibodies for compensation controls (if necessary) for 30 minutes at 4^{o}C. Samples were washed with PBS spun down then resuspended in complete RPMI for live cell sorting on the BD FACS ARIA II (BD Biosciences, San Jose, CA) to isolate $CD45^+EpCAM^-CD200^-$ immune cells. Prior to loading, some BPH cell preps were labeled with TotalSeq-B

Antibodies (Biolegend) CD3 (clone UCHT1), CD4 (clone RPA-T4), CD8 (clone RPA-T8), CD11b (clone ICRF44), and CD19 (clone HIB19 per manufacturer instructions.

4.3.3 Single-cell RNA-Seq

scRNA-Seq of BPH samples was performed as described in Chapter 3, Section 3.3.4. In summary, sorted $CD45^{+}EpCAM^{-}CD200^{-}$ immune cells from each BPH sample were counted, prepped and loaded into the 10X Chromium chip for a 5000 target cell recovery per 10X Genomics protocols. cDNA synthesis and clean-up steps were performed per manufacturer protocols. cDNA content and quality were assessed via Agilent Bioanalyzer (Agilent Technologies, Santa Clara, CA). Sample library preparation was performed per 10X Genomics protocols prior to sequencing. The resulting data was combined with previously published scRNA-Seq data from three normal prostates [25].

4.3.4 Sample sequencing and data analysis

BPH samples were sequenced and analyzed as described in detail in Chapter 3, Section 3.3.4. In summary, BPH samples were sequenced by the Purdue Genomics Core using a NovaSeq S4 flow cell on a NovaSeq 6000 platform (Illumina, San Diego, CA). Paired-end, 2x150 base-pair reads were sequenced to a depth of 50,000 reads per cell. TotalSeq-B antibody libraries for quantification of cell surface proteins were sequenced at a depth of 5,000 reads per cell. Distinct immune cell clusters were identified based on gene expression patterns and marker genes, as well as using the protein expression observed from the CD3, CD4, CD8, CD11b, and CD19 CITE-seq data and subsequently classified based on known immune phenotypes.

4.3.5 Interaction score calculation

BPH sample scRNA-Seq data were combined with previously published scRNA-Seq data (Henry et al., 2018) from three normal non-BPH prostates. Ligand-receptor interaction scores were then calculated using methods previously published by Kumar et al (2018) based on ligand and receptor gene expression and cell number and referencing databases of known ligand-receptor pairs [24, 26]. Ligand and receptor pairs with experimentally observed interactions from two databases were filtered to include only those that were identified by a Wilcoxon rank sum test (FDR<0.05) as

differentially expressed between condition (large prostatic tissue BPH associated leukocytes, small prostatic tissue BPH associated leukocytes, and normal prostatic tissue associated leukocytes) [23, 32]. For these filtered ligand-receptor pairs, interaction scores were calculated as in equation 1 [26].

Eq 1. $$Interaction\ score = \frac{1}{n_{cell\ type\ 1}} \sum_{i \in cell\ type\ 1} e_{i,receptor} \times \frac{1}{n_{cell\ type\ 2}} \sum_{j \in cell\ type\ 2} e_{j,ligand}$$

$e_{i,j}$ = normalized expression of gene *j* in cell *i*

n_c = number of cells of cell type *c*

4.3.6 RNA isolation, cDNA synthesis and qPCR

RNA was isolated from TRK buffer-lysed cell samples using the Promega Total RNA Kit (Promega, Madison, WI) and per manufacturer protocols. cDNA was synthesized using reverse transcriptase (New England Biolabs, Ipswich, MA). qPCR was performed using Quanta PerfeCTa FastMix II (QuantaBio, Beverly, MA) and commercial probes (Integrated DNA Technologies, Coralville, IA) for the following genes: TIMP1, CD63, VIM, CD44, VEGFA, NRP2.

4.4 Results

4.4.1 Immune cell clustering analysis identifies immune cell subtypes

BPH patient selection and tissue collection were discussed in Chapter 3. In summary, TZ tissues were collected from 10 small (<60 grams) "early-stage" BPH prostates and 3 large (>70 grams) "late-stage" BPH prostates from patients undergoing prostatectomy surgery for low Gleason score (≤7) PZ prostate tumors or symptomatic BPH, respectively. Patient ages ranged from 61 to 76 years with no significant difference in age between small BPH and large BPH patients. Other patient criteria included no previous history of chronic prostatitis or uncontrolled diabetes, and no prior indwelling catheter. Clinical data from BPH patients are summarized in Table 3.1.

For BPH prostate immune cell scRNA-Seq, $CD45^{+}EpCam^{-}CD200^{-}$ immune cells were isolated and analyzed as described in Chapter 3. Initial analysis of the combined samples (10 small BPH, 3 large BPH, and 3 normal prostates) separated all immune cells into 11 clusters (Fig 4.1). Overall, immune cells from the three sample types clustered in a generally similar manner, indicating the presence of similar immune cell subtypes among sample types.

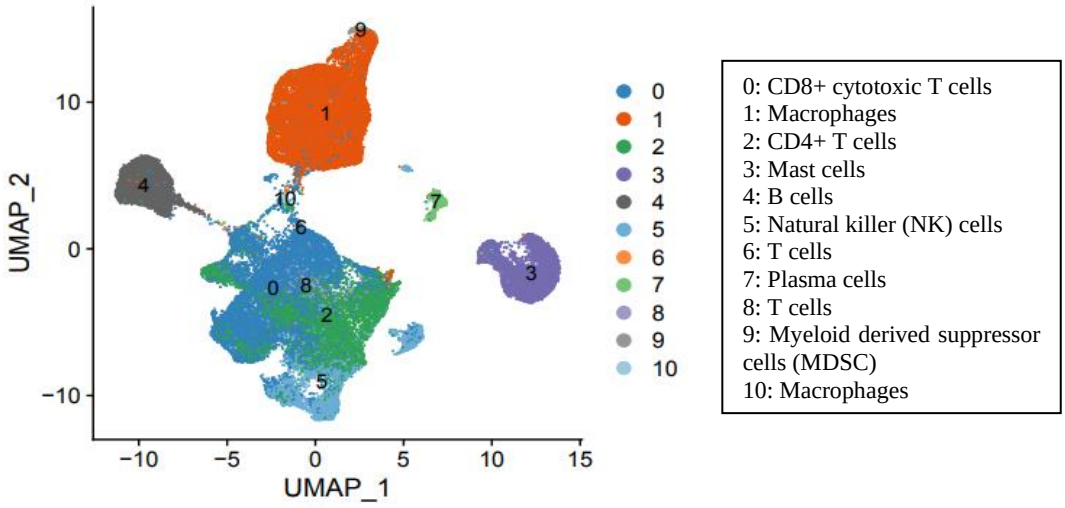

Figure 4.1 Combined immune cell clustering and the identification of cell type of each cluster.

Overall, these results demonstrate that immune cells from large, small, and normal prostates generally cluster in a similar manner, with T cells the predominate cell type in both BPH and normal prostates, followed by macrophages, B cells, and mast cells. These findings are consistent with previous studies which identified T lymphocytes and macrophages as the predominate immune cell types in the prostate [3, 12, 13, 17]. These findings indicate that while similar immune cell types are present in each sample type, the distribution and proportions of immune cell types vary among small and large BPH and normal prostate, which may suggest a role for a particular immune cell type or types in BPH.

4.4.2 Interaction scoring predicts immune cell ligand-receptor interactions

Since immune cell infiltration has been associated with BPH progression and ligand-receptor interactions between prostate cell types are known to influence immune cell recruitment and activation, we hypothesized that immune cell interactions between symptomatic BPH and early

non-symptomatic prostates and between BPH and normal non-BPH prostates would be altered, and these alterations may contribute to the immune cell composition, gene expression, and signaling observed in BPH. To examine alterations in immune cell interactions among the BPH and normal prostates, we adapted a method to use single cell gene expression data to predict and score ligand-receptor interactions previously developed by Kumar et al (2018) to predict ligand-receptor interactions in tumors [26]. In summary, this method uses scRNA-Seq data of ligand and receptor gene expression and cell number to predict and score interactions between known ligand-receptor pairs referencing published databases. This method was applied to the scRNA-Seq data from the three sample types and predicted interaction scores were compared between sample types to identify differences. As we were interested in interactions between live cells, predicted interactions that involved proteins released from dying or dead cells or interactions between components of receptor complexes such as B2M and HLA were removed from the analysis.

To elucidate the ligand and receptor expression within each cell type in each sample type, we examined the correlation between expression of ligand and receptor genes. In general, expression of ligands increased in BPH specimens compared to normal, while expression of receptor genes remained low for most cell types. In contrast, Cluster 0 $CD8^+$ T cells and Cluster 1 macrophages showed relatively high expression of receptors, and both receptor and ligand expression were increased in BPH cells compared to normal. This suggests that cell-cell communication is enhanced in BPH. Interestingly, in both $CD8^+$ T cells (Cluster 0) and macrophages (Cluster 1), the number of ligand genes expressed in each sample type was strongly correlated with the number of receptor genes expressed in those clusters, suggesting that these cell types may be involved in more extensive interactions to and from other cells compared to other immune cell types (Fig. 4.2 A). Furthermore, this correlation was even stronger in Cluster 0 and Cluster 1 cells from both Small and Large BPH compared to normal prostate, suggesting that ligand/receptor interactions involving $CD8^+$ T cells and macrophages are altered in BPH (Fig. 4.2 A). Also, the expression of ligands and receptors involved in autocrine interactions was strongly correlated in macrophage Cluster 1 and in myeloid/macrophage Cluster 10 and increased in BPH compared to normal, while the correlation of autocrine ligands and receptors among $CD8^+$ T cell Cluster 0 was low (Fig. 4.2 B). Additionally, the correlations among the other T cell clusters were generally near or below the average percentage of ligand and receptor expression. These results suggest that myeloid/macrophage cells may strongly influence their own activity through ligand/receptor

interactions on the same cell, while T cell activity is influenced mostly through interactions with other cells and less so through autocrine interactions.

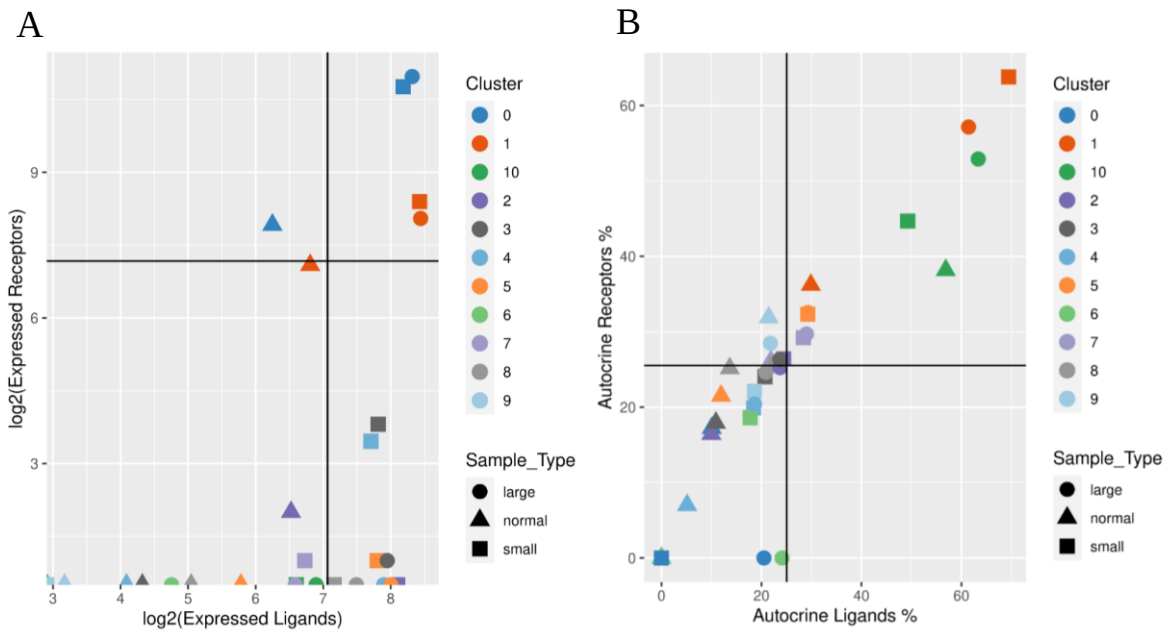

Figure 4.2. (A) Correlation of the number of ligand and receptor genes expressed in each cluster. (B) Percentage of autocrine ligands and receptors expressed among cells within each cluster.

To predict alterations in ligand-receptor interactions between sample types, interaction scores for individual ligand-receptor pairs were compared between sample types. For most interactions between the various immune cell subsets, particularly those involving myeloid/macrophage clusters, scores were overall increased between Small BPH normal, between Large BPH and normal, and between Small BPH and Large BPH. In all, 2415, 959, and 333 significantly different scores were identified between small BPH and normal, between large BPH and normal, and between Large BPH and Small BPH, respectively. Overall, most ligand-receptor pairs that were predicted to be altered between and within various clusters among all sample types fell into three broad and overlapping categories: pairs associated with 1) cell migration and adhesion, 2) immune cell recruitment and activity, and 3) angiogenesis and wound repair in various tissues (Table 4.1). While many pairs have not been previously studied in the context of the prostate, a few predicted pairs have been previously implicated in prostate disease, particularly in prostate cancer [35, 36]. Also, several pairs involving interleukins and their receptors were predicted to be altered between sample types, indicating that interleukin signaling networks are also altered in BPH (Table 4.1).

These results suggest alterations in immune cell interactions involved in cell migration and recruitment and in inflammatory signaling in BPH compared to normal prostates, and these alterations may contribute to the overall increased immune cell numbers and composition in BPH.

Table 4.1 Previously described functions of select predicted ligand-receptor pairs.

Function	**Ligand/Receptor**
Interleukin signaling	IL10/IL10RA IL1RN/IL1R1 IL1RN/IL1R2 IL2/IL2RA IL2/IL2RB ICAM1/IL2RA
Cell adhesion and migration	VIM/CD44 TIMP1/CD63 ICAM1/ITGAX MMP9/CD44 PLAU/PLAUR
Immune cell recruitment and activation	CCL5/SDC4 CCL20/CXCR3 TNF/TNFRSF1B LTB/CD40 TGFB1/SDC2 TGFB1/TGFBR2
Angiogenesis and wound repair	VEGFA/NRP2 HBEGF/CD44 SPP1/CD44
Prostate disease (PCa)	CXCL16/CXCR6 HBEGF/CD9 HBEGF/CD44

The ligand-receptor pair with the greatest increase in scores between small BPH and normal, large BPH and normal, and large BPH and small BPH was vimentin (VIM) and CD44. Interactions between vimentin and CD44 have been associated with adhesion and migration of various cell types [37, 38]. Also, VIM expression by immune cells, including macrophages and lymphocytes, has also been associated with activation and modulation of immune cell function [39]. Alterations in this interaction were predicted between and within multiple clusters, with the greatest score difference within the mast cell cluster (Cluster 3). This increase in VIM/CD44 scoring in BPH suggests enhanced immune cell migration involving multiple immune cell types in BPH.

Interestingly, many of the VIM/CD44 interactions with the greatest difference in scores between BPH and normal were between macrophage and mast cell subsets, either as macrophage/mast cell or as macrophage/macrophage or mast cell/mast cell subset interactions, suggesting that this interaction may be of particular importance for myeloid cell migration and adhesion in BPH.

Interaction between tissue inhibitor of metalloproteinase 1 (TIMP1) and CD63 was among the next most significantly increased interactions in BPH compared to normal. The greatest TIMP1/CD63 score difference between small BPH and normal was between Cluster 1 macrophages and Cluster 3 mast cells, and between large BPH and normal were within Cluster 3 mast cells. Like vimentin and CD44, the interaction between TIMP1 and CD63 has been associated with adhesion and migration in various cell types [37, 38, 40]. Also, CD63 has been associated with mast cell activation and cytokine production [41].

Table 4.2. Predicted ligand-receptor interactions with the greatest score difference between sample types.

Ligand	Receptor	Cluster from	Cluster to	Score Difference	P Value
Small BPH vs Normal					
VIM	CD44	3	3	5.837826	1.91E-08
VIM	CD44	10	3	5.066115	9.12E-05
VIM	CD44	3	2	4.666841	3.14E-08
VIM	CD44	3	1	4.207507	2.64E-07
VIM	CD44	3	5	4.120679	4.27E-06
Large BPH vs Normal					
VIM	CD44	3	3	6.130169	0.017364
VIM	CD44	10	3	5.885330	0.006101
VIM	CD44	6	3	4.828236	0.032099
VIM	CD44	3	2	4.790438	0.022711
VIM	CD44	10	2	4.422772	0.010246
Large BPH vs Small BPH					
VIM	CD44	6	3	3.192855	0.038176
VIM	CD44	9	3	2.539327	0.035532
VIM	CD44	6	2	2.379563	0.042859
VIM	CD44	3	9	2.305077	0.010252
VIM	CD44	10	9	2.054921	0.003231

When expression of CD44, VIM, TIMP1, and CD63 was compared across all clusters, CD44 was differentially expressed in the myeloid/macrophage clusters 1 and 9, as well as in mast cells (Table 4.2). Its predicted ligand, VIM, was highly expressed in mast cells (Cluster 3) and either not differentially expressed or reduced in other clusters (Table 4.2). TIMP1 expression was increased in the three myeloid/macrophage clusters (clusters 1, 9, and 10), and the expression of its receptor CD63 was increased in the mast cell cluster 3 and myeloid/macrophage cluster 10 compared to other immune cell clusters (Table 4.2). VIM and CD44 expression were increased in Cluster 1 macrophages from Large BPH compared to normal, and expression of VIM, CD44, and CD63 were increased in mast cells from Small BPH and Large BPH compared to normal prostate mast cells. Also, distribution of cells expressing these genes varied among and within individual clusters, suggesting cellular heterogeneity within clusters (Fig. 4.3). In all, interactions within and between all identified myeloid populations (including mast cells) accounted for 37% and 51% of

Table 4.3. Differential gene expression of VIM, CD44, TIMP1, and CD63 among clusters.

	Fold Change			
Cluster	**VIM**	**CD44**	**TIMP1**	**CD63**
0	-5.74095	-2.25817	-4.98425	-2.42679
1	-2.78363	**1.979624**	**4.123172**	-
2	-2.88182	-2.43932	-5.47265	-2.41372
3	**5.536098**	**0.943176**	-1.96339	**3.099975**
4	-6.60369	-0.83193	-4.35794	-2.31268
5	-3.3439	-2.49576	-4.44904	-
6	-	-	-7.16008	-2.32219
7	-3.36997	-3.39739	-3.42794	-1.56351
8	-	-2.63655	-	-2.39396
9	-3.30279	**0.827007**	**1.898189**	-1.42855
10	-1.16745	-1.27789	**0.84946**	**1.297197**

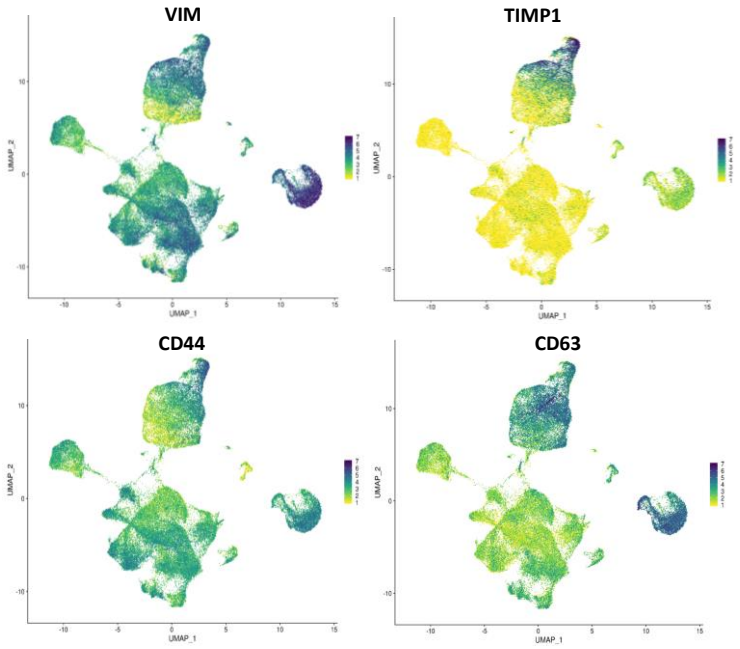

Figure 4.3. Distribution of cells expressing VIM, CD44, TIMP1, and CD63 among clusters.

altered interaction scores between Small BPH and normal and between Large BPH and normal, respectively. These findings indicate significant alterations in communication among myeloid populations within the BPH microenvironment, particularly involving myeloid cell recruitment and activation, which may indicate an important role for these cell types in the increase in immune cell infiltration in BPH.

When predicted interaction scores between Cluster 0 $CD8^+$ T cell ligands and myeloid cell receptors were compared, IFNG/IFNGR1, IFNG/IFNGR2, and TNF/TNFRSF1B were the highest score differences between BPH and normal, particularly with Cluster 1 macrophages (Table 4.4). VIM/CD44 was also significantly increased in Large BPH vs Small BPH, and overall there were fewer significantly different scores and those differences were usually smaller. TNF/TNFRSF1B interaction between Cluster 0 and Cluster 9 MDSC was predicted to be increased between Small BPH and normal and between Large BPH and normal. IFNγ has been associated with promoting a pro-inflammatory M1 macrophage phenotype [43]. TNFα has also been associated with M1 macrophage polarization; however, TNFα has also been associated with enhanced immunosuppressive activity by MDSC [43-45]. When gene expression of these ligand and receptors was compared between samples, TNFRSF1A, TNFSFR1B, and IFNGR2 expression was

increased in Cluster 1 macrophages from Large BPH compared to normal. Additionally, Cluster 0 $CD8^+$ T cell expression of TNF and TNFRSF1A were increased in large BPH, and IFNG was increased in both large and small BPH compared to normal. TNF/TNFRSF1B was slightly decreased in Large BPH compared to Small BPH, which may suggest this interaction may play a greater role in the early stages of BPH than the later. In all, these findings suggest that CD8+ T cells may promote pro-inflammatory macrophage polarization and activity but may also influence anti-inflammatory activity by immunosuppressive myeloid subsets, thereby contributing to the mixed inflammatory BPH microenvironment.

Table 4.4. Ligand-receptor interactions involving Cluster 0 CD8+ T cells and myeloid/macrophage clusters (1,9,10) with the highest significantly different scores (P value ≤ 0.05) between sample types.

Ligand	Receptor	Ligand Cluster	Receptor Cluster	Score Difference	P value
Small BPH vs Normal					
VIM	CD44	0	1	2.183866364	1.90E-06
VIM	CD44	0	10	1.971719769	1.04E-05
IFNG	IFNGR1	0	1	0.495798822	6.06E-05
TNF	TNFRSF1B	0	1	0.493181731	2.81E-05
IFNG	IFNGR2	0	1	0.466891045	7.88E-05
Large BPH vs Normal					
VIM	CD44	0	9	1.754291532	0.001051
VIM	CD44	0	1	1.65592721	0.042691
IFNG	IFNGR1	0	1	0.442489395	0.00746
TNF	TNFRSF1B	0	9	0.226397853	1.34E-04
TNF	TNFRSF1B	0	1	0.224885189	0.00133
Large BPH vs Small BPH					
VIM	CD44	0	9	1.201072839	0.00495
TGFB1	TGFBR2	0	10	-0.069938954	0.026362
TNF	TNFRSF1A	0	1	-0.087733808	0.020748
CCL5	SDC4	0	1	-0.19926251	0.038316
TNF	TNFRSF1B	0	1	-0.268296543	0.002186

When interactions from Cluster 1 macrophages to Cluster 0 $CD8^+$ T cells were examined, score differences between Small BPH and normal were overall small and included interactions associated with anti-inflammatory processes including IL10/IL10RA and TGFB1/TGFBR2 (Table 4.5). Differences between Large BPH and normal included those involved in tissue repair (HBEGF/CD44) but also interactions involved in T cell recruitment (CXCL16/CXCR6) and cell adhesion and migration (MMP9/CD44) (Table 4.5). This suggests that macrophage-T cell

communications are a mix of anti- and pro-inflammatory signals but may shift towards a more pro-inflammatory character as BPH progresses and further promote T cell migration to the prostate microenvironment. This is consistent with the increase in T cells and progressive nature of BPH inflammation over time.

Table 4.5. Cluster 1 to Cluster 0 interactions with the greatest score differences between sample types.

Ligand	Receptor	Ligand Cluster	Receptor Cluster	Score Difference	P value
Small BPH vs Normal					
VIM	CD44	1	0	1.969244037	0.027968
IL10	IL10RA	1	0	0.165152776	0.036489
TGFB1	TGFBR2	1	0	0.136288537	0.008063
SPP1	ITGA4	1	0	0.06210286	0.026753
ICAM2	ITGB2	1	0	0.038566173	9.85E-06
Large BPH vs Normal					
VIM	CD44	1	0	2.140174417	4.73E-05
HBEGF	CD44	1	0	0.521394753	2.51E-06
TIMP1	CD63	1	0	0.512408962	0.001529
CXCL16	CXCR6	1	0	0.47478817	2.36E-04
MMP9	CD44	1	0	0.417065382	0.001104
Large BPH vs Small BPH					
HBEGF	CD9	1	0	-0.027088783	0.004821
THBS1	ITGA6	1	0	-0.04384413	0.00286
CCL20	CXCR3	1	0	-0.081219256	0.023094
THBS1	ITGA4	1	0	-0.236495885	0.026458
TIMP1	CD63	1	0	-0.341927359	6.96E-04

Since autocrine ligand and receptor expression was predicted to be enhanced among Cluster 1 macrophages, interaction scores among these cells were examined. The top altered interactions between BPH and normal samples included multiple interactions associated with anti-inflammatory and tissue repair processes, including IL10/IL10RA, VEGFA/NRP2, and PLAU/PLAUR (Table 4.6). Score differences in these interactions were lower between Large BPH and normal compared to Small BPH and normal and predicted scores for other anti-inflammatory/tissue repair-associated interactions (TGFB1/SDC2, HBEGF/CD44) were slightly reduced in Large BPH compared to Small BPH, suggesting a reduction in M2-associated interactions in Large BPH macrophages (Fig. 4.6). These results suggest that macrophage populations shift to a more M1-like pro-inflammatory character as BPH progresses, consistent with the progressive nature of BPH inflammation.

Table 4.6. Cluster 1 to Cluster 1 interactions with the greatest score differences between sample types.

Ligand	Receptor	Ligand Cluster	Receptor Cluster	Score Difference	P value
Small BPH vs Normal					
VIM	CD44	1	1	2.321394803	8.75E-06
TIMP1	CD63	1	1	1.265134245	0.03396
PLAU	PLAUR	1	1	1.140680591	1.09E-05
VEGFA	NRP2	1	1	0.999275627	2.34E-05
ICAM1	ITGAX	1	1	0.967648908	1.04E-05
Large BPH vs Normal					
VIM	CD44	1	1	1.38695725	0.027604
PLAU	PLAUR	1	1	0.767430422	0.162595
VEGFA	NRP2	1	1	0.628476797	0.179169
ICAM1	ITGB2	1	1	0.590943669	0.032386
ICAM1	ITGAX	1	1	0.589913591	0.121451
Large BPH vs Small BPH					
CD14	ITGA4	1	1	0.047156234	0.037896
TGFB1	SDC2	1	1	-0.053866031	0.027692
HBEGF	CD44	1	1	-0.306237309	0.031045
VIM	CD44	1	1	-0.934437553	0.044888
TIMP1	CD63	1	1	-1.014542139	0.00462

All together, the results of the interaction analysis indicate that communications between and among specific immune cell populations, particularly $CD8^+$ T cell and macrophages, are altered between BPH and normal prostate populations. Also, differences in predicted interactions between Small BPH and normal, Large BPH and normal, and Large BPH and Small BPH indicate a shift in favor of an overall more pro-inflammatory microenvironment in late-stage symptomatic BPH, consistent with the progressive nature of BPH inflammation and association of inflammation with clinical symptoms of BPH.

4.4.3 Myeloid/macrophage Reactome pathway analysis and subclustering analysis reveal a mixed inflammatory phenotype

Comparison of interaction scores between sample types predicted that interactions between several interleukins and their receptors were altered in BPH (Table 4.1). To identify interleukin signaling pathways that may be associated with predicted ligand-receptor interactions, Reactome pathway analysis was performed to identify enriched pathways in each cluster. Signaling by interleukins was the top enriched pathway in most of the combined sample clusters, including macrophage Cluster 1 (Table 4.3), MDSC Cluster 9 (Table 4.4), and macrophage Cluster 10 (Table 4.5). In

addition, several specific interleukin pathways associated with both M2 (IL-4 and IL-13, IL-10) and M1 (IL-12, IL-1) macrophage cytokines were also enriched in myeloid/macrophage clusters (Table 4.3). Additionally, differential expression of several interleukin and interleukin receptor genes included in the Reactome pathways were increased in at least one the myeloid/macrophage clusters (Table 4.6).

Table 4.7. Reactome pathways enriched in Cluster 1 macrophages.

Description	Gene Ratio	Bg Ratio	P value
Signaling by Interleukins	129/1480	462/10554	1.053534e-15
Interleukin-4 and Interleukin-13 signaling	45/1480	108/10554	1.507093e-12
Interleukin-10 signaling	23/1480	47/10554	1.100926e-08
Interleukin-12 family signaling	19/1480	58/10554	0.000222
Interleukin-2 signaling	7/1480	12/10554	0.000436
Interleukin-12 signaling	16/1480	48/10554	0.000551
Interleukin-1 processing	5/1480	7/10554	0.000884
Interleukin-3, Interleukin-5 and GM-CSF signaling	15/1480	48/10554	0.001716

Table 4.8. Reactome pathways enriched in Cluster 9 MDSC.

Description	Gene Ratio	Bg Ratio	P value
Signaling by Interleukins	96/1035	462/10554	3.695715e-13
Interleukin-4 and Interleukin-13 signaling	31/1035	108/10554	2.31557e-08
Interleukin-10 signaling	15/1035	47/10554	2.480339e-05
Interleukin-12 family signaling	16/1035	58/10554	9.835425e-05
Interleukin-2 signaling	6/1035	12/10554	0.000481
Interleukin-3, Interleukin-5 and GM-CSF signaling	13/1035	48/10554	0.000529
Interleukin-12 signaling	12/1035	48/10554	0.001840

Table 4.9. Reactome pathways enriched in Cluster 10 macrophages.

Description	Gene Ratio	Bg Ratio	P value
Signaling by Interleukins	98/916	462/10554	1.665857e-17
Interleukin-4 and Interleukin-13 signaling	34/916	108/10554	1.156741e-11
Interleukin-10 signaling	18/916	47/10554	2.679285e-08
Interleukin-3, Interleukin-5 and GM-CSF signaling	14/916	48/10554	3.635110e-05
Interleukin-1 family signaling	26/916	139/10554	0.000136
Interleukin-2 signaling	6/916	12/10554	0.000245
Interleukin-12 family signaling	14/916	58/10554	0.000336
Interleukin-2 family signaling	11/916	44/10554	0.001049
Interleukin-12 signaling	11/916	48/10554	0.002245
Interleukin-1 signaling	18/916	103/10554	0.003078

Table 4.10. Interleukins and interleukin receptor genes with increased expression (bolded) in one or more myeloid/macrophage cluster (1, 9,10).

	Fold Change					
Cluster	*IL2*	*IL18*	*IL23A*	*IL10*	*IL1B*	*IL1RN*
1	-2.63304	**3.807845**	**3.163462**	**2.461996**	**4.72333**	**5.004052**
9	-4.33391	-	-5.34852	-4.92162	-0.89029	**0.305958**
10	**0.870774**	**0.899996**	-	**0.377268**	**2.227179**	**1.317848**

	Fold Change					
Cluster	*IL2RA*	*IL6R*	*IL1R1*	*IL1R2*	*IL3RA*	*IL18R1*
1	**1.159399**	**2.560562**	**2.308341**	**3.699734**	**1.23135**	-3.76025
9	-3.99331	**3.122597**	**1.500373**	**2.01518**	-2.7164	**0.788215**
10	**1.844642**	-2.74995	**0.289477**	-	-1.65192	-2.14529

Taken together, these findings point to mixed pro- and anti-inflammatory signaling among myeloid/macrophage populations, which contributes to the overall mixed inflammatory response in the BPH prostate microenvironment. This is in keeping with a previous study, which observed variable inflammatory responses among immune cells associated with BPH nodules and immune cells associated with areas of histologically normal prostate tissue within BPH patient specimens [19]. This mix of pro-and anti-inflammatory signals is hypothesized to contribute to the non-resolving nature of BPH inflammation, and myeloid/macrophage populations contribute to these mixed signals.

Since each immune cell cluster was identified based on a limited number of general immune cell subtype markers, we presumed that each cluster was composed of smaller related subsets which likely differ in their cell-cell interactions. Immunostaining for the macrophage-associated marker

CD68 and the M2 macrophage-associated marker CD163 indicate the presence of macrophage subsets (Chapter 3, Fig. 3.4). Also, predicted cluster interactions indicate a mix of pro- and anti-inflammatory signaling in BPH, which may indicate a mix of pro- and anti-inflammatory M1 and M2 phenotypes and differential signaling among these subsets. To further characterize the composition of immune cell populations, individual clusters and closely related cluster groupings were analyzed to identify subsets within the larger subtype populations. Additionally, subclustering aided in identifying contaminating cell types as well as potentially damaged or dying cells based on their expression of genes associated with cell damage such as mitochondrial genes and allowed for exclusion of these cells from subsequent analyses. As interactions among myeloid/macrophage cells were some of the highest predicted interactions and the autocrine ligand/receptor correlation analysis predicted significant autocrine interactions among these cells (Fig. 4.2 B), we initially focused on myeloid/macrophage subclustering. Three myeloid/macrophage clusters (clusters 1, 9 and 10) were analyzed together.

The combined myeloid/macrophage populations were divided into 8 subclusters (Fig. 4.4 A). Myeloid/macrophages from normal prostates segregated almost exclusively into Subcluster (SC) 5 (Fig. 4.4 A). DGE expression patterns among these subclusters indicate a mix of myeloid/macrophage phenotypes, with most subclusters variably expressing both M1-associated and M2-associated genes identified by previous studies [43, 45, 46, 47]. While some subclusters preferentially expressed either M1 or M2-associated genes, all subclusters contained cell expressing a mix of M1 and M2 genes and did not separate into one type or the other (Fig. 4.4 B). For example, SC 3 and SC 6 shifted towards an M1 profile, while SC 1 was slightly more M2-like (Fig 4.4 B). In addition to M1 and M2 genes, SC 3 also expressed S100A8 and S100A9, which are associated with human monocytic MDSC [46]. These genes were also differentially expressed in SC 5 and 6.

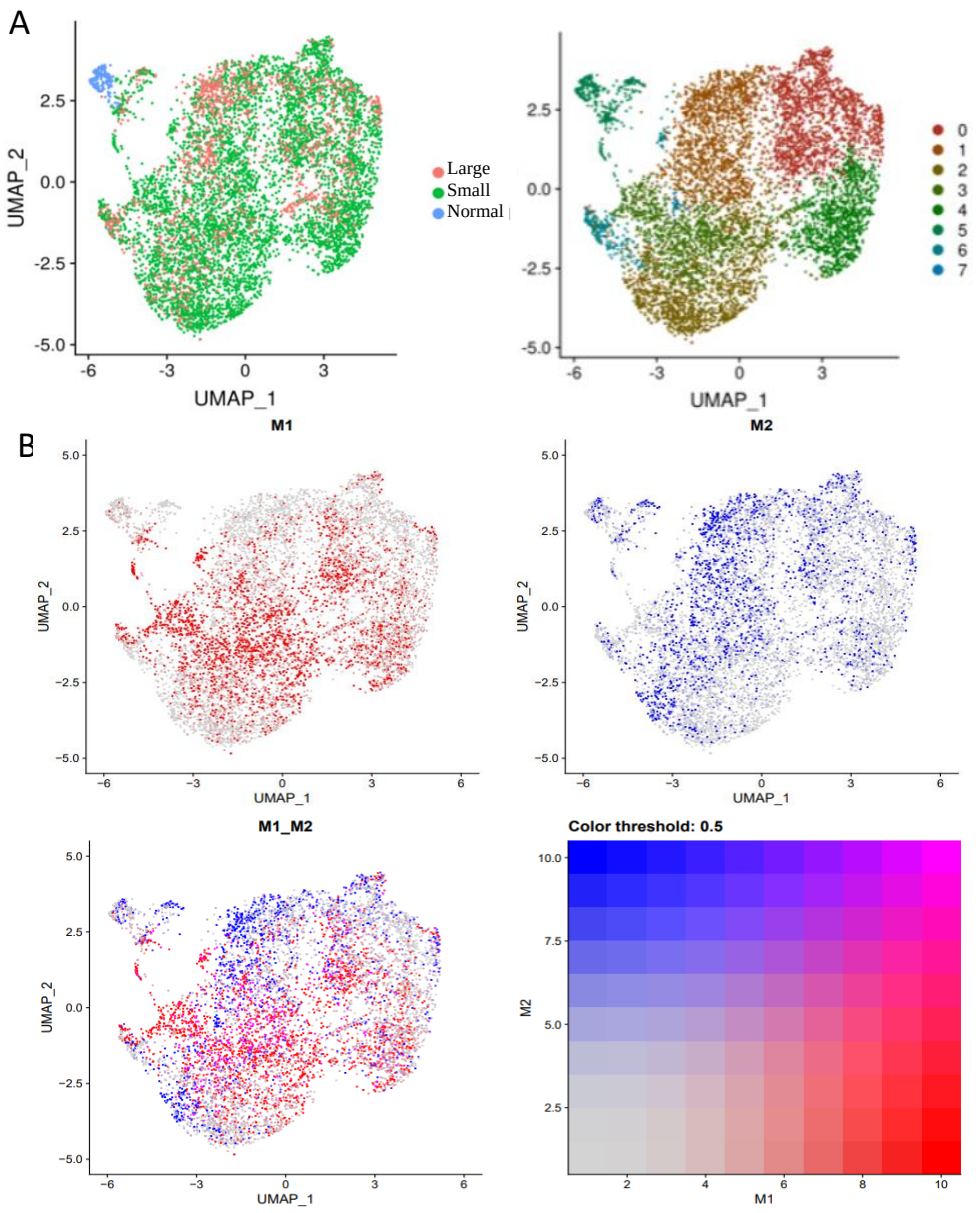

Figure 4.4. (A) Distribution of combined myeloid/macrophage cells from each sample type (left) among the 8 subclusters (right). (B) Expression and distribution of M1 and M2-associated genes among myeloid/macrophage subclusters.

Overall, these finding suggest that macrophage populations are of a mixed phenotype in these prostate samples and do not separate cleanly into the traditional M1 or M2 groupings based on scRNA-Seq gene expression data. This may relate to the inadequacy of a strict M1/M2 classification for macrophages *in vivo*, as well as the complexity and plasticity of

myeloid/macrophage cells and their gene expression *in vivo*. This is consistent with previous studies that have indicated this classification and associated markers do not accurately reflect macrophage populations *in vivo* [45, 49].

4.4.4 Subcluster interaction analysis predicts interactions between myeloid/macrophage subsets

Correlation of autocrine ligands and receptors suggest that communication among myeloid/macrophage cells may be enhanced in BPH (Fig. 4.2 B). To further evaluate interactions among myeloid/macrophage populations, the interaction analysis was applied to the myeloid/macrophage subclusters. Predicted pairings were similar to those predicted in the initial cluster interaction analysis, with ligand-receptor pairs involved in adhesion and migration among the highest predicted interactions. In the combined samples, the highest interaction score among the myeloid/macrophage subclusters was VIM/CD44 between SC 6 and SC 3, followed by ICAM1/ITGAX within SC 4 and TIMP1/CD63 between SC 7 and SC 2. Expression of ligands and receptors identified in the interaction analysis were differentially expressed among the combined sample subclusters. TIMP1 expression was increased in SC 3 and SC 6 and CD63 expression was highest in SC 6. VIM expression was highest in SC 6, and CD44 expression was highest in SC 3. When small BPH and normal prostate subcluster interactions were compared, as with the cluster interactions, VIM/CD44 was the most altered interaction between most subclusters. The most increased interaction overall was VIM/CD44 between SC 6 and SC 3. TIMP1/CD63 was also increased between SC 3 and SC 6. In the comparison between large BPH and normal, VIM/CD44 was also the most altered interaction between most subclusters. TIMP1/CD63 was most elevated within SC 6. These results suggest that certain myeloid/macrophage subsets, particularly SC 6 and SC 3, may preferentially participate in myeloid/macrophage migration and communication in BPH. Also, while no subclusters fell completely into one subtype. the overall M1/M2 gene expression of both SC 6 and SC 3 was shifted towards an M1 profile, which suggests that a more M1-like phenotype enhances cell-cell interactions involved in cell migration and adhesion among macrophages in BPH.

Table 4.11. Interactions with the greatest differences in scores among myeloid/macrophage subclusters between sample types.

Ligand	Receptor	Ligand Cluster	Receptor Cluster	Score Difference	P value
Small BPH vs Normal					
VIM	CD44	mac_6	mac_3	7.09173533	1.45E-08
VIM	CD44	mac_3	mac_3	6.529645675	2.35E-09
VIM	CD44	mac_2	mac_3	5.807280866	2.03E-08
VIM	CD44	mac_7	mac_3	5.694991964	2.39E-04
TIMP1	CD63	mac_3	mac_6	5.633397008	9.01E-08
Large BPH vs Normal					
TIMP1	CD63	mac_6	mac_6	6.881977386	0.063603
VIM	CD44	mac_6	mac_3	6.307100782	0.001804
VIM	CD44	mac_7	mac_3	5.468825022	1.98E-04
TIMP1	CD63	mac_6	mac_2	5.353595318	0.02642
TIMP1	CD63	mac_6	mac_3	5.092791476	0.021997
Large BPH vs Small BPH					
TIMP1	CD63	mac_6	mac_6	2.189884892	0.072751
ICAM1	ITGB2	mac_6	mac_6	0.484655116	0.006765
SPP1	ITGA4	mac_6	mac_2	0.254748525	0.038859
SPP1	ITGA4	mac_6	mac_6	0.241425461	0.033819
CD14	ITGA4	mac_6	mac_2	0.172198368	0.029559

4.5 Discussion

Immune cells and their interactions with other cell types through cell-cell signaling pathways modulate the prostate microenvironment, and alterations in these interactions are hypothesized to contribute to a dysregulated immune response that drives unresolving prostate inflammation and prostate cell hyperplasia in BPH. The purpose of this study was to identify and compare the immune cell populations and their interactions in small early-stage BPH, large late-stage BPH, and normal non-BPH prostates to elucidate potential immune-related mechanisms of BPH initiation and progression. This study intended to examine the contribution of immune cell populations and their interactions to BPH initiation from normal to hyperplastic as well as BPH progression from pre-clinical to clinical BPH. Overall, this study identified specific immune cell subtypes as well as subsets within the myeloid/macrophage subtypes and identified a mixed pro- and anti-inflammatory microenvironment in BPH. This is in keeping with previous studies that identified a mixed Th1/Th2 phenotype among lymphoid cells in BPH [19]. Interaction analysis predicted alterations in specific myeloid/macrophage-myeloid/macrophage and myeloid/macrophage-$CD8^+$

T cell ligand-receptor interactions in BPH compared to normal prostates, suggesting that communication among these cells may play a role in BPH. Furthermore, this study highlights the extent of prostate myeloid cell heterogeneity and suggests roles for specific immune cell subtypes in BPH that may be targets of further study. In addition, some interactions identified by this analysis have previously been implicated in prostate disease, particularly prostate cancer; however, their roles in BPH are generally not well studied (Table 4.1).

Significantly altered ligand-receptor interactions between samples were divided into broad and overlapping categories based on previously identified functions. Among all predicted interactions, ligand-receptor pairs involved in cell adhesion and migration were among the most frequently predicted to be altered between BPH and normal prostate and between small BPH and large BPH. VIM/CD44 interactions were predicted to be the most increased between the sample types and has been associated with adhesion and migration of many cell types [37, 38, 50]. Vimentin (VIM) is an intermediate filament expressed by mesenchymal cells and is typically an intracellular protein; however, it may be expressed on the cell surface or secreted under certain conditions by some cell types such as activated macrophages, lymphocytes, neutrophils, and endothelial cells [37, 50, 51]. CD44 is an adhesion molecule that exists in several isoforms and is expressed by various cell types [52]. CD44 mediates interactions between cells and between cells and extracellular matrix (ECM) components, particularly hyaluronic acid, and has been associated with various cell functions including immune cell migration, differentiation, and activation [52]. The next most increased predicted interaction, TIMP1/CD63, is involved in cell migration, and CD63 also has immunomodulatory effects in antigen-presenting cells (APCs) [53]. Interactions between several immunomodulatory cytokines and their receptors were also predicted to be altered between sample types. Predicted increased interactions of potent immune cell modulators, particularly TNF and IFNγ from $CD8^+$ T cells and their receptors TNFRSF1A and TNFRSF1B, and IFNGR1 and IFNGR2, respectively, on macrophages suggest that $CD8^+$ T cells may promote a pro-inflammatory M1-like macrophage phenotype in BPH. However, M2-associated interactions such as IL10-IL10RA were predicted to be increased between Cluster 1 macrophages and Cluster 0 $CD8^+$ T cells and between some myeloid/macrophage subclusters in BPH samples, and along with mixed M1/M2 gene expression profiles among these subclusters indicates a mix of myeloid/macrophage inflammatory phenotypes. Also, TNF may have varying effects on myeloid subsets, particularly MDSC [44]. In all, these results indicate that immune cell migration and

activation is enhanced in the BPH prostate compared to normal prostate, and immune cells drive the BPH inflammatory microenvironment through interactions between and within various immune cell populations. This enhanced immune cell recruitment and migration is consistent with previous observations of an overall increase in immune cells BPH compared to non-BPH prostates [3, 17]. Also, these results suggest that mixed pro-inflammatory and anti-inflammatory signals between $CD8^+$ T cells and myeloid/macrophage populations may contribute to the chronic non-resolving nature of BPH inflammation. Additionally, pathway analyses indicate enrichment of interleukin signaling pathways associated with both anti-inflammatory (IL4 and IL13, IL10) and pro-inflammatory (IL12, IL1, IL3, IL5) macrophage signaling, which may support the hypothesis of dysregulated macrophage responses in BPH.

Macrophage subsets have been classified in the literature as classically-activated (M1) or alternatively-activated (M2a, M2b, M2c) [45]. These classifications have largely been defined in *in vitro* polarization experiments, and several studies have suggested that this classification does not accurately describe and encompass the heterogeneity of macrophage populations *in vivo* [45, 49]. Several studies have attempted to identify and have proposed specific cytokine profiles and gene markers for each subset. M1 polarization has been associated with expression of pro-inflammatory cytokines such as IL-1β, IL-6, IL-12 and IL-23 and production of reactive oxygen and nitrogen species [43]. M2 polarization has been associated with an anti-inflammatory and pro-tissue repair expression profile, including IL-10, TGFβ, VEGFA, and insulin-like growth factor 1 (IGF-1) [43]. Macrophages in the inflammatory microenvironment may originate from tissue-resident macrophages of embryonal origin or recruited from the bone marrow via the peripheral blood [54]. Studies of lung macrophages suggest macrophage populations may respond differently to inflammatory stimuli based on their origin [55]. This may contribute to the heterogeneous nature of macrophage populations in inflammation. In the current study, subclusters expressed many genes previously associated with either M1 or M2 subsets, and also variably expressed both M1 and M2-associated genes. This finding may relate to the nature of macrophage polarization and gene expression as a continuum as opposed to discrete subsets, as well as the plasticity of myeloid cells *in vivo*. It may also suggest an overall dysregulated macrophage immune response in BPH, where the balance between pro-inflammatory and anti-inflammatory phenotypes may be in flux and consequently fail to resolve the inflammatory process.

Cell-cell interactions play critical roles in the development and function of cells within normal and diseased tissues [23, 56]. scRNA-Seq provides a powerful tool in defining the composition and characteristics of cell populations within tissues [23, 24, 26]. This technology also has allowed for comparison of cellular characteristics between normal and diseased tissues, providing a means for identification of potential disease-related genes and signaling pathways [23, 24, 26]. Additionally, several groups have devised methods for evaluating and quantifying ligand-receptor interactions in various tissues in an effort to define the cell-cell communication and signaling networks of specific tissues [23, 24, 26]. These studies have largely focused on various tumor tissue types and the potential roles of ligand-receptor interactions in cancer progression and metastasis [24, 26]. To our knowledge, this is the first study to apply this ligand-receptor prediction method to explore immune cell interactions in the prostate and in the context of BPH. Further studies are needed to establish the roles of the predicted interactions in prostate inflammation *in vivo*.

Several challenges were encountered in this study. The first challenge was identification and collection of suitable BPH patient samples. Patients with diagnosed with active prostatitis, bacterial infections of the urogenital tract, and indwelling catheters were excluded. To examine BPH progression, BPH samples were divided into two groups based on size to represent early-stage and late-stage BPH. The samples classified as small BPH were selected to represent "early-stage" pre-clinical BPH. As noted above, these samples were obtained from patients undergoing SP surgery for low-grade (Gleason score <7) PZ PCa. TZ tissue from low volume and low IPSS BPH prostates with no PCa would be the ideal small early-stage BPH tissue for comparison to large volume and high IPSS BPH tissues from patients undergoing SP specifically for BPH-related LUTS. However, as surgical intervention is not indicated for patients with low IPSS and no evidence of PCa, tissues from such cases are typically not readily available outside of autopsy specimens. SP specimens from PCa patients with small PZ-confined tumors are more readily available, and the field effects of PCa tumors are considered limited to within about 3mm of the tumor periphery [57, 58]. For these reasons, PCa-free TZ tissue obtained from these specimens is an accepted method for collection of these samples [57, 58]. However, potential effects of PZ tumor cells on TZ immune cells cannot be completely ruled out.

In this study, immune cells were isolated by FACS using the pan-leukocyte marker CD45 as well as the epithelial cell marker EpCAM and endothelial cell marker CD200 to exclude epithelial and endothelial cells, respectively. As immune cells represent a relatively small proportion of prostate cells compared to other cell types such as epithelial cells and smooth muscle cells, FACS sorting was used to enrich for immune cells. This would help to ensure that rare immune cell types were less likely to go undetected among other prostate cell types. And while FACS sorting is a useful tool to enrich samples for specific cell types, cell sorting is imperfect and contamination by unwanted cell types can occur. Henry et al (2018) noted how the use of various epithelial markers may affect the purity of epithelial populations isolated by FACS for bulk RNA sequencing [25]. In the current study, subclustering analyses helped to identify contaminating cell types by their expression of genes associated with non-immune cell types such as epithelial cell keratins, as well as confirm the identities of immune cell subtypes within each cluster.

Another challenge in this study was related to the previously published normal non-BPH prostate scRNA-Seq study by Henry et al. (2018), which performed whole sample scRNA-Seq rather than on isolated $CD45^+$ immune cells only [25]. The inclusion of more numerous prostate cell populations along with the relatively small number of immune cells normally present in non-BPH prostates meant there were relatively few normal prostate immune cells for analysis compared to our BPH specimens (Table 3.1). Consequently, this may bias some analyses as well as preclude comparison of some clusters/subclusters between normal and BPH samples.

scRNA-Seq is a powerful tool to generate large amounts of data regarding gene expression among individual cells. The interaction scoring method applied here is one way to utilize this data to predict how specific cell types are communicating within a specific tissue in the context of a specific pathologic condition. And while this study focused exclusively on immune cells and their interactions, intercellular communications between immune cells and other prostate cell types, such as epithelial cells and fibroblasts, also contribute to BPH. Whole BPH prostate scRNA-Seq data could be combined with the normal prostate scRNA-Seq data used here and, using the interaction scoring method, interactions between the various prostate cell types could be identified and compared. As scRNA-Seq becomes more widely used and these data become available, methods such as the one applied here may be another useful tool in future scRNA-Seq data analyses of BPH to identify cell-cell interactions that may be investigated as treatment targets.

4.6 References

1. Vital, P., P. Castro, and M. Ittmann, *Oxidative stress promotes benign prostatic hyperplasia.* Prostate, 2016. **76**(1): p. 58-67.

2. Berry, S.J., et al., *The development of human benign prostatic hyperplasia with age.* J Urol, 1984. **132**(3): p. 474-9.

3. Robert, G., et al., *Inflammation in benign prostatic hyperplasia: a 282 patients' immunohistochemical analysis.* Prostate, 2009. **69**(16): p. 1774-80.

4. Franks, L.M., *Benign nodular hyperplasia of the prostate; a review.* Ann R Coll Surg Engl, 1953. **14**(2): p. 92-106.

5. St Sauver, J.L., et al., *Longitudinal association between prostatitis and development of benign prostatic hyperplasia.* Urology, 2008. **71**(3): p. 475-9; discussion 479.

6. Krieger, J.N., S.O. Ross, and D.E. Riley, *Chronic prostatitis: epidemiology and role of infection.* Urology, 2002. **60**(6 Suppl): p. 8-12; discussion 13.

7. Roberts, R.O., et al., *Prevalence of a physician-assigned diagnosis of prostatitis: the Olmsted County Study of Urinary Symptoms and Health Status Among Men.* Urology, 1998. **51**(4): p. 578-84.

8. Done, J.D., et al., *Role of mast cells in male chronic pelvic pain.* J Urol, 2012. **187**(4): p. 1473-82.

9. Bharucha, A.E. and T.H. Lee, *Anorectal and Pelvic Pain.* Mayo Clin Proc, 2016. **91**(10): p. 1471-1486.

10. Moore, R.A., *Inflammation of the Prostate Gland.* The Journal of Urology, 1937. **38**(2): p. 173-182.

11. Nickel, J.C., et al., *Chronic Prostate Inflammation is Associated with Severity and Progression of Benign Prostatic Hyperplasia, Lower Urinary Tract Symptoms and Risk of Acute Urinary Retention.* J Urol, 2016. **196**(5): p. 1493-1498.

12. Di Carlo, E., et al., *The prostate-associated lymphoid tissue (PALT) is linked to the expression of homing chemokines CXCL13 and CCL21.* Prostate, 2007. **67**(10): p. 1070-80.

13. Kramer, G., D. Mitteregger, and M. Marberger, *Is benign prostatic hyperplasia (BPH) an immune inflammatory disease?* Eur Urol, 2007. **51**(5): p. 1202-16.

14. Kramer, G., et al., *Increased expression of lymphocyte-derived cytokines in benign hyperplastic prostate tissue, identification of the producing cell types, and effect of differentially expressed cytokines on stromal cell proliferation.* Prostate, 2002. **52**(1): p. 43-58.

15. Kohnen, P.W. and G.W. Drach, *Patterns of inflammation in prostatic hyperplasia: a histologic and bacteriologic study.* J Urol, 1979. **121**(6): p. 755-60.

16. Fibbi, B., et al., *Chronic inflammation in the pathogenesis of benign prostatic hyperplasia.* Int J Androl, 2010. **33**(3): p. 475-88.

17. Theyer, G., et al., *Phenotypic characterization of infiltrating leukocytes in benign prostatic hyperplasia.* Lab Invest, 1992. **66**(1): p. 96-107.

18. Steiner, G., et al., *Phenotype and function of peripheral and prostatic lymphocytes in patients with benign prostatic hyperplasia.* J Urol, 1994. **151**(2): p. 480-4.

19. Steiner, G.E., et al., *Cytokine expression pattern in benign prostatic hyperplasia infiltrating T cells and impact of lymphocytic infiltration on cytokine mRNA profile in prostatic tissue.* Lab Invest, 2003. **83**(8): p. 1131-46.

20. Ou, Z., et al., *Infiltrating mast cells enhance benign prostatic hyperplasia through IL-6/STAT3/Cyclin D1 signals.* Oncotarget, 2017. **8**(35): p. 59156-59164.

21. Kramer, G. and M. Marberger, *Could inflammation be a key component in the progression of benign prostatic hyperplasia?* Curr Opin Urol, 2006. **16**(1): p. 25-9.

22. AlJanahi, A.A., M. Danielsen, and C.E. Dunbar, *An Introduction to the Analysis of Single-Cell RNA-Sequencing Data.* Mol Ther Methods Clin Dev, 2018. **10**: p. 189-196.

23. Ramilowski, J.A., et al., *A draft network of ligand-receptor-mediated multicellular signalling in human.* Nat Commun, 2015. **6**: p. 7866.

24. Cabello-Aguilar, S., et al., *SingleCellSignalR: inference of intercellular networks from single-cell transcriptomics.* Nucleic Acids Res, 2020. **48**(10): p. e55.

25. Henry, G.H., et al., *A Cellular Anatomy of the Normal Adult Human Prostate and Prostatic Urethra.* Cell Rep, 2018. **25**(12): p. 3530-3542 e5.

26. Kumar, M.P., et al., *Analysis of Single-Cell RNA-Seq Identifies Cell-Cell Communication Associated with Tumor Characteristics.* Cell Rep, 2018. **25**(6): p. 1458-1468 e4.

27. Stoeckius, M., et al., *Simultaneous epitope and transcriptome measurement in single cells.* Nat Methods, 2017. **14**(9): p. 865-868.

28. Macosko, E.Z., et al., *Highly Parallel Genome-wide Expression Profiling of Individual Cells Using Nanoliter Droplets.* Cell, 2015. **161**(5): p. 1202-1214.

29. Hafemeister, C. and R. Satija, *Normalization and variance stabilization of single-cell RNA-seq data using regularized negative binomial regression.* Genome Biol, 2019. **20**(1): p. 296.

30. Zappia, L. and A. Oshlack, *Clustering trees: a visualization for evaluating clusterings at multiple resolutions.* Gigascience, 2018. **7**(7).

31. Benjamini, Y., Hochberg, Y., *Controlling the false discovery rate: a practical and powerful approach to multiple testing.* Journal of the Royal Atatistical Society Series B 57, 1995: p. 289-300.

32. Southan, C., et al., *The IUPHAR/BPS Guide to PHARMACOLOGY in 2016: towards curated quantitative interactions between 1300 protein targets and 6000 ligands.* Nucleic Acids Res, 2016. **44**(D1): p. D1054-68.

33. Baxter, E.W., et al., *Standardized protocols for differentiation of THP-1 cells to macrophages with distinct M(IFNgamma+LPS), M(IL-4) and M(IL-10) phenotypes.* J Immunol Methods, 2020. **478**: p. 112721.

34. Norstrom, M.M., et al., *Progression of benign prostatic hyperplasia is associated with pro-inflammatory mediators and chronic activation of prostate-infiltrating lymphocytes.* Oncotarget, 2016. **7**(17): p. 23581-93.

35. Singh, R., et al., *CXCR6-CXCL16 axis promotes prostate cancer by mediating cytoskeleton rearrangement via Ezrin activation and alphavbeta3 integrin clustering.* Oncotarget, 2016. **7**(6): p. 7343-53.

36. Duque, J.L., et al., *Heparin-binding epidermal growth factor-like growth factor is an autocrine mediator of human prostate stromal cell growth in vitro.* J Urol, 2001. **165**(1): p. 284-8.

37. Pall, T., et al., *Soluble CD44 interacts with intermediate filament protein vimentin on endothelial cell surface.* PLoS One, 2011. **6**(12): p. e29305.

38. Nieminen, M., et al., *Vimentin function in lymphocyte adhesion and transcellular migration.* Nat Cell Biol, 2006. **8**(2): p. 156-62.

39. Su, L., et al., *Role of vimentin in modulating immune cell apoptosis and inflammatory responses in sepsis.* Sci Rep, 2019. **9**(1): p. 5747.

40. Forte, D., et al., *The tissue inhibitor of metalloproteinases-1 (TIMP-1) promotes survival and migration of acute myeloid leukemia cells through CD63/PI3K/Akt/p21 signaling.* Oncotarget, 2017. **8**(2): p. 2261-2274.

41. Orinska, Z., et al., *Tetraspanins in the regulation of mast cell function.* Med Microbiol Immunol, 2020. **209**(4): p. 531-543.

42. Gunther, C., et al., *CXCL16 and CXCR6 are upregulated in psoriasis and mediate cutaneous recruitment of human CD8+ T cells.* J Invest Dermatol, 2012. **132**(3 Pt 1): p. 626-34.

43. Martinez, F.O., et al., *Transcriptional profiling of the human monocyte-to-macrophage differentiation and polarization: new molecules and patterns of gene expression.* J Immunol, 2006. **177**(10): p. 7303-11.

44. Sade-Feldman, M., et al., *Tumor necrosis factor-alpha blocks differentiation and enhances suppressive activity of immature myeloid cells during chronic inflammation.* Immunity, 2013. **38**(3): p. 541-54.

45. Martinez, F.O. and S. Gordon, *The M1 and M2 paradigm of macrophage activation: time for reassessment.* F1000Prime Rep, 2014. **6**: p. 13.

46. Zhao, F., et al., *S100A9 a new marker for monocytic human myeloid-derived suppressor cells.* Immunology, 2012. **136**(2): p. 176-83.

47. Lurier, E.B., et al., *Transcriptome analysis of IL-10-stimulated (M2c) macrophages by next-generation sequencing.* Immunobiology, 2017. **222**(7): p. 847-856.

48. Becker, M., et al., *Integrated Transcriptomics Establish Macrophage Polarization Signatures and have Potential Applications for Clinical Health and Disease.* Sci Rep, 2015. **5**: p. 13351.

49. Zilionis, R., et al., *Single-Cell Transcriptomics of Human and Mouse Lung Cancers Reveals Conserved Myeloid Populations across Individuals and Species.* Immunity, 2019. **50**(5): p. 1317-1334 e10.

50. Mor-Vaknin, N., et al., *Vimentin is secreted by activated macrophages.* Nat Cell Biol, 2003. **5**(1): p. 59-63.

51. Bilalic, S., et al., *Lymphocyte activation induces cell surface expression of an immunogenic vimentin isoform.* Transpl Immunol, 2012. **27**(2-3): p. 101-6.

52. Zhang, G., et al., *CD44 clustering is involved in monocyte differentiation.* Acta Biochim Biophys Sin (Shanghai), 2014. **46**(7): p. 540-7.

53. Saiz, M.L., V. Rocha-Perugini, and F. Sanchez-Madrid, *Tetraspanins as Organizers of Antigen-Presenting Cell Function.* Front Immunol, 2018. **9**: p. 1074.

54. Hashimoto, D., et al., *Tissue-resident macrophages self-maintain locally throughout adult life with minimal contribution from circulating monocytes.* Immunity, 2013. **38**(4): p. 792-804.

55. Mould, K.J., et al., *Single cell RNA sequencing identifies unique inflammatory airspace macrophage subsets.* JCI Insight, 2019. **4**(5).

56. Ricke, W.A., et al., *Hormonal and stromal regulation of normal and neoplastic prostatic growth.* Prog Mol Subcell Biol, 2005. **40**: p. 183-216.

57. Mehrotra, R., et al., *Spectrum of malignancies in Allahabad, North India: a hospital-based study.* Asian Pac J Cancer Prev, 2008. **9**(3): p. 525-8.

58. Moller, M., et al., *Heterogeneous patterns of DNA methylation-based field effects in histologically normal prostate tissue from cancer patients.* Sci Rep, 2017. **7**: p. 40636.

CHAPTER 5. MAST CELL INTERACTIONS IN BENIGN PROSTATIC HYPERPLASIA

Meaghan M Broman, Nadia A Lanman, Renee E Vickman, Gregory M Cresswell, Juan Sebastian Paez Paez, Susan Crawford, Simon W Hayward, Gervaise Henry, Douglas Strand, Timothy L Ratliff

5.1 Abstract

Various immune cell types including mast cells are commonly observed in BPH specimens, however the potential role of mast cells (MC) in the pathogenesis of BPH is unclear. Single cell RNA Sequencing (scRNA-Seq) is a powerful tool for the identification of cell types and signaling pathways in healthy and diseased tissues. Recent studies have used scRNA-Seq data to identify ligand-receptor interactions between cell types within tissue specimens. In this study, scRNA-Seq was used to identify and analyze MC populations and predict their interactions with other immune cells in BPH and normal prostate. Initial analyses predicted numerous interactions involving MC, suggesting a potential role for MC interactions in BPH.

scRNA-Seq was performed on immune cells isolated from 10 small (<60g) and 3 large (>70g) BPH prostates. Distinct immune cell subtypes were clustered based on differential gene expression (DGE). These data were combined with previously published scRNA-Seq data from three normal prostates. Ligand-receptor interactions were predicted and scored based on ligand and receptor gene expression and cell number while referencing databases of known ligand-receptor pairs. MC gene expression and ligand-receptor interactions scores were compared between sample types. HMC-1.2 human mast cell line and THP-1 human monocyte line were used for *in vitro* studies.

Unsupervised clustering of combined scRNA-Seq data segregated immune cells into 11 main clusters, including a prominent MC cluster, which was further divided into 6 subclusters. Significant gene expression alterations between BPH and normal samples MC included multiple inflammatory cytokines including CSF1, TNF, and CCL2. Initial interaction scoring across all immune cell subtypes predicted and scored a total of 5515 ligand-receptor pairs. 2040 scores were significantly different between BPH and normal samples. 1,001 of predicted interactions involved MC, 492 with significantly different scores between small BPH and normal and/or large BPH and

normal. These included both MC-MC interactions and MC interactions with other immune cell types, particularly macrophages. Highly scored interactions include ligand-receptor pairs that have been associated with cell adhesion and migration such as VIM/CD44, TIMP1/CD63, and HBEGF/CD9. CD63 and CD9 have been implicated in mast cell activation and chemotaxis. HMC-1.2 cells cultured in conditioned medium (CM) from cytokine-polarized THP-1 cells increased expression of specific DEG identified from the scRNA-Seq analysis, including CSF1, TNF, CCL2, and CD63.

While the role of MC in BPH is not well understood, these results indicate that BPH MC are a heterogeneous population of cells whose gene expression and interactions are altered in BPH compared to normal prostates, suggesting a potential role in the disease. Also, MC interactions with macrophages may play significant roles in driving the BPH inflammatory microenvironment. And while further studies are needed to define the significance of these alterations *in vivo*, the scRNA-Seq and bioinformatic analysis techniques described here aid in identification of potential targets for future studies.

5.2 Introduction

MC have been observed in various normal, hyperplastic, and neoplastic prostate tissues; however, the roles of MC in urologic disease are not entirely clear [13, 14]. MC have been observed in PCa specimens, and some studies have suggested that intratumoral mast cells may be a positive prognostic indicator in PCa [15]. In BPH tissues, MC have been observed particularly in the periglandular and perivascular stroma [13, 14]. MC have been implicated in CP/CPPS, and previous studies have suggested that MC may contribute to LUTS by promoting prostatic inflammation, smooth muscle contraction, and fibrosis [12, 16, 17]. Furthermore, MC may modulate various other immune cells including Treg, Th17 cells, and B cells to promote inflammatory responses in autoimmune disorders [18, 19]. It has been proposed that MC may exacerbate the prostate inflammation observed in CP/CPPS, and may also promote the non-resolving inflammation observed in BPH [17]. Also, studies in a mouse model of experimental autoimmune prostatitis (EAP) observed that targeting of MC activation may reduce urinary dysfunction, immune cell infiltration, and fibrosis, and suggest MC as a potential therapeutic target for BPH and LUTS [12].

MC are derived from $CD34^+$ myeloid progenitor cells that migrate to and mature in most body tissues and reside long-term [22, 23]. They are commonly identified by their metachromatic cytoplasmic granules in toluidine blue-stained tissue sections and by their expression of the cell surface markers c-kit (CD117) and the high-affinity IgE receptor FcεRI [24]. Their prominent cytoplasmic granules contain various inflammatory mediators including histamine, heparin, and neutral proteases [25, 26]. MC subsets have been previously identified by their expression of neutral proteases, particularly tryptase, chymase, cathepsin-G like protease, and carboxypeptidase A3 [27]. MC may also produce a variety of inflammatory mediators and growth factors including TNFα, IL-6, GM-CSF, CCL2, and VEGF [25, 26]. While MC are best known and studied for their role in IgE-mediated hypersensitivity reactions and parasitic diseases, they may also participate in innate and adaptive immune responses [23-25]. Additional roles for MC in various physiologic and pathologic processes have been proposed, including wound repair and angiogenesis, fibrosis, autoimmunity, and cancer [26]. However, the extent of these roles in many cases is not fully understood [23, 25].

MC have been observed in various normal, hyperplastic, and neoplastic prostate tissues; however, the roles of MC in urologic disease are not entirely clear [20, 21]. MC have been observed in PCa specimens, and some studies have suggested that intratumoral mast cells may be a positive prognostic indicator in PCa [22]. In BPH tissues, MC have been observed particularly in the periglandular and perivascular stroma [20, 21]. MC have been implicated in CP/CPPS, and previous studies have suggested that MC may contribute to LUTS by promoting prostatic inflammation, smooth muscle contraction, and fibrosis [12, 13, 23]. Furthermore, MC may modulate various other immune cells including Treg, Th17 cells, and B cells to promote inflammatory responses in autoimmune disorders [24, 25]. It has been proposed that MC may exacerbate the prostate inflammation observed in CP/CPPS, and may also promote the non-resolving inflammation observed in BPH [13].

MC heterogeneity has been demonstrated in various tissues including the prostate; however, the significance of this heterogeneity on the prostate is not known [27]. An immunohistochemical study of prostate tumors and adjacent non-neoplastic BPH tissue identified three and two MC subsets in PCa tissue and adjacent BPH tissue, respectively, based on their expression of chymase, tryptase, and CD117, suggesting a degree of MC heterogeneity in the prostate [14]. While previous

studies have identified the presence of MC and MC subsets in neoplastic and non-neoplastic prostate tissue, the extent of their heterogeneity and potential roles in prostate disease are not clear. It is hypothesized that MC subsets may play different roles in BPH inflammation.

The development of single-cell RNA sequencing (scRNA-Seq) has become a useful tool in transcriptome analysis [26-28]. The 10X Chromium platform employs a microfluidics system by which single cells are paired with DNA oligo-coated beads within an oil droplet. This platform allows for characterization of the transcriptome of several thousand cells from a single sample at one time [27]. Advances in scRNA-Seq methods over the past decade have elucidated the extent of gene expression, regulation and signaling networks in cells from normal and diseased tissues [26]. scRNA-Seq has been used to identify and define cell types and subtypes by differential gene expression patterns within various tissues and cell populations, as well as to identify cell surface markers for these subtypes [27]. More recently, analysis of scRNA-Seq data has been used to elucidate ligand-receptor interactions within a particular tissue [28].

In an effort to further characterize BPH MC populations and elucidate their potential roles in hyperplastic disease, this study used scRNA-Seq data obtained from BPH and normal prostate MC to identify MC subsets based on gene expression profiles. Furthermore, scRNA-Seq data was used to predict and compare ligand-receptor interactions among immune cells in BPH and non-BPH prostates. To do this, scRNA-seq data from small and large BPH tissues was combined with previously published scRNA-seq data from normal non-BPH tissues to compare MC gene expression and ligand-receptor interactions as described in Chapter 4. Overall, significant differences were noted in the composition and gene expression in BPH MC compared to normal prostate MC. Also, predicted ligand/receptor interactions involving MC often involved macrophages, and several of these interactions were predicted to be significantly altered between BPH and normal prostates, suggesting potential roles for these MC-macrophage interactions in BPH. *In vitro* treatment of the human MC cell line HMC-1.2 with conditioned medium (CM) from polarized macrophages found that macrophages modulate MC cytokine gene expression. It is anticipated that identification and comparison of MC subsets and prediction of MC interactions with other immune cells (particularly macrophages) in normal and BPH prostates may contribute to our understanding of the roles of these cells and their interactions in the pathogenesis and progression of BPH and may also indicate potential treatment targets.

5.3 Methods

5.3.1 Human prostate samples

BPH prostatic tissues were obtained from BPH patients undergoing simple prostatectomy (SP) or robot-assisted laparoscopic prostatectomy (RALP) surgery for symptomatic BPH or prostate cancer (PCa) as described in Chapter 3, Section 3.3.1. In summary, transitional zone tissues from 10 Small BPH (<60g) and 3 Large BPH (>70g) were collected and processed for scRNA-Seq. Sections from each prostate were fixed in 10% NBF for histology and immunohistochemistry.

5.3.2 BPH tissue processing, sorting and isolation of BPH prostate cell populations

BPH tissues were processed for histology and immune cell isolation as described in Chapter 3, Section 3.3. In summary, transition zone tissues from each sample were digested and processed to a single cell suspension. Samples were incubated with 5ul Human TruStain Fx Blocking reagent (Biolegend) and 0.5ul Zombie Viability Dye (Biolegend) in 100ul PBS per sample then incubated with an antibody cocktail of CD45-PE (clone HI30, Biolegend) pan-leukocyte marker, EpCAM-APC (clone 9C4, Biolegend) epithelial cell marker, and CD200-PE/Cy7 (clone OX-104, Biolegend) endothelial cell marker or single antibodies for compensation controls (if necessary) for 30 minutes at 4^{o}C. Samples were washed with PBS spun down then resuspended in complete RPMI for live cell sorting on the BD FACS ARIA II (BD Biosciences, San Jose, CA) to isolate $CD45^{+}EpCAM^{-}CD200^{-}$ immune cells. Prior to loading, some BPH cell preps were labeled with TotalSeq (Biolegend) antibodies per manufacturer protocols for the following cell surface immune cell markers: CD3, CD8a, CD4, CD11b, CD19, and CD279.

5.3.3 BPH sample single-cell RNA-Seq

scRNA-Seq was performed as described in Chapter 3. In summary, sorted $CD45^{+}EpCAM^{-}CD200^{-}$ immune cells from each BPH sample were counted, prepped and loaded into the 10X Chromium chip for a 5000 target cell recovery per 10X Genomics protocols. cDNA synthesis and clean-up steps were performed per manufacturer protocols. cDNA content and quality were assessed via Agilent Bioanalyzer (Agilent Technologies, Santa Clara, CA). Sample library preparation was

performed per 10X Genomics protocols prior to sequencing. The resulting data was combined with previously published scRNA-Seq data from three normal prostates [25].

5.3.4 Sample sequencing and data analysis

BPH samples were sequenced and analyzed as described in detail in Chapter 3, Section 3.3.4. In summary, BPH samples were sequenced by the Purdue Genomics Core using a NovaSeq S4 flow cell on a NovaSeq 6000 platform (Illumina, San Diego, CA). Paired-end, 2x150 base-pair reads were sequenced to a depth of 50,000 reads per cell. TotalSeq-B antibody libraries for quantification of cell surface proteins were sequenced at a depth of 5,000 reads per cell. Distinct immune cell clusters were identified based on gene expression patterns and marker genes, as well as using the protein expression observed from the CD3, CD4, CD8, CD11b, and CD19 CITE-seq data and subsequently classified based on known immune phenotypes.

5.3.5 Ligand-receptor interaction score calculation

Ligand-receptor interaction scores were calculated as described in Chapter 4. BPH sample scRNA-Seq data were combined with previously published scRNA-Seq data (Henry et al., 2018) from three normal non-BPH prostates. Ligand-receptor interaction scores were then calculated using methods previously published by Kumar et al (2018) based on ligand and receptor gene expression and cell number and referencing databases of known ligand-receptor pairs [30, 36]. Ligand and receptor pairs with experimentally observed interactions from two databases were filtered to include only those that were identified by a Wilcoxon rank sum test (FDR<0.05) as differentially expressed between condition (large prostatic tissue BPH associated leukocytes, small prostatic tissue BPH associated leukocytes, and normal prostatic tissue associated leukocytes) [28, 37]. Interaction scores were calculated using the following equation [30].

Eq 1. $$Interaction\ score = \frac{1}{n_{cell\ type\ 1}} \sum_{i \in cell\ type\ 1} e_{i,receptor} \times \frac{1}{n_{cell\ type\ 2}} \sum_{j \in cell\ type\ 2} e_{j,ligand}$$

$e_{i,j}$ = normalized expression of gene *j* in cell *i*

n_c = number of cells of cell type *c*

5.3.6 Monocyte differentiation and conditioned medium generation

The human monocyte cell line THP-1 (kindly provided by Dr. Emily Dykhuizen, Medicinal Chemistry and Molecular Pharmacology, Purdue University) were differentiated as previously described [38]. 300,000 THP-1 cells/ml were seeded in each well of a 24 well culture plate in complete RPMI 1640 medium, treated with 5ng/ml PMA for 24 hours, then rested in PMA-free medium for 72 hours at 37^{o} C and 5% CO_2. Cells were then cultured with 20ng/ml IFNγ (Biolegend) and 250ng/ml LPS (Sigma), 30 ng/ml IL-4 (Biolegend), or no cytokines for 48 hours to generate M(LPS,IFNγ), M(IL-4), and M(0) THP-1 cells, respectively. Media was replaced with fresh complete RPMI and cells were cultured for 24 hours. Conditioned medium (CM) was collected and cells were lysed in 350ul TRK buffer for RNA isolation and cDNA synthesis.

5.3.7 THP-1 conditioned medium culture

300,000 THP-1 cells/ml were plated in a 24 well or 96 well plate and treated with 5ng/ml PMA for 24 hours and rested for 72 hours as described above. CM from cytokine-treated THP-1 cells was added in a 1:1 CM:RPMI ratio and cultured for 48 hours. Media was removed and fresh media was added and cells were cultured for 24 hours to generate CM.

5.3.8 HMC-1.2 conditioned media treatment

HMC-1.2 cells were plated at a density of 300,000/ml in a 96 well plate and treated with polarized THP-1 CM generated as described above at a 1:1 ratio with IMDM for 48 hours. After 48 hours, fresh medium was added to all wells and CM and cells were collected after 24 hours as described above.

5.3.9 RNA isolation, cDNA synthesis and qPCR

RNA was isolated from TRK buffer-lysed cell samples as described in Chapter 4. using the Promega Total RNA Kit (Promega, Madison, WI) and per manufacturer protocols. qPCR was performed using Quanta PerfeCTa FastMix II (QuantaBio, Beverly, MA) and commercial probes (Integrated DNA Technologies, Coralville, IA) for the following genes: CSF1, TNF, CCL2, TIMP1, CD63, CD44, CD9.

5.3.10 Mouse prostate inflammation models

Intact POET-3 mouse prostates were inflamed as described in Chapter 2 [34, 47]. POET-3 prostates were harvested at 6 days post-inflammation. Aire KO mouse prostates were inflamed and harvested as described in Chapter 3. Prostates were fixed in 10% NBF and processed for hematoxylin and eosin (H&E) and toluidine blue staining.

5.4 Results

5.4.1 Mast cell localization within the prostate stroma

To localize and evaluate MC in BPH and normal prostate tissues, BPH and normal prostate (n=2) sections were stained with MC stain toluidine blue. The overall distribution in both BPH and normal prostates was similar, with MC predominately located in the stroma adjacent to vascular structures or occasionally in perineural areas or in the periglandular stroma (Fig. 5.1 A). MC in normal prostates were generally sparse, while in BPH prostates MC were more abundant. MC were often arranged in loose perivascular aggregates, frequently in association with few lymphocytes (Fig. 5.1 A). MC in normal prostates were generally densely granulated, while BPH MC varied in granularity with many MC partially or fully releasing their granules, indicative of an active state (Fig. 5.1 A) [12]. Consistent with previous studies, the average percentage of these activated MC was significantly higher in BPH sections compared to normal prostate sections (Fig. 5.1 B). The percentage between small BPH and large BPH was not significantly different.

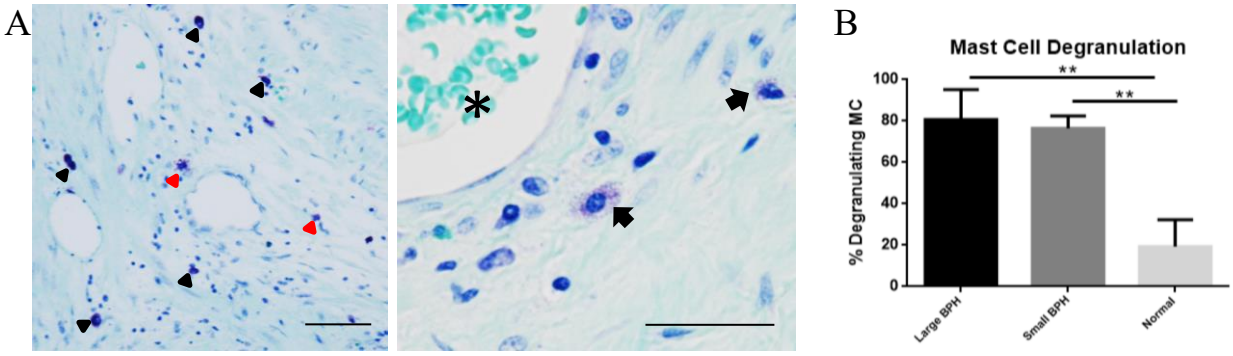

Figure 5.1. (A) Toluidine blue-stained sections of human BPH prostate showing (left) quiescent (black arrows) and degranulating (red arrows) mast cells scattered within the perivascular stroma of large BPH specimen. Right, degranulating mast cells (arrows) adjacent to a blood vessel (asterisk) in small BPH specimen. (B) Percent degranulating MC observed in Large BPH, Small BPH, and normal prostate toluidine blue-stained sections. Scale bars=50µm.

5.4.2 Combined sample immune cell clustering identifies a prominent mast cell cluster

Clustering analysis was performed on scRNA-Seq data from the combined sample types (Small BPH, Large BPH, normal) as described in Chapter 3, resulting in identification of 11 clusters (Fig. 5.2). MC (Cluster 3) were identified based on differential expression of MC-associated genes such as tryptases (TPSAB1, TPSB2), carboxypeptidase A3 (CPA3), and c-kit/CD117 (KIT) [14]. These findings are consistent with previous studies which identified immune cell populations in BPH prostates [7, 8, 10].

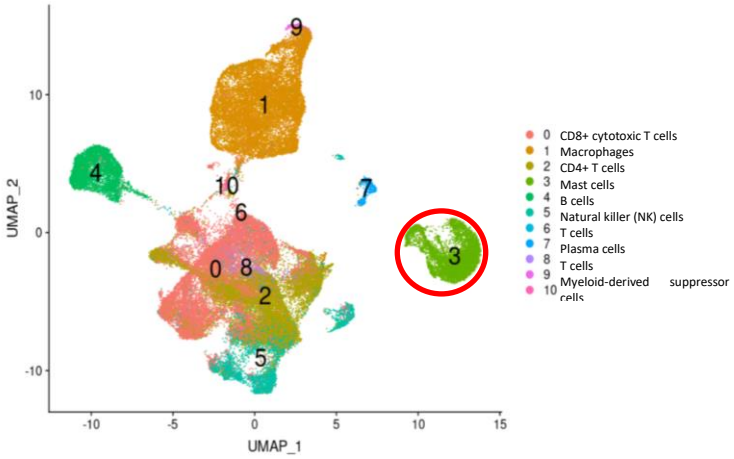

Figure 5.2. Immune cell clustering and identity of each cluster. Cluster 3 was identified as MC based on DGE patterns.

5.4.3 Mast cell cluster 3 cytokine gene expression-sample comparison

MC are hypothesized to contribute to BPH inflammation through inflammatory mediators involved in the recruitment and activation of other immune cells. Gene expression of various cytokines were compared between sample types. In both small and large BPH, expression of CSF1, CCL2, and TNF were increased compared to normal prostate MC (Table 5.2). Also, CXCL2 expression was increased in large prostate MC compared to normal prostate MC (Table 5.2. CSF1 promotes the proliferation and differentiation of monocytes and macrophages [41]. CCL2 may be expressed by a variety of cell types including myeloid cells and T cells and promotes the recruitment and chemotaxis of monocytes, dendritic cells, and T cells to sites of inflammation [42]. TNFα released from MC may induce expression of adhesion molecules in endothelial cells and promote immune cell adhesion and migration [26, 43]. CXCL2, or macrophage inflammatory protein 2-alpha (MIP-2α), is most often associated with neutrophil chemotaxis in inflammation

[44]. These results indicate that MC may contribute to recruitment and differentiation of immune cells, particularly monocytes and macrophages, and contribute to the overall inflammatory microenvironment of the BPH prostate.

Table 5.1. Cytokine genes differentially expressed in Cluster 3 MC between sample types.

	Fold Change		
Gene	*Large BPH vs Normal*	*Small BPH vs Normal*	*Large BPH vs Small BPH*
CXCL2	6.498	-	1.263
CSF1	5.439	5.174	-
TNF	3.421	4.065	-
CCL2	2.823	3.625	-

5.4.4 Cluster interaction scoring

Initial interaction scoring across all immune cell subtypes predicted and scored a total of 5515 ligand-receptor pairs involving all cell types included in the analysis. Similar to the myeloid/macrophage clusters (Chapter 4), the highest overall predicted score among all immune cell types for both small BPH and large BPH was within the mast cell population between the ligand vimentin (VIM) and the receptor CD44, which have been previously associated with cell adhesion and migration in several cell types (Chapter 4).

Next, interaction scores were compared between sample types to identify differences in interactions among and between similar cell subtypes. Overall, 2018 scores were significantly different between BPH and normal samples. 1,001 of predicted interactions involved MC, 492 with significantly different scores between small BPH and normal and/or large BPH and normal. These included both MC-MC interactions and MC interactions with other immune cell types. VIM/CD44 represented the top significant score differences between BPH and normal (Table 5.2). As many of the greatest significant score differences between sample types involved MC/MC, MC/macrophage, or Macrophage/MC clusters, suggesting that interactions among MC and other myeloid populations may play a prominent role in BPH inflammation. Overall, the most prominent differences between BPH and normal prostate interactions within MC and between MC and macrophages involved ligand/receptor pairs associated with cell migration and adhesion and immune modulation. After VIM/CD44, the interaction between TIMP1 and CD63 was among the next highest significant score differences, particularly between macrophages expressing TIMP1

and MC expressing CD63, as well as between MC and MC (Table 5.3). TIMP1/CD63 has been associated with migration in various cell types (Chapter 4) [48]. Also, receptors of the tetraspanin family which includes CD63 have been previously associated with MC activation [49]. The interaction between another tetraspanin family member associated with MC activation, CD9, on MC and the growth factor HBEGF from Cluster 1 macrophages was also predicted to be altered between BPH and normal [49, 50]. HBEGF/CD9 interaction has also been associated with monocyte migration [51].

Table 5.2. Ligand-receptor pairs with the highest significant difference in interaction scores between sample types involving Cluster 3 MC and all other clusters.

Ligand	**Receptor**	**Ligand Cluster**	**Receptor Cluster**	**Score Difference**	**P value**
Small BPH vs Normal					
VIM	CD44	3	3	5.837825757	1.91E-08
VIM	CD44	10	3	5.066115167	9.12E-05
VIM	CD44	3	2	4.66684137	3.14E-08
VIM	CD44	3	1	4.207507287	2.64E-07
VIM	CD44	3	5	4.129678836	4.27E-06
Large BPH vs Normal					
VIM	CD44	3	3	6.130169691	0.017364
VIM	CD44	10	3	5.885330828	0.006101
VIM	CD44	6	3	4.828236779	0.032099
VIM	CD44	3	2	4.790438253	0.022711
VIM	CD44	3	8	4.415011405	0.040115
Large BPH vs Small BPH					
VIM	CD44	6	3	3.192855238	0.038176
VIM	CD44	9	3	2.539327101	0.035532
VIM	CD44	3	9	2.305076968	0.010252
TIMP1	CD63	3	6	0.550428145	0.001418
ICAM1	ITGB2	3	10	0.339398331	0.019925

Table 5.3. Ligand-receptor interactions involving MC and myeloid/macrophage clusters with the greatest difference in scores between sample types.

Ligand	Receptor	Ligand Cluster	Receptor Cluster	Score Difference	P value
Small BPH vs Normal					
TIMP1	CD63	1	3	2.159554417	1.34E-05
TIMP1	CD63	3	3	1.500435171	8.43E-09
VEGFA	NRP2	3	1	1.163063525	2.26E-06
TIMP1	CD63	3	1	1.083514675	0.001561452
TIMP1	CD63	10	3	1.018586665	0.020971231
Large BPH vs Normal					
TIMP1	CD63	3	3	1.5978051	0.002592
TIMP1	CD63	1	3	1.322152576	0.009959
VEGFA	NRP2	3	1	0.993581757	0.102316
TIMP1	CD63	3	1	0.898479843	0.012907
TIMP1	CD63	9	3	-0.631454651	0.040732
Large BPH vs Small BPH					
ICAM1	ITGB2	3	10	0.339398331	0.019925
TNF	TNFRSF1B	3	1	-0.052888961	0.020093
ICAM1	IL2RA	1	3	-0.088574889	0.001015
VEGFA	NRP2	3	10	-0.09162062	0.036085
TIMP1	CD63	3	1	-0.185034832	0.045107
TIMP1	CD63	1	3	-0.837401841	0.029919

Overall, the most prominent differences between BPH and normal prostate interactions within MC and between MC and macrophages involved ligand/receptor pairs associated with cell migration and adhesion and immune modulation, indicating MC may contribute to the inflammatory microenvironment by influencing immune cell recruitment and activity. Furthermore, predicted interactions between macrophage ligands and MC receptors associated with MC activation indicate a role of modulation of MC activity by macrophages in BPH. Also, while the top altered interaction between Small BPH and Large BPH was also VIM/CD44 within Cluster 3 MC, fewer interactions involving MC were predicted to be altered between Small BPH and Large BPH than between BPH and normal prostates, suggesting that interactions involving other cell types, particularly T cells, may be more prominent in late-stage BPH disease.

When gene expression of select ligands and receptors predicted by the interaction analysis was compared between sample types, expression of CD63, CD9, VIM, and CD44 was significantly increased in Cluster 3 MC from both Small BPH and Large BPH specimens compared to normal (Table 5.4). Expression of these genes was not significantly different between Small BPH and Large BPH MC.

Table 5.4. Comparison of select ligand and receptor genes between sample types.

	Fold Change		
Gene	*Large BPH vs Normal*	*Small BPH vs Normal*	*Large BPH vs Small BPH*
VEGFA	3.332	2.741	-
CD9	1.990	1.706	-
CD63	1.953	1.162	-
VIM	1.585	1.586	-
CD44	1.946	1.539	-

In all, the predicted alterations in interactions between MC and other myeloid populations in BPH indicate MC may contribute to the inflammatory microenvironment by influencing the recruitment and activity of other myeloid cell types. Furthermore, predicted interactions between macrophage ligands and MC receptors associated with MC activation, indicate a role for reciprocal modulation of MC activity by macrophages in BPH. Also, while the top altered interaction between Small BPH and Large BPH was also VIM/CD44 within Cluster 3 MC, fewer interactions involving MC were predicted to be altered between Small BPH and Large BPH than between BPH and normal prostates, suggesting that the roles of interactions involving other cell types, particularly T cells (Chapter 4), may be more prominent than MC interactions in late-stage BPH disease compared to early-stage BPH.

5.4.5 Impact of macrophage subtypes on MC gene expression

It is hypothesized that macrophage interactions with MC modulate MC gene expression. To examine the impact of polarized macrophages on MC *in vitro*, the human MC HMC-1.2 cells were exposed to conditioned medium from THP-1 cells differentiated and polarized using specific cytokines [38]. While *in vitro* polarization does not accurately reflect the in vivo heterogeneity of macrophage subsets and their activities (Chapter 4), this *in vitro* study can model the impact of

specific macrophage subsets on MC. HMC-1.2 cells were cultured in conditioned medium (CM) from polarized THP-1 cells and gene expression of specific ligands, receptors and cytokines was assessed by qPCR. Following treatment of HMC-1.2 cells with CM from polarized macrophages, expression of CD63 and CD9 was highest in HMC-1.2 cells cultured in M(IL10) CM (Fig. 5.4). CD44 was elevated in M(LPS) and M(IL10) CM-cultured HMC-1.2 cells over M(0) CM. M(IFN,LPS) CM decreased expression of CD63, CD9, and CD44. M(IL4,IL13) CM also increased CCL2, CSF1, and TNF expression. The greatest increase in CSF1 expression was induced by M(LPS) CM, while M(IFN,LPS) CM diminished CSF1 and CCL2 expression compared to M(0) CM. The results of *in vitro* experiments with the HMC-1.2 cell line suggest that the differential gene expression of specific cytokines (CCL2, CSF1, TNF) in BPH MC and expression of ligands (VIM) and receptors (CD9, CD63, CD44) identified in the interaction analysis may be influenced predominately by interactions with M2-like macrophages.

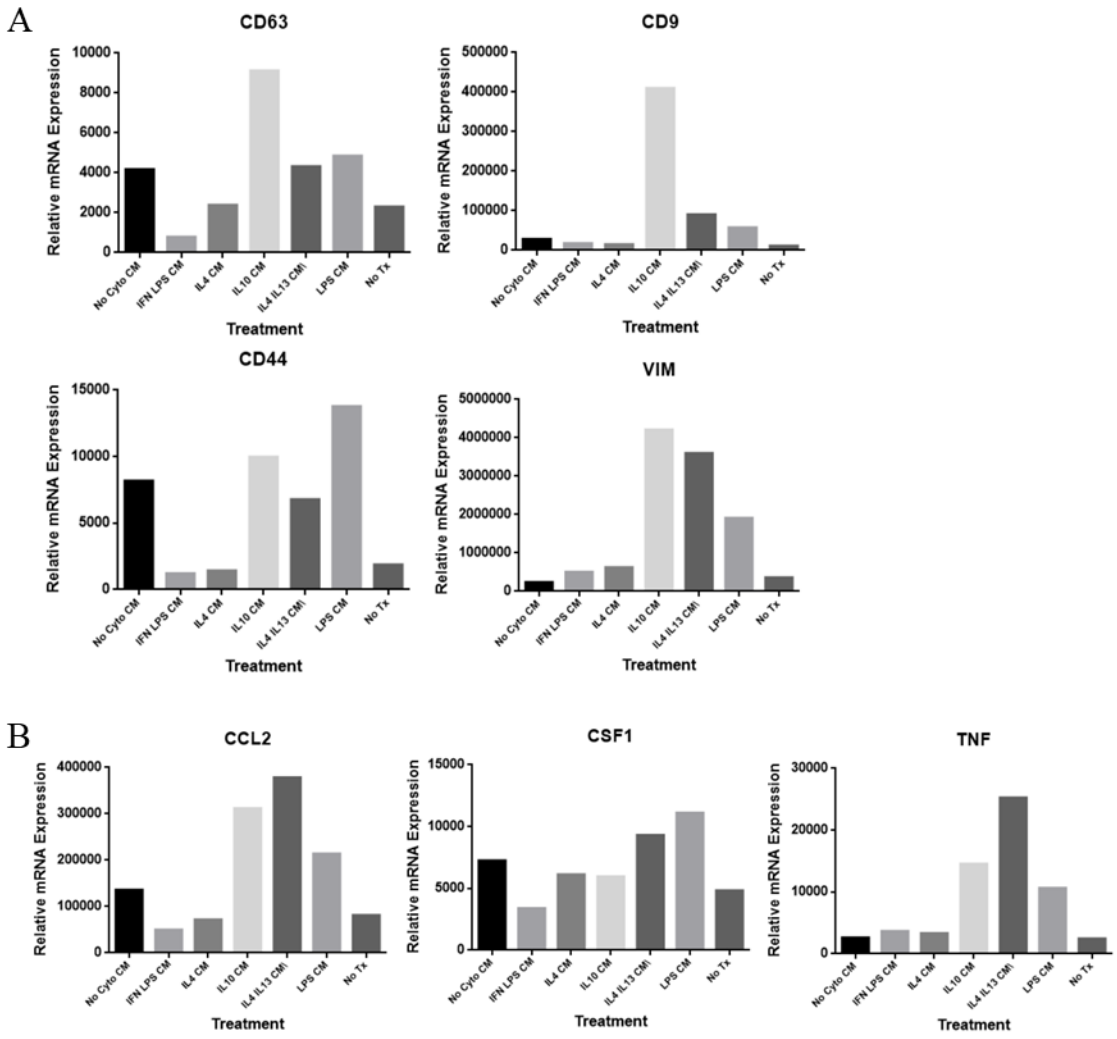

Figure 5.3 (A) Gene expression of ligand and receptors involved in highest scored MC/macrophage interactions in HMC-1.2 cells cultured in polarized THP-1 CM. (B) Expression of cytokines differentially expressed in BPH Cluster 3 MC in polarized THP-1 CM-treated HMC-1.2 cells.

5.4.6 Mast cell subclustering identifies mast cell subsets in the prostate

While previous studies have indicated that prostate MC are a heterogeneous cell type, the extent of their heterogeneity has yet to be defined. Previous studies have identified MC subsets based on their expression of the neutral proteases tryptase (TPSAB1, TPSB2), chymase (CMA1), cathepsin G (CTSG), and carboxypeptidase A3 (CPA3), the proportion of which varies among tissue types and location within tissues [22]. Mucosa-associated MC typically consist of tryptase-expressing cells, while mast cells within connective tissues often express chymase and carboxypeptidase A3

in addition to tryptase [22]. Other studies have included other MC-associated markers such as c-kit (CD117) to identify subsets in the prostate [14].

To characterize the composition of prostate MC, the combined sample MC cluster (Cluster 3) was further analyzed to identify MC subsets. Initial subclustering analysis identified contaminating cell types that were removed from subsequent analyses. Subclustering analysis separated the combined sample MC into 6 subclusters (SC) (Fig. 5.4 B). MC from normal prostates clustered predominately in one subcluster (Subcluster 4). MC from small and large BPH prostates were more widely distributed amongst the other subclusters (Fig. 5.4 A). Genes for markers associated with MC markers were differentially expressed among subclusters [27]. Consistent with previous studies, BPH MC subclusters generally expressed KIT and tryptase (TPSAB1, TPSB2) genes [14]. Most also expressed CPA3. Normal prostate MC (SC 4) also expressed KIT, TPSAB1, TPSB2, and CPA3 (Fig. 5.4 C). Some genes for MC-associated markers were differentially expressed among subclusters [27]. KIT was slightly decreased in SC 5 and increased in SC 4. TPSAB1 and TPSB2 were increased in subcluster 0 and TPSAB1 was increased in subcluster 4. Expression of these two genes was slightly decreased in SC 1 and 5, as was CPA3. CMA1 and CTSG were expressed by a small number of BPH MC mostly in SC 1, 2 and 3 (Fig 5.4 C). Overall, expression of specific MC-associated genes was generally similar among subclusters with the exception of CMA1 and CTSG. MC from normal prostates segregated almost exclusively to one subcluster distinct from the other subclusters, and BPH MC were more heterogeneous than normal MC based on protease gene expression and other DEG, which may suggest roles for MC subsets in BPH. Gene expression of some inflammatory mediators identified in the cluster analysis also varied among subclusters. TNF was differentially expressed in subcluster 5. CSF1 was differentially expressed in subcluster 3. CCL2 was not differentially expressed among the subclusters. These findings indicate prostate MC heterogeneity as defined by known MC markers as well as inflammatory mediator gene expression and suggest mixed functions for these subclusters within the prostate inflammatory microenvironment. Similar to cluster interaction predictions, the top predicted interactions among MC subclusters and between MC subclusters and other immune cell types involved VIM/CD44 between MC and MC and between MC and macrophages. TIMP1/CD63 interactions between macrophages and MC subclusters 4 and 0 were also increased in BPH. VIM and CD44 were differentially expressed in subcluster 0. CD63 was differentially expressed in subcluster 4.

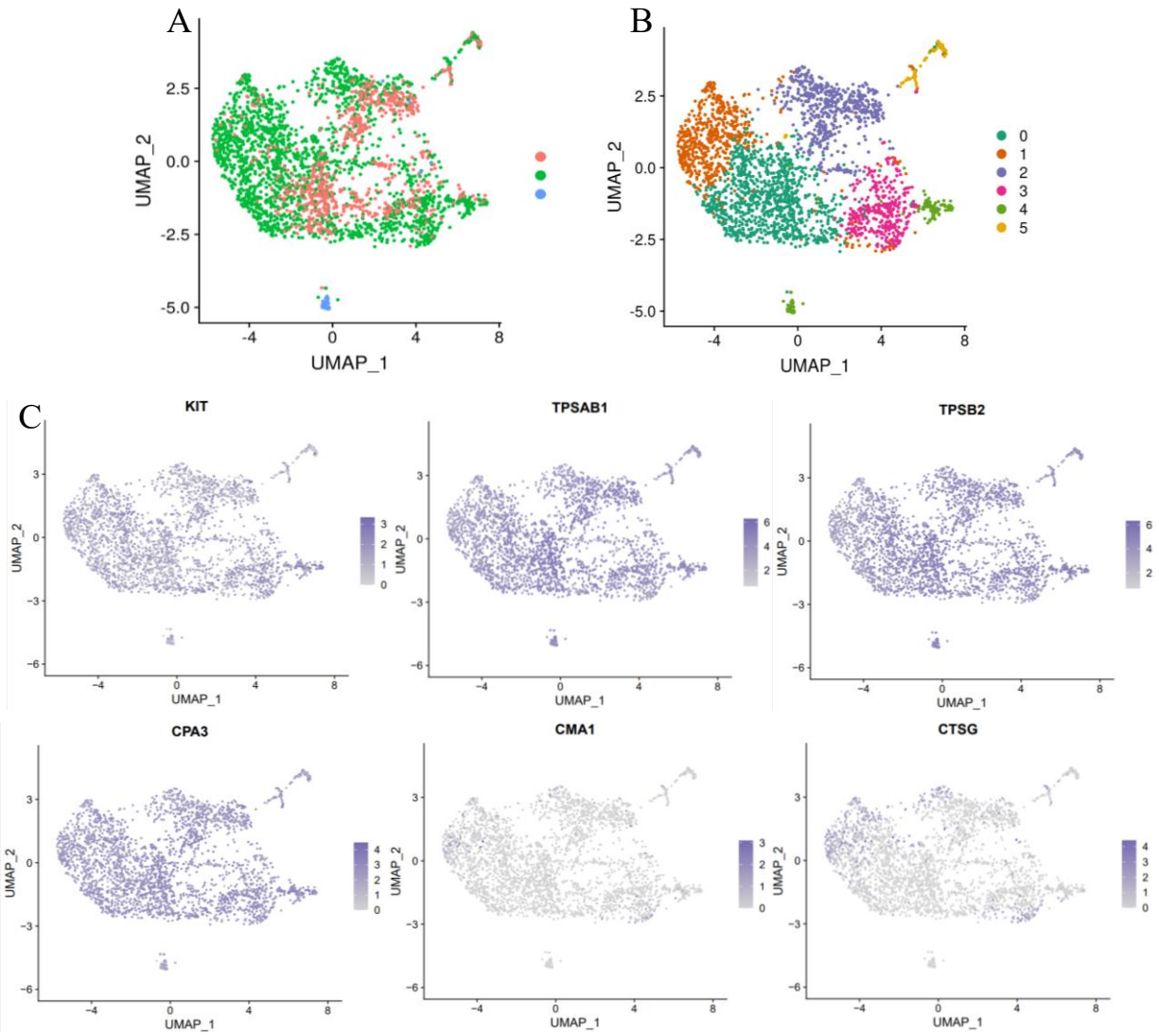

Figure 5.4. (A) Distribution of MC from large BPH (orange), small BPH (green) and normal (blue) samples among subclusters. (B) MC were divided into 6 subclusters. (C) Expression of MC-associated genes among subclusters.

Overall, subclustering analysis reveals heterogeneity among prostate MC beyond the subtypes identified in previous studies [14]. Based on sample type comparison of gene expression and in interactions among MC and between MC and other immune cells, particularly macrophages, this heterogeneity appears to be increased in BPH compared to normal prostates, although further investigation is needed to determine the significance of this heterogeneity and of certain subsets in BPH. It should be noted that some differences between BPH and normal samples may be due to the relatively small number of normal prostate MC included in this analysis.

5.4.7 Mast cells in immune prostatitis mouse models

MC have been associated with prostatic inflammation and pelvic pain in mouse models of autoimmune prostatitis [7, 12, 18, 20, 21]. As MC are hypothesized to contribute to the non-resolving inflammation of BPH, mouse models of resolving vs non-resolving autoimmune-type prostatitis were compared. The POET-3 model of resolving prostate inflammation and the Aire KO model of non-resolving prostate inflammation were examined histologically for mast cells. POET-3 and Aire KO mice were inflamed as described in Chapter 3 and fixed prostates were stained with toluidine blue as described. In the POET-3 model, MC were distributed within the periglandular stroma and generally well granulated (Fig. 5.5 A). In inflamed Aire KO mice, MC were also present in the periglandular stroma. However, many MC were also observed singly or in small loose aggregates adjacent to nerve ganglia (Fig. 5.5 B). This finding is consistent with findings in other immune mouse models and also consistent with the reported role of MC in pelvic pain [12, 17, 20]. MC in Aire KO mice were also generally well granulated with few degranulating MC. Previous studies have described degranulated MC in mouse models of experimental autoimmune prostatitis (EAP), and this difference may potentially be related to differences in mouse models or possibly related to the time of harvest [12, 20].

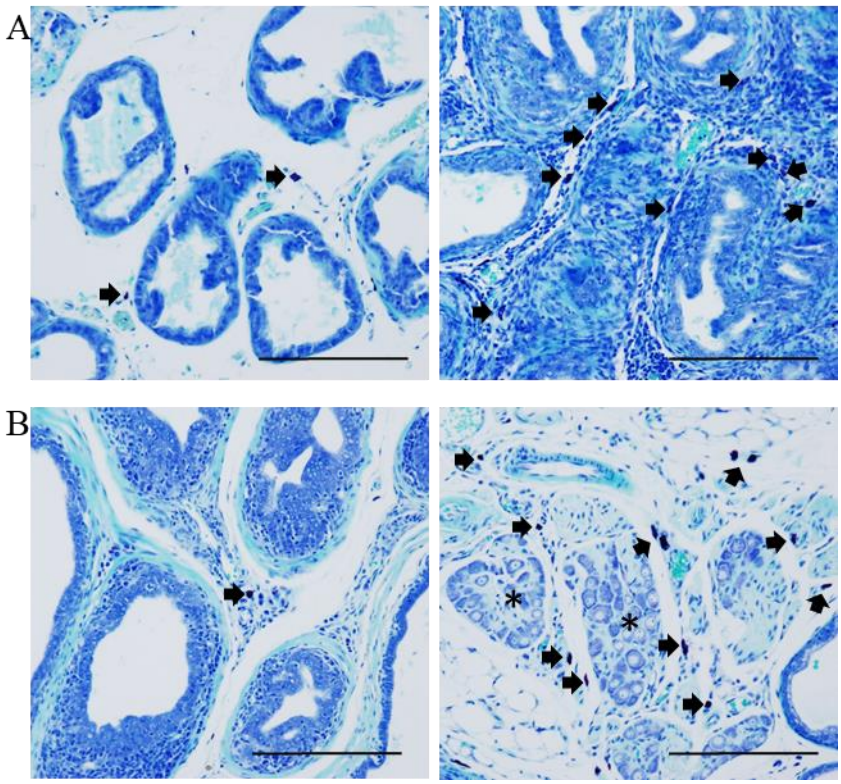

Figure 5.5. (A) Toluidine blue-stained sections of naïve (left) and inflamed (right) POET-3 mouse prostates showing MC within the stroma (arrows). (B) Toluidine blue-stained sections of inflamed Aire KO mouse prostate showing MC (arrows) within the periglandular stroma (left) and adjacent to nerve ganglia (asterisks) (right). Scale bars=100μm.

5.5 Discussion

This study examined the composition, gene expression, and interactions of prostate MC in an effort to further define their roles in BPH. MC were identified in normal and BPH tissues by histology and by scRNA-Seq clustering analyses. MC in BPH tissue sections were overall more abundant and activated than MC in normal prostate sections. MC in BPH tissues differentially expressed genes for cytokines involved in immune cell modulation and recruitment, and ligand/receptor interactions involved in these processes were also predicted to be increased in BPH MC compared to normal prostate MC, particularly interactions with macrophages and with other MC. Subclustering analyses identified MC subsets among sample types with variable expression of neutral protease genes, inflammatory mediator genes, and predicted ligand/receptor genes among these subsets. Also, MC from normal prostates predominately separated into one subcluster, suggesting an increased degree of heterogeneity among BPH MC. In all, these findings indicate

alterations in MC activation, gene expression, and cell-cell communications which may contribute to the chronic BPH inflammatory microenvironment.

Inflammation is commonly observed in association with BPH nodules, and it is hypothesized that chronic prostatic inflammation may play a role in BPH initiation and progression; however, the precise roles of specific immune cell populations in BPH is not clear. [7, 8]. Previous studies have shown that the immune cell infiltrate of the normal prostate is generally low and composed predominately of $CD8^+$ T lymphocytes, along with fewer CD4+ T lymphocytes, macrophages, B cells, NK cells, plasma cells, and mast cells [10]. In BPH, overall immune cell numbers increase [10]. CD4+ T lymphocytes infiltrate the prostate in response to pro-inflammatory cytokines such as interleukin 15 (Il-15) and interferon γ (IFNγ) [8, 10]. T lymphocytes present in BPH infiltrates produce various cytokines such as IL-2, IFNy, TNFα, and others [52]. Additionally, myeloid/macrophage subtypes may produce a variety of pro- and anti-inflammatory cytokines, and current scRNA-Seq data suggest a mixed M1/M2-type phenotype among these cells in BPH. MC are known to produce a variety of inflammatory mediators including TNF, IL4, IL6, GM-CSF, and many others [26]. This milieu of mixed signals is hypothesized to contribute to the non-resolving nature of BPH inflammation. The data presented here suggest that MC may contribute to the overall inflammatory microenvironment through cytokines associated with monocyte recruitment and differentiation, as well as predicted interactions with macrophages associated with MC activation.

As men age, the incidence of both BPH and diagnosed prostatitis increase [8, 10]. Inflammation is observed in the majority of clinical BPH specimens and has been associated with LUTS, and it is hypothesized that chronic prostatitis may play a role in BPH initiation and progression; however, the precise roles of specific immune cell populations in BPH are not clear. [7-9]. Prostatitis is a common male urologic condition, with estimates of overall prevalence between 2% and 16% in various studies [53-55]. The National Institutes of Health (NIH) divides prostatitis into four categories: acute bacterial prostatitis (Type I), chronic bacterial prostatitis (Type II), chronic prostatitis/chronic pelvic pain syndrome (CP/CPPS) (Type III), and asymptomatic inflammatory prostatitis (Type IV) [12, 56]. Around 90% of diagnosed prostatitis cases in men are categorized as CP/CPPS [12]. Around 90% of diagnosed prostatitis cases are categorized as CP/CPPS in which no infectious cause is identified and may involve a variety of symptoms including LUTS, sexual

dysfunction, and psychosocial symptoms [12, 56]. Various causes of CP/CPPS have been hypothesized, including autoimmune mechanisms, infections, neurologic dysfunction, or endocrine imbalance; however, the underlying etiology of CP/CPPS remains unclear [12, 56]. Previous studies have suggested MC involvement in pelvic pain, and elevated levels of the MC-associated proteins tryptase-β, carboxypeptidase A3 (CPA3), and nerve growth factor (NGF) have been identified in the prostatic secretions of CP/CPPS patients [12, 17, 20]. It has also been suggested that MC may be involved in suppressing Treg activity and promote loss of self-tolerance in CPPS [17]. In this study, Treg were sparsely scattered within many lymphoid aggregates and organizing lymphoid structures (Chapter 3), and it is hypothesized that loss of Treg activity may contribute to the failure of BPH inflammation to resolve. The potential role of MC in Treg activity in BPH inflammation has yet to be fully elucidated.

The significance of MC in prostate disease is not well understood. Previous studies have described the presence of MC and MC subsets in the normal prostate and in BPH mainly as a comparison with prostate tumor tissues and intertumoral MC populations [13, 14, 57]. These studies have identified MC subtypes in the prostate based on their expression of neutral proteases tryptase and/or chymase, indicating heterogeneity among prostate MC [14]. Globa et al (2014) observed two MC subsets (chymase$^+$ tryptase$^-$ CD117$^+$ and chymase$^-$ tryptase$^+$ CD117$^+$) in the non-neoplastic prostate and three subsets (chymase$^+$ tryptase$^-$ CD117$^+$, chymase$^-$ tryptase$^+$ CD117$^+$, chymase$^+$ tryptase$^+$ CD117$^-$) in peritumoral areas and a chymase$^+$ tryptase$^+$ CD117$^+$ subset within prostate tumors [14]. Tumor-associated mast cells may be involved in angiogenesis, and some studies suggest intertumoral mast cells are a positive prognostic indicator in PCa [15].

More recently, studies have explored the role of MC in benign prostatic disease, as well as their potential as a treatment target. MC have been observed in BPH specimens and have been associated with CP/CPPS, suggesting potential role in LUTS [12, 14]. MC have also been implicated in BPH prostate epithelial proliferation through IL6/STAT3 signaling and in prostate stromal cell expansion/proliferation in the context of *Trichomonas vaginalis* infection [16, 58]. Also, the roles of MC on smooth muscle activity, tissue fibrosis, and inflammation noted in other tissues suggest a potential impact on these processes in the prostate and on LUTS [9, 24, 59]. Additionally, as BPH has been speculated to be an autoimmune inflammatory process and MC have been associated with autoimmunity, studies involving MC in mouse models of EAP have

suggested a role for MC in autoimmune-type prostatic inflammation and associated CP/CPPS symptoms [7, 12, 18, 21]. Studies using EAP models noted have noted an increase in activated MC in inflamed EAP mouse prostates compared to controls [12, 21]. Additionally, Done et al (2012) observed diminished pelvic pain in MC deficient mice and in mice treated with a MC stabilizer that inhibited MC degranulation and a histamine receptor 1 antagonist, indicating MC-derived mediators are involved in CP/CPPS and indicating MC as a potential treatment target for CP/CPPS [12]. In the current study, MC were observed in both the resolving POET-3 and non-resolving Aire KO prostatitis models. Unlike previous descriptions of other immune prostatitis mouse models, degranulating MC were generally not observed in these models. This may potentially be due to differences in the mice themselves, or possibly the timing of inflammation to harvest. It is possible that MC may be more or less active at different stages of the inflammatory process, and a time course study in these mouse models may clarify how MC participate in the acute vs peak vs resolution/non-resolution stages of prostate inflammation. A study such as this may also shed light on how MC may participate in the initiation, resolution, or continuation of BPH inflammation in human patients. Further characterization of MC in the POET-3 and Aire KO models may provide contrasting resolving vs non-resolving models for the role of MC in BPH inflammation.

scRNA-Seq is a powerful tool to generate large amounts of data regarding gene expression among individual cells and can be used to assess transcriptional heterogeneity within cell populations and identify rare cell subtypes that might otherwise be overlooked in bulk samples [60]. Recent studies have used scRNA-Seq to examine prostate cellular anatomy in detail. Henry et al (2018) analyzed the whole cellular populations of three non-BPH prostates to elucidate the normal cellular composition of the prostate, and thus provided a dataset for comparison to BPH prostates. Recently, studies by this group have explored the use of scRNA-Seq data from immune cells obtained from BPH patient prostates to characterize the immune landscape of BPH. These studies have included immune cell identification and gene expression analyses, as well as prediction of ligand-receptor interactions between immune cells from BPH and normal prostates. Cell-cell communications via ligand-receptor interactions is known to be integral to tissue and organ function [28]. To explore these interactions in BPH, we have adapted and applied a previously-developed method using scRNA-Seq data to predict immune cell interactions within BPH and normal prostate tissue and subsequently compare these interactions between small early-stage and

large late-stage BPH and normal non-BPH prostates [30, 36]. The results of this method suggest a role for MC interactions in the prostate, both within the MC population and between MC and other immune cell subtypes. While this study focused on MC interactions with other immune cells, particularly macrophages, MC are known to impact various other cell types such as endothelial cells, fibroblasts, and smooth muscle cells [9, 22, 24, 26]. As only immune cells were isolated from the BPH tissues for scRNA-Seq in this study, it is not possible to use the mathematical method described here to predict ligand-receptor interactions among other cell types using this scRNA-Seq dataset. However, this method could be applied to scRNA-Seq obtained from whole prostate cell preparations to predict and compare interactions among the various prostate cell types. As scRNA-Seq becomes more widely used and these datasets become available, methods such as the one described here may be one more useful tool in scRNA-Seq data analyses.

The results described here indicate that MC and their interactions are altered in BPH compared to normal prostates, suggesting that these cells may play a role in driving BPH inflammation and potentially contribute to the hyperplastic response. This study also identifies potential immune-related targets for further validation and study, as well as highlight the utility of scRNA-Seq and bioinformatic analysis techniques in identification and comparison of cellular interactions in diseased and normal tissues. Further studies are needed to further explore and confirm the biological significance of these predictions *in vivo*.

5.6 References

1. Vital, P., P. Castro, and M. Ittmann, *Oxidative stress promotes benign prostatic hyperplasia.* Prostate, 2016. **76**(1): p. 58-67.

2. Berry, S.J., et al., *The development of human benign prostatic hyperplasia with age.* J Urol, 1984. **132**(3): p. 474-9.

3. McNeal, J.E., *The zonal anatomy of the prostate.* Prostate, 1981. **2**(1): p. 35-49.

4. De Nunzio, C., et al., *The controversial relationship between benign prostatic hyperplasia and prostate cancer: the role of inflammation.* Eur Urol, 2011. **60**(1): p. 106-17.

5. Henry, G.H., et al., *A Cellular Anatomy of the Normal Adult Human Prostate and Prostatic Urethra.* Cell Rep, 2018. **25**(12): p. 3530-3542 e5.

6. Hollingsworth, J.M. and T.J. Wilt, *Lower urinary tract symptoms in men.* BMJ, 2014. **349**: p. g4474.

7. Kramer, G., D. Mitteregger, and M. Marberger, *Is benign prostatic hyperplasia (BPH) an immune inflammatory disease?* Eur Urol, 2007. **51**(5): p. 1202-16.

8. Fibbi, B., et al., *Chronic inflammation in the pathogenesis of benign prostatic hyperplasia.* Int J Androl, 2010. **33**(3): p. 475-88.

9. Bushman, W.A. and T.J. Jerde, *The role of prostate inflammation and fibrosis in lower urinary tract symptoms.* Am J Physiol Renal Physiol, 2016. **311**(4): p. F817-F821.

10. Robert, G., et al., *Inflammation in benign prostatic hyperplasia: a 282 patients' immunohistochemical analysis.* Prostate, 2009. **69**(16): p. 1774-80.

11. Di Carlo, E., et al., *The prostate-associated lymphoid tissue (PALT) is linked to the expression of homing chemokines CXCL13 and CCL21.* Prostate, 2007. **67**(10): p. 1070-80.

12. Done, J.D., et al., *Role of mast cells in male chronic pelvic pain.* J Urol, 2012. **187**(4): p. 1473-82.

13. Gupta, R.K., *Mast cell variations in prostate and urinary bladder.* Arch Pathol, 1970. **89**(4): p. 302-5.

14. Globa, T., et al., *Mast cell phenotype in benign and malignant tumors of the prostate.* Pol J Pathol, 2014. **65**(2): p. 147-53.

15. Taverna, G., et al., *Mast cells as a potential prognostic marker in prostate cancer.* Dis Markers, 2013. **35**(6): p. 711-20.

16. Ou, Z., et al., *Infiltrating mast cells enhance benign prostatic hyperplasia through IL-6/STAT3/Cyclin D1 signals.* Oncotarget, 2017. **8**(35): p. 59156-59164.

17. Murphy, S.F., A.J. Schaeffer, and P. Thumbikat, *Immune mediators of chronic pelvic pain syndrome.* Nat Rev Urol, 2014. **11**(5): p. 259-69.

18. Sayed, B.A., et al., *The master switch: the role of mast cells in autoimmunity and tolerance.* Annu Rev Immunol, 2008. **26**: p. 705-39.

19. Walker, M.E., J.K. Hatfield, and M.A. Brown, *New insights into the role of mast cells in autoimmunity: evidence for a common mechanism of action?* Biochim Biophys Acta, 2012. **1822**(1): p. 57-65.

20. Roman, K., et al., *Tryptase-PAR2 axis in experimental autoimmune prostatitis, a model for chronic pelvic pain syndrome.* Pain, 2014. **155**(7): p. 1328-38.

21. Roman, K., et al., *TRPV1 in experimental autoimmune prostatitis.* Prostate, 2020. **80**(1): p. 28-37.

22. Krystel-Whittemore, M., K.N. Dileepan, and J.G. Wood, *Mast Cell: A Multi-Functional Master Cell.* Front Immunol, 2015. **6**: p. 620.

23. Metcalfe, D.D., *Mast cells and mastocytosis.* Blood, 2008. **112**(4): p. 946-56.

24. Beghdadi, W., et al., *Mast cells as cellular sensors in inflammation and immunity.* Front Immunol, 2011. **2**: p. 37.

25. Lyons, D.O. and N.A. Pullen, *Beyond IgE: Alternative Mast Cell Activation Across Different Disease States.* Int J Mol Sci, 2020. **21**(4).

26. Mukai, K., et al., *Mast cells as sources of cytokines, chemokines, and growth factors.* Immunol Rev, 2018. **282**(1): p. 121-150.

27. Irani, A.M. and L.B. Schwartz, *Human mast cell heterogeneity.* Allergy Proc, 1994. **15**(6): p. 303-8.

28. Ramilowski, J.A., et al., *A draft network of ligand-receptor-mediated multicellular signalling in human.* Nat Commun, 2015. **6**: p. 7866.

29. AlJanahi, A.A., M. Danielsen, and C.E. Dunbar, *An Introduction to the Analysis of Single-Cell RNA-Sequencing Data.* Mol Ther Methods Clin Dev, 2018. **10**: p. 189-196.

30. Kumar, M.P., et al., *Analysis of Single-Cell RNA-Seq Identifies Cell-Cell Communication Associated with Tumor Characteristics.* Cell Rep, 2018. **25**(6): p. 1458-1468 e4.

31. Stoeckius, M., et al., *Simultaneous epitope and transcriptome measurement in single cells.* Nat Methods, 2017. **14**(9): p. 865-868.

32. Macosko, E.Z., et al., *Highly Parallel Genome-wide Expression Profiling of Individual Cells Using Nanoliter Droplets.* Cell, 2015. **161**(5): p. 1202-1214.

33. Hafemeister, C. and R. Satija, *Normalization and variance stabilization of single-cell RNA-seq data using regularized negative binomial regression.* Genome Biol, 2019. **20**(1): p. 296.

34. Zappia, L. and A. Oshlack, *Clustering trees: a visualization for evaluating clusterings at multiple resolutions.* Gigascience, 2018. **7**(7).

35. Benjamini, Y., Hochberg, Y., *Controlling the false discovery rate: a practical and powerful approach to multiple testing.* Journal of the Royal Atatistical Society Series B 57, 1995: p. 289-300.

36. Cabello-Aguilar, S., et al., *SingleCellSignalR: inference of intercellular networks from single-cell transcriptomics.* Nucleic Acids Res, 2020. **48**(10): p. e55.

37. Southan, C., et al., *The IUPHAR/BPS Guide to PHARMACOLOGY in 2016: towards curated quantitative interactions between 1300 protein targets and 6000 ligands.* Nucleic Acids Res, 2016. **44**(D1): p. D1054-68.

38. Baxter, E.W., et al., *Standardized protocols for differentiation of THP-1 cells to macrophages with distinct M(IFNgamma+LPS), M(IL-4) and M(IL-10) phenotypes.* J Immunol Methods, 2020. **478**: p. 112721.

39. Wang, H.H., et al., *Characterization of autoimmune inflammation induced prostate stem cell expansion.* Prostate, 2015. **75**(14): p. 1620-31.

40. Haverkamp, J.M., et al., *An inducible model of abacterial prostatitis induces antigen specific inflammatory and proliferative changes in the murine prostate.* Prostate, 2011. **71**(11): p. 1139-50.

41. Stanley, E.R., et al., *Biology and action of colony--stimulating factor-1.* Mol Reprod Dev, 1997. **46**(1): p. 4-10.

42. Gschwandtner, M., R. Derler, and K.S. Midwood, *More Than Just Attractive: How CCL2 Influences Myeloid Cell Behavior Beyond Chemotaxis.* Front Immunol, 2019. **10**: p. 2759.

43. Walsh, L.J., et al., *Human dermal mast cells contain and release tumor necrosis factor alpha, which induces endothelial leukocyte adhesion molecule 1.* Proc Natl Acad Sci U S A, 1991. **88**(10): p. 4220-4.

44. De Filippo, K., et al., *Mast cell and macrophage chemokines CXCL1/CXCL2 control the early stage of neutrophil recruitment during tissue inflammation.* Blood, 2013. **121**(24): p. 4930-7.

45. Mor-Vaknin, N., et al., *Vimentin is secreted by activated macrophages.* Nat Cell Biol, 2003. **5**(1): p. 59-63.

46. Bilalic, S., et al., *Lymphocyte activation induces cell surface expression of an immunogenic vimentin isoform.* Transpl Immunol, 2012. **27**(2-3): p. 101-6.

47. Pall, T., et al., *Soluble CD44 interacts with intermediate filament protein vimentin on endothelial cell surface.* PLoS One, 2011. **6**(12): p. e29305.

48. Forte, D., et al., *The tissue inhibitor of metalloproteinases-1 (TIMP-1) promotes survival and migration of acute myeloid leukemia cells through CD63/PI3K/Akt/p21 signaling.* Oncotarget, 2017. **8**(2): p. 2261-2274.

49. Orinska, Z., et al., *Tetraspanins in the regulation of mast cell function.* Med Microbiol Immunol, 2020. **209**(4): p. 531-543.

50. Kabashima, K., et al., *Biomarkers for evaluation of mast cell and basophil activation.* Immunol Rev, 2018. **282**(1): p. 114-120.

51. Schenk, G.J., et al., *Roles for HB-EGF and CD9 in multiple sclerosis.* Glia, 2013. **61**(11): p. 1890-905.

52. Steiner, G.E., et al., *Cytokine expression pattern in benign prostatic hyperplasia infiltrating T cells and impact of lymphocytic infiltration on cytokine mRNA profile in prostatic tissue.* Lab Invest, 2003. **83**(8): p. 1131-46.

53. St Sauver, J.L., et al., *Longitudinal association between prostatitis and development of benign prostatic hyperplasia.* Urology, 2008. **71**(3): p. 475-9; discussion 479.

54. Roberts, R.O., et al., *Prevalence of a physician-assigned diagnosis of prostatitis: the Olmsted County Study of Urinary Symptoms and Health Status Among Men.* Urology, 1998. **51**(4): p. 578-84.

55. Krieger, J.N., S.O. Ross, and D.E. Riley, *Chronic prostatitis: epidemiology and role of infection.* Urology, 2002. **60**(6 Suppl): p. 8-12; discussion 13.

56. Bharucha, A.E. and T.H. Lee, *Anorectal and Pelvic Pain.* Mayo Clin Proc, 2016. **91**(10): p. 1471-1486.

57. Aydin, O., et al., *Immunohistological analysis of mast cell numbers in the intratumoral and peritumoral regions of prostate carcinoma compared to benign prostatic hyperplasia.* Pathol Res Pract, 2002. **198**(4): p. 267-71.

58. Kim, J.H., et al., *Proliferation of Prostate Stromal Cell Induced by Benign Prostatic Hyperplasia Epithelial Cell Stimulated With Trichomonas vaginalis via Crosstalk With Mast Cell.* Prostate, 2016. **76**(15): p. 1431-44.

59. Overed-Sayer, C., et al., *Are mast cells instrumental for fibrotic diseases?* Front Pharmacol, 2013. **4**: p. 174.

60. Haque, A., et al., *A practical guide to single-cell RNA-sequencing for biomedical research and clinical applications.* Genome Med, 2017. **9**(1): p. 75.

CHAPTER 6. CONCLUSIONS AND FUTURE DIRECTIONS

6.1 Introduction

Prostatic inflammation has been implicated in the pathogenesis of BPH, yet the interactions and activities of immune cell populations in driving the inflammatory microenvironment and its impact on prostate cell hyperplasia has not yet been fully elucidated. The purpose of the research presented here is to explore the impact of inflammation on prostate morphology and cellular growth and to better define immune cell interactions and roles in hyperplastic disease. This was done through the use of murine models of prostatitis as well as morphologic and transcriptomic analyses of human BPH specimens. Previous studies involving histology and immunohistochemistry in animal models and human specimens have described the composition and distribution of prostatic immune cells in normal and BPH prostates [1-3]. Additional studies have examined the expression of immune cell-derived inflammatory mediators in the BPH microenvironment [4, 5]. Still others have examined the gene expression profiles of BPH specimens [6]. However, these studies have been limited in their scope due to the limitations of the technologies available at the time. Advances in scRNA-seq technology and the development of various scRNA-Seq data analysis methods have allowed for not only a broader and deeper examination of the gene expression of individual cells in tissues but also describe their behavior and functions in tissues through signaling pathway analyses, ligand-receptor interaction prediction, correlations with clinical data, and more. To the author's knowledge, this research represents the first studies combining isolated immune cell scRNA-Seq data analysis techniques and histologic analyses to define and describe immune cell populations and predict their activity through gene expression, signaling pathway, and ligand-receptor interaction prediction analyses. Here, we have seen that immune cell distribution and morphology, gene expression, and predicted ligand/receptor interactions involving immune modulatory molecules are altered in BPH compared to normal prostate immune cells and suggests roles for specific immune cell types and their interactions in driving prostate inflammation.

The studies presented here demonstrated the impact of autoimmune-type inflammation on basal epithelial cells in driving basal cell expansion and directing their growth and differentiation under conditions mimicking ADT. Also, analysis of human specimens indicates a mixed inflammatory

microenvironment in BPH and altered cell-cell communication between and among immune cell populations via ligand-receptor interactions. In all, these studies indicate that immune cells and their interactions drive the chronic inflammatory phenotype of BPH and that inflammation can promote basal epithelial cell proliferation and differentiation under conditions mimicking androgen-targeted therapy.

While the current study focused mainly on the impact of inflammation on murine basal epithelial cells and interactions involving myeloid/macrophage, $CD8^+$ T cell, and mast cell populations, the development and progression of BPH involves complex interactions between and among the various epithelial, stromal, and immune cell populations present in the prostate, and many of these interactions remain to be explored. The analyses and techniques used here may be applied to the exploration of other prostate cell populations and their interactions. Here is discussed the potential future directions for this research.

6.2 Ligand-receptor interactions in BPH

The purpose of the immune cell interaction study was to further define immune cell populations and their activities in BPH compared to normal non-BPH prostates. This involved histologic evaluation of BPH specimens and scRNA-Seq analyses of BPH and normal prostate immune cell populations. Previous studies involving histology and immunohistochemistry have discussed the immune microenvironment in normal and BPH prostates [1-6]. Here, we have seen that immune cell distribution and morphology, gene expression, and predicted ligand/receptor interactions involving immune modulatory molecules are altered in BPH compared to normal prostate immune cells and suggests roles for specific immune cell types and their interactions in driving prostate inflammation.

Future studies in immune cell interactions offer a variety of possible directions. In the current studies, select immune cell populations were explored. Clinical correlations indicated a role for T cell populations in BPH symptoms, and interaction analysis indicated alterations in the communications between and among macrophages and mast cells (Chapter 3, Chapter 5). However, these analyses also indicated roles for other immune cell types in BPH. Interaction analysis predicted interactions among all identified immune cell populations, suggesting that many

immune cell types may contribute to BPH inflammation, either to drive the continuation or promote resolution of inflammation.

The findings in the current study indicate that mast cells and their interactions with other immune cells (particularly macrophages) may play a role in driving the ongoing inflammation of BPH (Chapter 5). Previous studies have associated prostate mast cells with CP/CPPS and with epithelial and stromal hyperplasia and fibrosis [7-10]. It is hypothesized that mast cells may contribute to the non-resolving BPH inflammation though their receptor-ligand interactions and stimulation of and by macrophages and of and by each other. Additional studies into the role of mast cells and their interactions in prostate disease could further explore the significance of the predicted alterations in ligand/receptor interactions involving these cells in BPH.

One important area of study would be to explore ligand-receptor interactions among all prostate cell types, including epithelial and stromal cells. The interaction analysis used here was first used to define interactions among cells within tumors [11]. Whole prostate cell preps could be analyzed by scRNA-Seq and cell-cell interactions predicted among all cell types. scRNA-Seq data from whole cell preps of BPH and normal prostates generated by Strand et al (2019) indicate that expression of the lymphoid chemotactic cytokine genes CXCL13 and CCL21 associated with TLS formation and maintenance are increased in the fibroblasts and endothelial cells of BPH prostates [12]. Interaction analysis may predict alterations in cytokine and chemokine interactions involved in immune cell recruitment and activation, as well as factors associated with stromal and/or epithelial hyperplasia. Such studies may provide specific ligand-receptor targets for treatment.

In these studies, prostate tissue from symptomatic BPH patients and age-matched non-BPH prostates could be compared histologically and by scRNA-Seq to evaluate morphology, gene expression, and cell-cell interactions between BPH and non-BPH prostates. Whole cell scRNA-Seq would allow the inclusion of non-immune cell types in the analysis, as other cell types such as follicular dendritic cells and endothelial cells have been implicated in immune cell recruitment and TLS formation [1, 13]. It is anticipated that predicted interactions between stromal cells and immune cells will include ligands and receptors implicated in TLS formation and maintenance, and that these interactions will be altered between BPH and normal prostates.

The current studies in basal epithelial progenitor cells indicate communication between epithelial cells and immune cells and likely stromal cells. Induced inflammation drove basal epithelial progenitor cell proliferation *in vivo* and differentiation *in vitro*. The precise mechanisms by which inflammation alters the proliferation and differentiation programs of epithelial cells so that they resist ADT is not known. To explore this, whole prostate scRNA-Seq and a similar ligand-receptor interaction prediction analysis and signaling pathway analysis as described here may elucidate the immune cell-epithelial cell interactions that may drive these changes. Also, as interactions between stromal cells and immune cells contribute to the recruitment and maintenance of the inflammatory microenvironment, these analyses may also further clarify the role of stromal cells in driving inflammation and epithelial proliferation [14].

In addition to exploring the roles of stromal cells in recruitment and organization of immune cells, interaction analyses may be useful in predicting interactions between immune cells and stromal cells that may drive stromal expansion. As stromal proliferation is often a dominant feature of BPH, it is hypothesized that the chronic non-resolving inflammation of the BPH microenvironment contributes to stromal proliferation and expansion. scRNA-Seq analysis of whole prostate cell populations and interaction analysis may predict cell interactions that are altered between stromal cells and immune cells.

6.3 The role of TLS in BPH

TLS represent a largely unexplored feature of BPH stromal immune cells. While these structures have been observed in the prostates of older men without histologic evidence of BPH as well as in PCa, it is uncertain whether these structures represent a normal age-related change or contribute to prostate cell hyperplasia [1, 15]. In the current study, the general morphology and cellular composition of these structures was described and was consistent with a previous study by Di Carlo (2007) describing prostate lymphoid populations and their organization in the prostates of aged men without histologic evidence of BPH (Chapter 3) [1]. The Di Carlo study also noted $FoxP3^+$ Treg by IHC in association with TLS. In BPH specimens, $FoxP3^+$ cells were generally sparsely distributed in TLS by immunohistochemistry (Chapter 3). It has been hypothesized that the perpetuation of BPH inflammation may be, at least in part, due to diminished Treg suppressive activity, and the sparse distribution of $FoxP3^+$ cells in BPH specimens in the current study may

indicate a loss of Treg control of BPH inflammation, thereby contributing to the progressive and non-resolving nature of BPH inflammation. However, it is difficult to determine the significance of this observation based on this and the previous study.

To determine the significance of TLS and their cellular populations (including Treg) In BPH, prostate tissue from symptomatic BPH patients and age-matched non-BPH prostates could be compared histologically and by scRNA-Seq to evaluate morphology, gene expression, and cell-cell interactions between BPH and non-BPH prostates. Whole cell scRNA-Seq would allow the inclusion of non-immune cell types in the analysis, as other prostate cell types such as follicular dendritic cells and endothelial cells have been implicated in TLS formation [1, 13]. Additionally, the use of spatial transcriptomic technology would provide information on the distribution and spatial relationships of immune cells within TLS in addition to scRNA-Seq data.

To model the inflammatory microenvironment, the Aire KO mouse may be used as a model of non-resolving prostatic inflammation. Current and previous studies in the POET-3 mouse have demonstrated the impact of autoimmune-type inflammation on prostate cell types and morphology, but the resolving nature of the POET-3 prostate inflammation differs from that observed in human BPH patients [16-18]. The Aire KO mouse can form stromal lymphoid structures resembling TLS following prostate antigen injection with complete Freud's adjuvant and boosted with incomplete Freud's adjuvant. Although further characterization is needed, this model may prove useful in exploring the mechanisms and impact of TLS formation in the prostate.

In addition to the TLS-associated T cells discussed in this research, B cells contribute to the composition of TLS. Some studies have investigated B cells in association with prostate tumors and have observed B cells infiltrating prostate tumors, and B cell-derived lymphotoxin has been associated with CRPC [19, 20]. However, the role of B cells in BPH has not been extensively studied. In the current studies, the proportion of B cells was found to be significantly positively correlated with BMI (Chapter 3). The significance of this observation is yet unknown. A study of BPH patient and age-matched non-BPH prostate tissue from both obese and non-obese individuals may indicate if this correlation is associated with any characteristic morphologic changes or if obesity modulates B cell gene expression and/or activity in the prostate.

6.4 PCa and inflammation

Inflammation has been associated with PCa, however the precise roles of inflammation in prostate carcinogenesis are not fully understood [22, 23]. Previous studies conducted by this lab have investigated the role of inflammation in carcinogenesis in POET-3/PTEN^{het} and POET-3/PTEN$^{fl/fl}$ mice [24]. Previous and current studies in this lab have indicated that inflammation promotes AR expression (Chapter 2)[18]. In murine basal progenitor cell studies, inflammation promoted AR expression in organoids despite AR signaling blockade (Chapter 2). Preliminary studies in an orthotopic model of PCa using murine high Myc-expressing prostate cancer cell line (Myc-CaP) indicate that induction of inflammation typically resulted in larger tumor regrowth in castrate mice and induced nuclear expression of AR in castrate mice (Fig. 6.1 A, B). The mechanisms by which inflammation promotes AR expression and activity are currently under investigation.

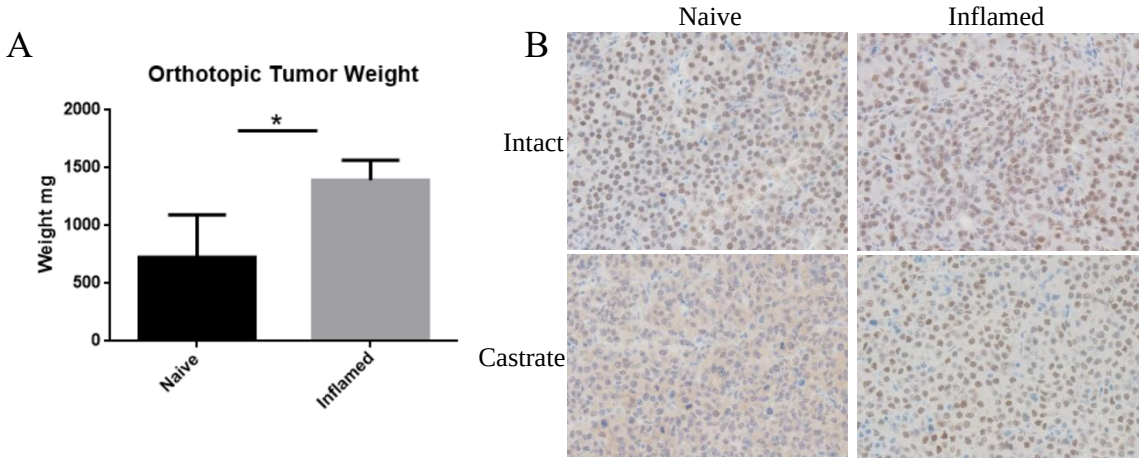

Figure 6.1. (A) Weights of naïve and inflamed MycCaP orthotopic tumors harvested from castrate mice (P=0.0464). (B) AR IHC demonstrating nuclear localization in orthotopic tumors from intact (top) mice and in inflamed castrate (bottom right) mouse.

6.5 Conclusions

Overall, the research presented here further characterizes the impact of inflammation on prostate cells and investigates the roles of immune cell populations and their interactions in the perpetuation of BPH inflammation. The precise mechanisms by which inflammation exerts its effects on prostate cell populations is not fully known and is currently under investigation. It is anticipated that the analysis techniques described here in combination with emerging

transcriptomic technologies will likely expand our understanding of BPH inflammation that may uncover potential therapeutic targets.

6.6 References

1. Di Carlo, E., et al., *The prostate-associated lymphoid tissue (PALT) is linked to the expression of homing chemokines CXCL13 and CCL21.* Prostate, 2007. **67**(10): p. 1070-80.

2. Theyer, G., et al., *Phenotypic characterization of infiltrating leukocytes in benign prostatic hyperplasia.* Lab Invest, 1992. **66**(1): p. 96-107.

3. Robert, G., et al., *Inflammation in benign prostatic hyperplasia: a 282 patients' immunohistochemical analysis.* Prostate, 2009. **69**(16): p. 1774-80.

4. Steiner, G.E., et al., *Cytokine expression pattern in benign prostatic hyperplasia infiltrating T cells and impact of lymphocytic infiltration on cytokine mRNA profile in prostatic tissue.* Lab Invest, 2003. **83**(8): p. 1131-46.

5. Kramer, G., et al., *Increased expression of lymphocyte-derived cytokines in benign hyperplastic prostate tissue, identification of the producing cell types, and effect of differentially expressed cytokines on stromal cell proliferation.* Prostate, 2002. **52**(1): p. 43-58.

6. Luo, J., et al., *Gene expression signature of benign prostatic hyperplasia revealed by cDNA microarray analysis.* Prostate, 2002. **51**(3): p. 189-200.

7. Done, J.D., et al., *Role of mast cells in male chronic pelvic pain.* J Urol, 2012. **187**(4): p. 1473-82.

8. Murphy, S.F., A.J. Schaeffer, and P. Thumbikat, *Immune mediators of chronic pelvic pain syndrome.* Nat Rev Urol, 2014. **11**(5): p. 259-69.

9. Ou, Z., et al., *Infiltrating mast cells enhance benign prostatic hyperplasia through IL-6/STAT3/Cyclin D1 signals.* Oncotarget, 2017. **8**(35): p. 59156-59164.

10. Krystel-Whittemore, M., K.N. Dileepan, and J.G. Wood, *Mast Cell: A Multi-Functional Master Cell.* Front Immunol, 2015. **6**: p. 620.

11. Kumar, M.P., et al., *Analysis of Single-Cell RNA-Seq Identifies Cell-Cell Communication Associated with Tumor Characteristics.* Cell Rep, 2018. **25**(6): p. 1458-1468 e4.

12. Strand, D.W. *Single-Cell RNA-sequencing Data-Strand Lab*. 2019; Available from: https://dev.strandlab.net/sc.data/.

13. Luo, S., et al., *Chronic Inflammation: A Common Promoter in Tertiary Lymphoid Organ Neogenesis.* Front Immunol, 2019. **10**: p. 2938.

14. Pitzalis, C., et al., *Ectopic lymphoid-like structures in infection, cancer and autoimmunity.* Nat Rev Immunol, 2014. **14**(7): p. 447-62.

15. Garcia-Hernandez, M.L., et al., *A Unique Cellular and Molecular Microenvironment Is Present in Tertiary Lymphoid Organs of Patients with Spontaneous Prostate Cancer Regression.* Front Immunol, 2017. **8**: p. 563.

16. Haverkamp, J.M., et al., *An inducible model of abacterial prostatitis induces antigen specific inflammatory and proliferative changes in the murine prostate.* Prostate, 2011. **71**(11): p. 1139-50.

17. Wang, H.H., et al., *Characterization of autoimmune inflammation induced prostate stem cell expansion.* Prostate, 2015. **75**(14): p. 1620-31.

18. Cooper, P.O., *The impacts of inflammation on adult prostate stem cells* in *Comparative Pathobiology*. 2020, Purdue University.

19. Ammirante, M., et al., *B-cell-derived lymphotoxin promotes castration-resistant prostate cancer.* Nature, 2010. **464**(7286): p. 302-5.

20. Woo, J.R., et al., *Tumor infiltrating B-cells are increased in prostate cancer tissue.* J Transl Med, 2014. **12**: p. 30.

21. Shalapour, S., et al., *Immunosuppressive plasma cells impede T-cell-dependent immunogenic chemotherapy.* Nature, 2015. **521**(7550): p. 94-8.

22. De Marzo, A.M., et al., *Proliferative inflammatory atrophy of the prostate: implications for prostatic carcinogenesis.* Am J Pathol, 1999. **155**(6): p. 1985-92.

23. De Marzo, A.M., et al., *Inflammation in prostate carcinogenesis.* Nat Rev Cancer, 2007. **7**(4): p. 256-69.

24. Burcham, G.N., et al., *Impact of prostate inflammation on lesion development in the POET3(+)Pten(+/-) mouse model of prostate carcinogenesis.* Am J Pathol, 2014. **184**(12): p. 3176-91.